UMinho|2015

Susana Amorim Lopes **A biodegradable PLGA – coating releasing DNase I to prevent bacterial adhesion and biofilm formation**

Universidade do Minho
Escola de Engenharia

Susana Amorim Lopes

A biodegradable PLGA – coating releasing DNase I to prevent bacterial adhesion and biofilm formation

setembro de 2015

Universidade do Minho
Escola de Engenharia

Susana Amorim Lopes

A biodegradable PLGA – coating releasing DNase I to prevent bacterial adhesion and biofilm formation

Mestrado Integrado em Engenharia Biomédica
Ramo Engenharia Clínica

Trabalho efetuado sob a orientação da
Professora Doutora Henny van der Mei
e da
Professora Doutora Lígia Rodrigues
e a supervisão do
Doutor Jan Swartjes

setembro de 2015

DECLARAÇÃO

Nome: Susana Amorim Lopes

Endereço Eletrónico: susana.amorim.l@gmail.com

Cartão de Cidadão: 14182218

Título da Dissertação:
A biodegradable PLGA – coating releasing DNase I to prevent bacterial adhesion and biofilm formation

Prevenção da adesão bacteriana e formação de biofilmes através de um revestimento biodegradável de PLGA com libertação de DNase I

Orientadores: Professora Doutora Henny van der Mei e Professora Doutora Lígia Rodrigues

Supervisor: Doutor Jan Swartjes

Ano de conclusão: 2015

Designação do Mestrado:
Mestrado Integrado em Engenharia Biomédica – Ramo Engenharia Clínica

É AUTORIZADA A REPRODUÇÃO INTEGRAL DESTA DISSERTAÇÃO APENAS PARA EFEITOS DE INVESTIGAÇÃO, MEDIANTE DECLARAÇÃO ESCRITA DO INTERESSADO, QUE A TAL SE COMPROMETE.

Universidade do Minho, _____/_____/_______

Assinatura: ____

To my dear parents

Acknowledgements

My first words are to my supervisor, Prof. Dr. Jan Swartjes, for the endless support, patience, availability, and dedication along this work. I thank specially the criticisms that made me rethink and move forward. This work would not be possible without his ideas and suggestions. Thank you for introduce me to the world of research and for challenge me.

Thanks to Prof. Dr. Lígia Rodrigues, for the guidance, confidence and encouragement always present, and for the helpful recommendations, ideas and wise advices that contributed to the realization of this work.

I would like to show my gratitude to everyone who helped with advices, insightful suggestions, and clarifications, especially to Prof. Dr. Henny van der Mei, Prof. Dr. Theo van Kooten, Prof. Dr. Daniëlle Neut and Dr. Niels Grasmeijer. A sincere thank for sharing knowledge.

Thanks to the laboratory people, mainly to Willem, for all the assistance provided, for the hospitality and sympathy, valuable insights, and for, even far, making me feel at home.

I want to express my appreciation to all the friends I made in Groningen, in particular to Raquel, Vera, Gülcan, Fernanda, Minnie and Delia for the support, the optimism, the unique and unforgettable moments. I also would like to thank to my Erasmus mates, Carolina and Luís, for all experiences and adventures we lived together.

I also thank my colleagues and friends, especially Carolina, Fábio, Rita and Márcio, for the exchange of experiences, for their help, comfort and encouragement, for the friendship and the words that, in the most difficult times, made me grow and continue.

I would like to express my deepest gratitude to Luís Pedro. Thank you for caring me day by day, for being a pillar in my life and the only constant in the short and long plans.

Finally, I thank my family, in particular my parents, without whom nothing of this would be possible. Thank you for making me who I am.

Thank you.

The present work as developed with the help of Erasmus+ and University Medical Center of Groningen (UMCG).

Abstract

Biofilms are highly complex bacterial aggregates, surrounded by extracellular polymeric substances (EPS). Each matrix component has specific functions contributing to the maintenance of the biofilm health. In the EPS matrix, extracellular deoxyribonucleic acid (eDNA) is present at the bacterial cell surface and plays an essential role in several stages of biofilm formation, namely it determines biofilm architecture, provides mechanical stability to biofilms, protects bacterial cells in biofilms from physical stress, antibiotics and detergents and could be a significant source of organic nutrients in the environment whilst disseminating genes amongst different microorganisms. In this context, attacking this essential component of the EPS matrix by deoxyribonuclease I (DNase I), an endonuclease that digests DNA through hydrolysis of the phosphodiester bonds, has been considered a possible approach to prevent biofilm formation.

In this work, covering titanium, a common orthopaedic implant material, with a protective biodegradable poly(lactic-co-glycolic acid) (PLGA) coating containing embedded DNase I, has been found to be a promising strategy to prevent the initial bacterial adhesion and biofilm formation *in vitro*. Employing coatings of PLGA-DNase I and PLGA-inulin packaged DNase I, bacterial adhesion and biovolumes of biofilms of up to 120 h old, of both *Staphylococcus aureus* ATTCC 12600^{GFP} or *Staphylococcus aureus* Newman D2C^{GFP}, decreased substantially with respect to uncoated titanium. It is expected that a timescale of 120 h is sufficiently long to prevent infection arising from peri-operatively introduced bacteria as is currently done with a dose of post-operatively administered antibiotics. Without the risk of bacterial resistance development, the PLGA-inulin packaged DNase I coating provides an appropriate and effective strategy to prevent biofilm formation on the surface of biomaterial implants and devices. In addition, the contact between U2-OS cells and the developed PLGA coatings does not negatively affect their viability and proliferative capacity, as well as the adhesion to the surface of the coatings. Therefore, this approach should be further explored to determine whether it can mitigate the occurrence of biomaterial-associated infections (BAI) *in vivo*, which are responsible for several clinical complications and high healthcare costs.

Keywords: Biomaterial-associated infections (BAI); eDNA; anti-biofilm strategies; DNase I; poly(lactic-co-glycolic acid) (PLGA).

Resumo

Os biofilmes são agregados bacterianos altamente complexos, rodeados por substâncias extracelulares poliméricas (EPS). Na matriz da EPS, o ácido desoxirribonucleico extracelular (eDNA) está presente na superfície das células bacterianas e desempenha um papel essencial em várias fases da formação do biofilme, nomeadamente determina a sua arquitetura, proporciona estabilidade mecânica, protege as células bacterianas de stress físico, antibióticos e detergentes, e pode ser uma fonte significativa de nutrientes orgânicos no ambiente enquanto dissemina genes entre diferentes microrganismos. Neste contexto, atacar este componente essencial da matriz de EPS utilizando desoxirribonuclease I (DNase I), uma endonuclease que digere DNA por hidrólise das ligações fosfodiéster, tem sido considerada uma possível abordagem para evitar a formação de biofilmes.

No presente trabalho, o revestimento de titânio, material comummente utilizado em implantes ortopédicos, com uma proteção biodegradável de poli(ácido láctico-co-ácido glicólico) (PLGA) incorporando DNase I, mostrou ser uma estratégia promissora para prevenir a adesão bacteriana inicial e a formação de biofilmes *in vitro*. Comparativamente à superfície de titânio não revestida, os revestimentos PLGA-DNase I e PLGA-inulina incorporando DNase I diminuíram significativamente a adesão bacteriana e os biovolumes dos biofilmes constituídos por *Staphylococcus aureus* ATTCC 12600^{GFP} ou *Staphylococcus aureus* Newman D2C^{GFP} com 24 h, 72 h e 120 h de crescimento. É expectável que 120 h seja um período de tempo suficientemente longo para evitar a ocorrência de infecções resultantes da entrada de bactérias no período peri-operatório. Sem apresentar risco de desenvolvimento de resistência bacteriana, o revestimento PLGA-inulina incorporando DNase I constitui uma estratégia adequada e eficaz para prevenir a formação de biofilmes na superfície de implantes de biomateriais e dispositivos. Adicionalmente, o contacto entre as células U2-OS e os revestimentos de PLGA desenvolvidos não afecta negativamente a sua viabilidade e capacidade proliferativa, assim como a sua adesão à superfície dos revestimentos. Portanto, esta abordagem deve ser explorada no futuro de forma a concluir se pode mitigar *in vivo* a ocorrência de infecções associadas aos biomateriais (BAI) responsáveis por várias complicações clínicas e altos custos de saúde.

Palavras-chave: Infeções associadas aos biomateriais (BAI); eDNA; estratégias anti-biofilme; DNase; revestimentos de poli(ácido láctico-co-ácido glicólico) (PLGA).

Scientific output

PAPERS SUBMITTED TO PEER REVIEWED JOURNALS:

Jan J.T.M. Swartjes, **Susana Amorim Lopes**, Prashant K. Sharma, Niels Grasmeijer, Henderik W. Frijlink, Wouter L.J. Hinrichs, Henny C. van der Mei, Henk J. Busscher, *PLGA and Inulin Protection of DNase I Microparticles Increases Functionality Against Bacterial Adhesion and Biofilm Formation*, (manuscript in preparation for Advanced Functional Materials).

Table of contents

Chapter 1 | Introduction..1

1.1. Contextualization and aims.. 3

1.2. Biomaterial-Associated Infections... 4

1.2.1. Biofilms on medical devices 4

1.2.2. Microorganisms commonly associated with medical devices 6

1.2.3. Risk factors underlying the development of BAI 10

1.3. Biofilms 12

1.3.1. Biofilm formation and development 12

1.3.2. The life cycle of a biofilm 13

1.3.3. Biofilm structure: Extracellular polymeric substances matrix............................ 15

1.3.3.1. Definition, composition and spatial distribution.................................. 15

1.3.3.2. Functionality.. 16

1.3.3.3. Extracellular DNA 17

1.3.3.3.1. Origin 17

1.3.3.3.2. Role.. 17

1.4. Anti-biofilm strategies 21

1.4.2. Biofilm prevention 22

1.4.3. Biofilm weakening.. 23

1.4.4. Biofilm disruption 24

1.4.4.1. Biofilm disruption enzymes.. 25

1.4.4.1.1. eDNA as a target in biofilm treatment.. 27

1.4.5. Biofilm Killing.. 28

1.4.6. Combined strategies.. 29

Chapter 2 | Materials and Methods 31

2.1. Particle preparation.. 33

2.1.1. Particle formulations and dimension 33

2.2. Surface coating... 33

2.2.1. Titanium substrate preparation.. 33

2.2.2. Coating of the titanium substrata 34

2.2.3. Coatings roughness and thickness.. 35

2.2.4. Coatings degradation time 35
2.3. DNase I release kinetics 36
2.3.1. DNase I calibration curve 36
2.3.2. Inulin calibration curve 36
2.3.3. DNase I release kinetics 36
2.3.4. Inulin release kinetics 37
2.3.5. Scanning electron microscopy 37
2.3.6. Initial burst release 37
2.4. Bacterial culture and harvesting 38
2.4.1. Bacterial strains 38
2.4.2. Growth conditions 39
2.4.3. Bacterial harvesting 39
2.5. Initial bacterial adhesion and biofilm growth 40
2.5.1. Initial bacterial adhesion 40
2.5.2. Biofilm growth 40
2.6. U-2 OS adhesion and XTT assay using U-2 OS 41
2.6.1. U-2 OS cell line 41
2.6.2. Growth conditions 41
2.6.3. XTT assay 42
2.6.4. Cell adhesion assay 42
2.7. Pilot experiment: effect of gentamicin when combined with the PLGA coatings containing either DNase I or inulin-packaged DNase I 44
2.7.1. Minimum inhibitory concentration and minimum bactericidal concentration 44
2.7.2. Biofilm susceptibility to gentamicin 44
2.8. Statistics 45
Chapter 3 | Results 47
3.1. Particle preparation 49
3.1.1. Particle dimension 49
3.2. Surface coating 49
3.2.1. Coating roughness and thickness 49
3.2.2. Coating degradation 52
3.3. Release kinetics 53

3.3.1. DNase I and inulin release kinetics 53
3.3.2. Initial burst release 55
3.4. Initial bacterial adhesion and biofilm growth 56
3.4.1. Initial bacterial adhesion 56
3.4.2. Biofilm growth 58
3.5. XTT assay and cell adhesion assay using U-2 OS 63
3.5.1. XTT assay 63
3.5.2. Cell adhesion assay 64
3.6. Pilot experiment: effect of gentamicin when combined with the PLGA coatings containing either DNase I or inulin-packaged DNase I 65
3.6.1. Minimum inhibitory concentration and minimum bactericidal concentration 65
3.6.2. Biofilm susceptibility to gentamicin 66
Chapter 4 | Discussion 69
4.1. Particle preparation 71
4.1.1. Particle dimension 71
4.2. Surface coating 72
4.2.1. Roughness and thickness of the coatings 72
4.2.2. Degradation of the coatings 73
4.3. Release kinetics 74
4.3.1. DNase I and inulin release kinetics 74
4.3.2. Prevention of the initial burst release 76
4.4. Initial bacterial adhesion and biofilm growth 77
4.5. XTT assay and cell adhesion assay using U-2 OS cells 83
4.5.1. XTT assay 83
4.5.2. Cell adhesion assay 84
4.6. Pilot experiment: effect of gentamicin when combined with the PLGA coatings containing either DNase I or inulin-packaged DNase I on the staphylococcal strains 86
4.6.1. Minimum inhibitory concentration and minimum bactericidal concentration 86
4.6.2. Biofilm susceptibility to gentamicin 88
Chapter 5 | Conclusion and future perspectives 91
5.1. Concluding remarks 93
5.2. Future perspectives 94

References 97

Appendices 115

Appendix A – Particles dimension 117

Appendix B – DNase I and inulin calibration curves 120

List of abbreviations and acronyms

2-D	2-Dimensional
3-D	3-Dimensional
Abs	Absorbance
ANOVA	Analysis of Variance
AHLs	Acylated Homoserine Lactones
ATCC	American Type Culture Collection
BAI	Biomaterial Associated Infections
c-di-GMP	Cyclic Diguanosine-5'-monophosphate
CFU	Colony-Forming Units
CLSI	Clinical and Laboratory Standards Institute
CLSM	Confocal Laser Scanning Microscopy
CoNS	Coagulase negative staphylococci
DAPI	4',6-diamidino-2-phenylindole
DMEM	Dulbecco's Modified Eagle's Medium
DMSO	Dimethyl Sulfoxide
DNA	Deoxyribonucleic Acid
DNase	Deoxyribonuclease
eDNA	Extracellular Deoxyribonucleic Acid
EDTA	Ethylene Diamine Tetraacetic Acid
EGTA	Ethylene Glycol Tetraacetic Acid
EPS	Extracellular Polymeric Substances
FBS	Fetal Bovine Serum
FDA	Food and Drug Administration
GFP	Green Fluorescent Protein
HAI	Healthcare Associated Infections
MBC	Minimum Bactericidal Concentration
MIC	Minimum Inhibitory Concentration
MRSA	Methicillin-Resistant *S. aureus*
MTT	3-(4,5-dimethyl-2-thiazol)-2,5-di-phenyl-2H-tetrazolium bromide
MV	Membrane Vesicles

M_{wb}	Molecular Weight Average
NIH	National Institutes of Health
OCT	Optical Coherence Tomography
P-value	Significance Value
PBS	Phosphate-Buffered Saline
PEO	Poly (ethylene oxide)
PGA	Poly (glycolide)
PIA	Polysaccharide Intercellular Adhesin
PJIs	Prosthetic Joint Infections
PLA	Poly (lactic acid)
PLGA	Poly (lactic-co-glycolic acid)
PNAG	Poly-N-acetyl-glucosamine
QS	Quorum Sensing
QSIs	Quorum Sensing Inhibitors
R^2	Correlation Coefficient
Ra	Average Roughness
rhDNase	Recombinant Human Deoxyribonuclease
RNA	Ribonucleic Acid
SD	Standard Deviation
SEM	Scanning Electron Microscopy
SPEP	Metalloprotease Serratopeptidase
spp.	Species
SPSS	Statistical Package for the Social Sciences
sRNA	Small Ribonucleic Acid
TRITC	Tetramethylrhodamine
TSB	Tryptone Soy Broth
UV	Ultraviolet
XTT	2,3-bis(2-methoxy-4-nitro-5-sulfophenyl)-2H-tetrazolium-5-carboxanilide

List of figures

Chapter 1

Figure 1.1. Schematic representation of the bacterial biofilms development from planktonic bacteria. The pathway on the top describes the development of non-surface-attached biofilms (host materials embedded). The pathway below shows the surface-attached biofilms. Adapted from [13]. 4

Figure 1.2. Frequency of the main pathogenic species found among orthopaedic clinical isolates of implant-associated infections. Adapted from [20]. 6

Figure 1.3. Projections of the worldwide increase of arthroplasties from 2005 to 2030. Taken from [24]. 8

Figure 1.4. A false-color scanning electron micrograph of *S. aureus* illustrating the typical grape-like cluster of cocci. Scale bar represents 1 μm. Adapted from [29]. 9

Figure 1.5. The major biofilm exopolysaccharide of staphylococci is intercellular polysaccharide adhesin (PIA) (blue: deacetylation creates free amino groups that at neutral or acid pH give the molecule a cationic character). Adapted from [36]. 9

Figure 1.6. Patient-associated risk factors underlying the development of BAI. Revision surgery patients are at greater risk than primary surgery implant patients. The risk of an implant or device becoming infected hematogenously decreases with time after implant placement due to more extensive host tissue integration. Taken from [6]. 10

Figure 1.7. Sequential steps of biofilms development. From right to left: initial attachment, irreversible attachment, early development of biofilm architecture, maturation and dispersion. Taken from [40]. 13

Figure 1.8. The complex structure of bacterial biofilms. Microcolonies in the mature biofilm are characterized by an EPS matrix typically constituted by exopolysaccharides, proteins, eDNA, amyloid fibres, bacteriophages and other macromolecules. Adapted from [40]. 16

Figure 1.9. Removal of eDNA influences acid-base interactions (named AB) B,D) and Ca^{2+} mediated cationic bridging between bacterial cells and consequently A,C) bacterial aggregation. Adapted from [57]. 18

Figure 1.10. Interactions between eDNA and other matrix components. Adapted from [59]. . 20

Figure 1.11. Anti-biofilm strategies. Adapted from [13]. 21

Figure 1.12. Schematic illustration of the biofilm disassembly. Taken from [75]. 24

Figure 1.13. Schematic representation of several matrix-degrading enzymes used for biofilm inhibition and dispersal. Taken from [77]. 26

Figure 1.14. Mechanism of biofilm dispersal caused by DNase I. A) eDNA acting as a bridge between a bacterial cell surface and various biopolymers in EPS. B) Disruption of EPS by DNase I coating attacking the eDNA component of the EPS, preventing bacterial adhesion to the substratum surface. Adapted from [58]. 28

Chapter 2

Figure 2.1. Schematic representation of the procedure used to coat each titanium substrata (only PLGA, PLGA-DNase I, PLGA-DNase I (1/5) and PLGA-inulin packaged DNase I). 34

Figure 2.2. Schematic illustration of the procedure used to avoid the initial burst release of DNase I from titanium coated with A) PLGA-DNase I and B) PLGA-inulin packaged DNase I (first approach). 38

Figure 2.3. Schematic representation of the procedure used to analyse the metabolic activity of U-2 OS cells around the material and cells adhered to the material (XTT assay), as well as the number of live cells in both cases (cell adhesion assay). 43

Chapter 3

Figure 3.1. Height map generated through white light interferometry in i) 2-Dimensional (2-D) and ii) 3-D for A) uncoated titanium surface; B) PLGA; C) PLGA-Inulin; D) PLGA-DNase I; E) PLGA-DNase (1/5); and F) PLGA-inulin-packaged DNase I. Total area is 2 mm × 2 mm and colours are artificially generated to yield a height map. 51

Figure 3.2. Pictures of the different PLGA coatings: i) PLGA; ii) PLGA-inulin; iii) PLGA-DNase I; iv) PLGA-DNase I (1/5); and v) PLGA-inulin packaged DNase I after A) 0 d, B) 14 d, C) 35 d and D) 56 d of immersion on a PBS solution. The red arrows point to some points of the surface where the coating is still present. 52

Figure 3.3. Release of DNase I from PLGA-DNase I. A) Cumulative amounts of DNase I released (μg) from PLGA-DNase I immersed in PBS for different periods of time (h) obtained specphotometrically, using the calibration curve presented in Figure B.1. Error bars indicate SD over three experiments with separately prepared coatings. B) SEM images of the PLGA-DNase I coating after immersion in PBS for i) 1 h (scale bar represents 604 μm) and ii) 120 h (scale bar represents 566 μm). 54

Figure 3.4. Release of DNase I and inulin from PLGA-inulin packaged DNase I. A) Cumulative amounts of DNase I and inulin released (μg) from PLGA-inulin-packaged DNase I immersed in PBS for different periods of time (h) obtained spectrophotometrically, using the calibration curve presented in Figure B.2. Error bars indicate SD over three experiments with separately prepared coatings. B) SEM images of the PLGA-inulin packaged DNase I coating after immersion in PBS during i) 1 h (scale bar represents 133 μm) and ii) 120 h (scale bar represents 156 μm). 54

Figure 3.5. Cumulative amount of DNase I released (μg) from A) PLGA-DNase I and B) PLGA-Inulin-packaged DNase I (after immersion in PBS for 1 h, 4 h and 8 h) coatings with an extra layer of PLGA on the top of the first coating or after increasing the thickness of the PLGA layer. The values were obtained spectrophotometrically using the calibration curve for DNase I (Figure B.1). Error bars indicate SD over three experiments with separately prepared coatings. *Indicate significant differences in the amount of DNase I released when compared to the quantity of DNase I released in the release kinetics (Figure 3.3.A) for the PLGA-DNase I coating or Figure 3.4.A) for the PLGA-Inulin-packaged DNase I coating) at the same time point ($p<0.05$). 55

Figure 3.6. Fluorescence microscopy images of A) *S. aureus* ATCC 12600^{GFP} and B) *S. aureus* Newman D2C^{GFP} adhesion after 1 h in PBS to i) titanium surfaces and the various coatings: ii) PLGA; iii) PLGA-inulin; iv) PLGA-DNase I; v) PLGA-DNase I (1/5); and vi) PLGA-inulin-packaged DNase I. Scale bar denotes 100 μm. 57

Figure 3.7. Number of adhering *S. aureus* ATCC 12600^{GFP} and *S. aureus* Newman D2C^{GFP} (x 10^6 cm^{-2}) after 1 h adhesion in PBS to titanium surfaces and the various coatings. Error bars represent the SD over three experiments with separately grown bacteria. *Indicates significant differences in the numbers of adhering bacteria, within the same strain, compared to titanium and coatings not containing DNase I ($p<0.05$). 57

Figure 3.8. Confocal Laser Scanning Microscopy (CLSM) 3-D images of A) 24 h, B) 72 h and C) 120 h old biofilms of *S. aureus* ATCC 12600^{GFP} on i) titanium surfaces and various coatings: ii) PLGA; iii) PLGA-inulin; iv) PLGA-DNase I; v) PLGA-DNase I (1/5) and vi) PLGA-inulin-packaged DNase I. The base of the biofilm is 375 x 375 μm. 59

Figure 3.9. Confocal Laser Scanning Microscopy (CLSM) 3-D images of A) 24 h, B) 72 h and C) 120 h old biofilms of *S. aureus* Newman D2C^{GFP} on i) titanium surfaces and various coatings: ii) PLGA; iii) PLGA-inulin; iv) PLGA-DNase I; v) PLGA-DNase I (1/5) and vi) PLGA-inulin-packaged DNase I. The base of the biofilm is 375 x 375 μm. 60

Figure 3.10. Average biovolumes (μm^3 μm^{-2}) of A) 24 h, B) 72 h and C) 120 h old biofilms of *S. aureus* ATCC 12600^{GFP} and *S. aureus* Newman D2C^{GFP} grown in TSB on titanium surfaces and on the various coatings. Error bars represent SD over three experiments with separately grown bacteria and different batches of coated samples. *, # and τ indicate significant differences in the biovolumes, within the same strain, compared to titanium, PLGA and PLGA-Inulin, respectively ($p<0.05$) 61

Figure 3.11. In-situ optical coherence tomography (OCT) observations of biofilm formation. 3-D (top) (scale bar represents 1 mm) and side (bottom) (scale bar represents 10 μm) views of A) *S. aureus* ATCC 12600^{GF} and B) *S. aureus* Newman D2C^{GF} biofilms 72 h old obtained using non-fluorescence-based, optical coherence tomography on i) titanium surfaces and various coatings: ii) PLGA; iii) PLGA-inulin; iv) PLGA-DNase I; v) PLGA-DNase I (1/5) and vi) PLGA-inulin-packaged DNase I. 63

Figure 3.12. Metabolic activity of the U-2 OS cells (%) in each coated substrata (material) and on the surrounding substrata (well) compared to the U-2 OS cell in the same conditions but in the presence of titanium (dashed line). Error bars represent SD over three experiments with separately grown U-2 OS cells and different batches of coated samples. 63

Figure 3.13. Confocal Laser Scanning Microscopy (CLSM) images of adhering U-2 OS cells after 24 h of growth on A) each one of the substrata: i) titanium surfaces; ii) PLGA; iii) PLGA-inulin; iv) PLGA-DNase I; v) PLGA-DNase I (1/5); and vi) PLGA-inulin-packaged DNase I and B) the surface of the well surrounding each one of the substrata mentioned. Scale bar denotes 100 μm. 64

Figure 3.14. Number of adhering U-2 OS cells (x 10^4 cm^{-2}) after 24 h of growth on titanium surfaces and the various coatings and the surface of the well surrounding each one of the substrata. Error bars represent SD over three experiments with separately grown U-2 OS cells and different batches of coated samples. 65

Figure 3.15. Confocal Laser Scanning Microscopy (CLSM) overlay images for 24 h old biofilm (9 h of biofilm growth without gentamicin and 15 h of biofilm growth in the presence of 8 μg/ml gentamicin) of A) *S. aureus* ATCC 12600^{GFP} and B) *S. aureus* Newman D2C^{GFP} for i) titanium; ii) PLGA-DNase I; and iii) PLGA-Inulin-packaged DNase I. Living cells fluoresced green and dead cells appeared red. Scale bar represents 100 μm. 66

Figure 3.16. Biovolume live bacteria/biovolume dead bacteria for 24 h old biofilm (9 h of biofilm growth without gentamicin and 15 h of biofilm growth in the presence of 8 μg/ml gentamicin) for titanium, PLGA-DNase I, and PLGA-Inulin-packaged DNase I. 66

Figure 3.17. Confocal Laser Scanning Microscopy (CLSM) overlay images for 48 h old biofilm (24 h of biofilm growth without gentamicin and 24 h of biofilm growth in the presence of 8 μg/ml gentamicin) of A) *S. aureus* ATCC 12600^{GFP} and B) *S. aureus* Newman D2C^{GFP} for i) titanium; ii) PLGA-DNase I; and iii) PLGA-Inulin-packaged DNase I. Living cells fluoresced green and dead cells appeared red. Scale bar represents 100 μm. 67

Figure 3.18. Biovolume live bacteria/biovolume dead bacteria for 48 h old biofilm (24 h of biofilm growth without gentamicin and 24 h of biofilm growth in the presence of 8 μg/ml gentamicin) for titanium, PLGA-DNase I, and PLGA-Inulin-packaged DNase I......................... 67

Chapter 4

Figure 4.1. Schematic illustration of the process that led to the initial burst release of DNase I particles: A) after deposition of the coating on the titanium surface; B) after 1 h immersion in PBS. The same happens for the PLGA-inulin packaged DNase I coating................................ 75

Appendices

Figure A.1. Size distribution (μm) of inulin particles... 117

Figure A.2. Size distribution (μm) of DNase I particles... 118

Figure A.3. Size distribution (μm) of inulin-packaged DNase I (ratio 4:1) particles. 119

Figure B.1. Calibration curve of DNase I (595 nm) solution as a function of their concentration in solution (μg/ml) obtained spectrophotometrically. Error bars indicate SD over three experiments with separately prepared DNase I solutions. 120

Figure B.2. Calibration curve of inulin (630 nm) solution as a function of their concentration in solution (μg/ml) obtained spectrophotometrically. Error bars indicate SD over three experiments with separately prepared inulin solutions. 120

List of tables

Chapter 1

Table 1.1. Variables affecting the bacterial adhesion and colonization onto biomaterial surfaces. Taken from [18] 5

Table 1.2. Incidence and major causative agents of infections associated with commonly used medical devices and implants. Adapted from [4] 7

Table 1.3. Variables important in cell attachment and biofilm formation. Adapted from [25] . 12

Table 1.4. Components of biofilms. Adapted from [25] 15

Table 1.5. Biofilm-disrupting enzymes........ 26

Chapter 3

Table 3.1. Geometric mean diameter (μm) of inulin, DNase I and inulin-DNase I (ratio 4:1) particles and SPAN values of dry powders ± standard deviations (SD) over two measurements calculated automatically by the laser diffraction software. SPAN is the width of distribution based on the x_{10}, x_{50} and x_{90} quantile. 49

Table 3.2. Average roughness (Ra) (μm) and thickness (μm) of the various coatings applied on the titanium surface. Values are expressed as means ± SD over three experiments with separately prepared coatings. *Indicates significant differences in Ra and thickness compared to the titanium surface coated with only PLGA ($p<0.05$) 49

Table 3.3. Degradation time (d) in PBS solution of the various coatings applied on titanium surfaces........ 52

Table 3.4. MIC (μg/ml) and MBC (μg/ml) of gentamicin for the *S. aureus* strains studied 65

Chapter 1

Introduction

1.1. Contextualization and aims

Currently, the average prevalence of healthcare-associated infections (HAI) in Europe is 7.1%, resulting in costs exceeding € 7 billion annually [1]. An interesting aspect is that hospital acquired infections increased, even though the average length of hospitalization has decreased [2]. The major proportion of HAI consist of biomaterials-associated infections (BAI) [3], which is due to the increased use of biomaterials and biomedical devices (as the presence of a foreign body considerably reduces the number of bacteria required to produce an infection [2]), caused by an aging population and improved materials technologies development [4,5]. BAI is the number one cause of failure of biomaterial implants or devices [6,7] and usually results from the presence of biofilms [3].

The microorganisms most frequently associated with BAI are staphylococci [8]. Their capability to adhere to materials and to promote the formation of biofilms is the key feature of their pathogenicity [9]. Therefore, this study involves two *Staphylococcus aureus* strains, ATCC 12600 (common reference strain in biofilm research) and Newman D2C (extremely virulent clinical isolate, known to cause persistent infections) [10].

Biomedical engineers are involved not only in the creation and construction of biomaterials and biomedical devices, aimed to significantly contribute to improving quality of life, but also in the development of strategies to prevent the occurrence of problems during their use. In this context, it is also in part their responsibility to seek ways of preventing BAI. This objective can be achieved by the use of materials, as well as the development of coatings, which are less susceptible to colonization by pathogenic microorganisms [11].

This thesis focusses on the implementation of an enzymatic coating aiming to prevent bacterial adhesion and biofilm formation on titanium surfaces (titanium is a commonly used orthopaedic biomaterial) [12]. More specifically, the ultimate goal is to avoid the occurrence of BAI using biodegradable coatings of poly-(lactic-co-glycolic acid) (PLGA) incorporating deoxyribonuclease (DNase) I subjected to inulin packaging. In order to achieve this goal, the release kinetics of DNase I from both protective PLGA coatings with DNase I and inulin packaged DNase I were determined, the “initial burst” of DNase I released from the PLGA coatings was mitigated or eliminated, an *in vitro* model for the assessment of biofilm formation over prolonged periods of time (120 h) was developed, and finally, it was determined whether the approach developed increases bacterial susceptibility to gentamicin.

1.2. Biomaterial-Associated Infections

1.2.1. Biofilms on medical devices

Embedded in a biopolymeric matrix, infectious biofilms can be categorized into tissue-associated or mucus-embedded cellular aggregates, for instance, in chronic wounds or in the lumen of the bronchi in patients with cystic fibrosis, and surface-related, when attached to the surface of devices such as implants or catheters (Figure 1.1) [13].

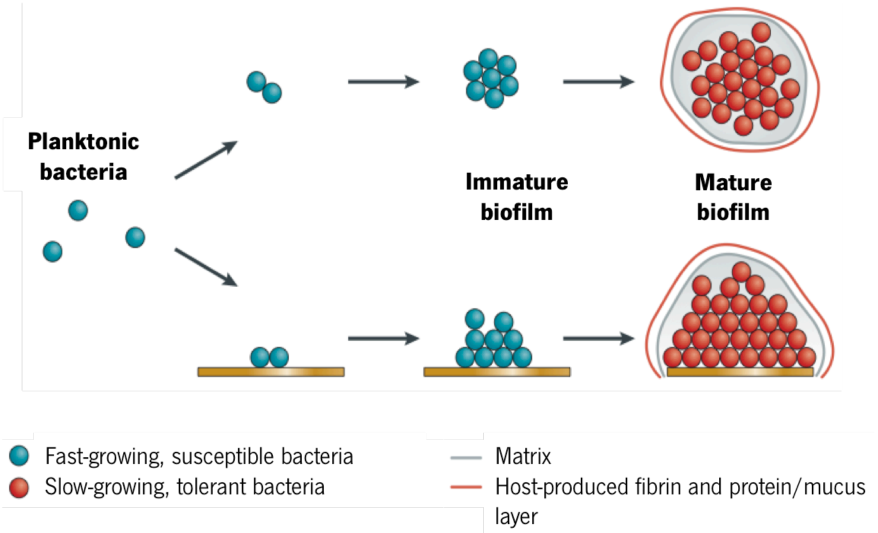
Planktonic bacteria
Immature biofilm
Mature biofilm
Fast-growing, susceptible bacteria
Slow-growing, tolerant bacteria
Matrix
Host-produced fibrin and protein/mucus layer

Figure 1.1. Schematic representation of the bacterial biofilms development from planktonic bacteria. The pathway on the top describes the development of non-surface-attached biofilms (host materials embedded). The pathway below shows the surface-attached biofilms. Adapted from [13]**.**

During the past decades there has been an increase in the use of biomaterials and biomedical devices (both used for restoration or support of human functions) due to an aging population and to improved materials technologies (including biocompatibility, functionality, and durability). However, the application of these devices can lead to BAI, usually resulting from the presence of biofilms [4,5]. Biofilms are abundant in nature [3] and it is estimated that 80% of human infections are related to biofilm formation [4]. The presence of an implanted material alone increases the risk of infection dramatically and it has been demonstrated that 10^4 times fewer bacteria are necessary to infect human volunteers receiving a suture compared to those suture-free [14]. Biofilm formation has been demonstrated for numerous pathogens associated with chronic infections and it is evidently an essential microbial survival strategy [8,15]. In that aspect, biofilm growth can be considered as a virulence factor, even though perhaps not completely correct as by definition, it does represent a bacterial tactic that contributes to its capability to cause an infection [8].

The first step of biofilm formation on an indwelling medical device is the surface conditioning by a layer of organic material (the constitution of this layer depends on the anatomical place of utilization of the medical device, although many of the molecules are proteinaceous and influence bacterial adhesion), which is deposited on the surface as a consequence of the contact between the material and body fluids [16-18]. This step influences all the following phases of biofilm formation (initial attachment, irreversible attachment, early development of biofilm architecture, maturation and dispersion – detailed in section 1.3.2), since the bond formed between the proteinaceous film and the bacteria represents the link to the growing biofilm [7,17,18]. When settled, the developed biofilm on the biomaterial surface shares the fundamental features of all bacterial biofilms [16].

It is of crucial relevance for the first steps of biofilm formation whether microbial contamination of the biomaterial surface occurs in a dry state, by mechanical transfer directly from contaminated objects and by airborne bacteria, or in wet conditions, from the contact with artificial aqueous solutions or physiological fluids. In the first two cases of contamination, the deposition of bacteria can be avoided by adequate sterility of the operating room and rigorous aseptic procedures during manipulation of sterile devices and surgery. On the other hand, the procedures to eradicate the microbial contamination resulting from the contact with liquid carriers (like blood, serum, saliva, eye aqueous humour and urine) are more complex, since in aqueous solutions bacterial adhesion on biomaterial surfaces is affected by numerous variables such as surface morphometry, physico-chemical properties, environmental conditions and the type of pathogen (Table 1.1) [18].

Table 1.1. Variables affecting the bacterial adhesion and colonization onto biomaterial surfaces. Taken from [18]

Variables controlling bacterial adhesion and colonization	
Surface morphometry	Macroporosity, microporosity, micro-roughness, nano-roughness
Physico-chemical properties	Surface energy, hydrophylicity/superhydrophylicity, hydrophobicity/superhydrophobicity, hydrophobic functional group, polar functional groups, charged functional groups, functional groups with specific activities, degree of hydration
Environmental conditions	Electrolytes, pH, temperature, host proteins/host adhesins, shear rate/fluid viscosity, fluid flow rate
Pathogen	Gram-positive/Gram-negative, genus/species, bacterial shape, surface energy, strain type and specific set of expressed adhesins

1.2.2. Microorganisms commonly associated with medical devices

A diversity of microorganisms has been unambiguously associated with BAI. Various microorganisms, including several species of bacteria and fungi [4], share a common ability to form biofilms and colonize human tissues in the presence of foreign bodies [17]. However, BAI is typically caused by commensal bacteria [19].

The microorganisms that are most frequently associated with orthopaedic medical devices are staphylococci (particularly *Staphylococcus epidermidis* and *S. aureus*), followed by *Pseudomonas aeruginosa* and other environmental bacteria (Figure 1.2) that opportunistically infect an immunologically susceptible host [8]. Other bacterial genera and staphylococcal species are emerging as new pathogens such as *Enterococcus faecalis* (a strong biofilm producer showing many virulence factors and differently resisting antibiotics) and *Staphylococcus lugdunensis* (a producer of mainly proteinaceous biofilms) [18].

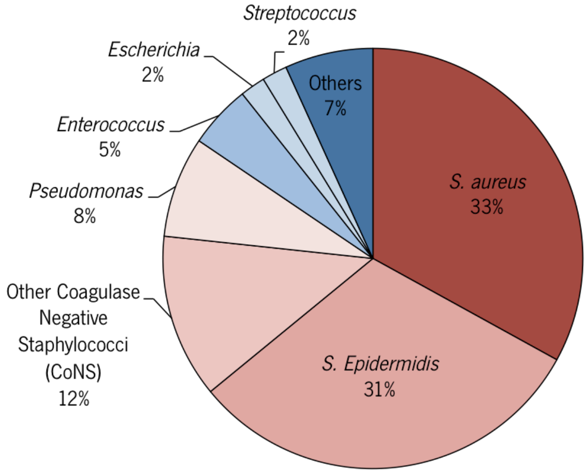

Figure 1.2. Frequency of the main pathogenic species found among orthopaedic clinical isolates of implant-associated infections. Adapted from [20]**.**

Despite the development of several strategies to control BAI, few biomaterials have been designed that effectively reduce the incidence of BAI [6,7]. Implanted medical devices are especially susceptible to microbial biofilm formation, since these surfaces are not well protected by host defences, thus offering sites to which the pathogens have access [17]. Biofilm growth occurs even in permanent, completely internal implants and devices particularly developed to selectively favor host tissue integration over bacterial adhesion, since numerous microorganisms use equivalent adhesive mechanisms as host tissue cells [6].

According to Busscher *et al.* [6], all biomaterial implants and devices can be affected by microbial contamination and clinical infection. Thus, numerous indwelling medical devices are colonized by biofilms, resulting in measurable rates of BAI (Table 1.2) [3].

Table 1.2. Incidence and major causative agents of infections associated with commonly used medical devices and implants. Adapted from [4]

Implants or devices	**Major causative organisms**	**Incidence**
Urinary catheter	*Escherichia coli, candida spp.,* coagulase negative staphylococci (CoNS), *E. faecalis, Proteus mirabilis*	33 %
Central venous catheter	CoNS, *S. aureus, Enterococcus spp., Candida spp., Klebsiella pneumoniae*	2 – 10 %
Peritoneal catheter	*S. aureus, P. aeruginosa, Candida spp.*	3 – 5 %
Mechanical heart valve	CoNS, *S. aureus, Streptococcus spp., Enterococcus spp.*	1 – 4 %
Ventricular assist device	CoNS, *S. aureus, Candida spp., P. aeruginosa*	13 – 80 %
Coronary stents	*S. aureus,* CoNS, *P. aeruginosa, Candida spp.*	< 0.1 %
Cardiac pacemakers	*S. aureus,* CoNS, *Streptococcus spp., Candida spp.*	0.1 % - 20 %
Vascular grafts	*S. aureus, S. epidermidis, Pseudomonas spp., Enterococcus spp., Enterobacter spp.*	1 % – 6 %
Contact lenses	*P. aeruginosa, Serratia marcescens, S. aureus*	0.1 %
Intraocular lenses	*S. epidermidis*	0.1 % – 0.5 %
Fracture fixation devices	CoNS, *S. aureus, Propionibacterium spp., Streptococcus spp., Corynebacterium spp.*	5 %
Hip/knee implants	*S. aureus,* CoNS, *Streptococcus spp., Enterobacteriaceae*	0.5 % – 4 %
Dental implants	*Streptococcus spp., Actinomyces spp., Porphyromonas spp., Prevotella spp.*	5 % – 8 %
Penile implants	CoNS, *Staphylococcus spp., Enterobacter spp., Pseudomonas spp.*	2 % – 5 %
Pelvic organ prolapse mesh	CoNS, *Streptococcus spp., Enterobacter spp., Pseudomonas spp.*	0 – 8 %
Cochlear implants	*S. aureus, P. aeruginosa, Haemophilus influenza, Streptococcus spp.*	1.4 % – 17 %
Sutures	*S. aureus, S. epidermidis,* CoNS, *Peptostreptococcus spp., Bacteroides fragilis, E. coli, Enterococcus spp., P. aeruginosa, Serratia spp.*	Unknown
Breast implants	*S. aureus,* CoNS, *Streptococcus, Propionibacterium spp.*	1 % – 2. 5 %
Intrauterine device	*Candida albicans,* CoNS [3]	Unknown
Artificial voice prosthesis	*C. albicans,* CoNS [3]	Unknown

Staphylococci are responsible for an increasing number of infections in joint prostheses, immunosuppressants and catheters [21]. Nowadays, *S. epidermidis* and *S. aureus* together account for about 65% of prosthetic joint infections (PJIs). These two species are the most commonly reported microorganisms both in early and late infections in total knee and hip arthroplasty [22]. It is important to emphasize that, although in the last five decades technical and operational measures to reduce the risk of infection in the use of prosthetic joints have been implemented, the increasing number of joint replacements makes the absolute number of such infections remain significant, representing substantial costs to healthcare systems around the world (Figure 1.3) [23].

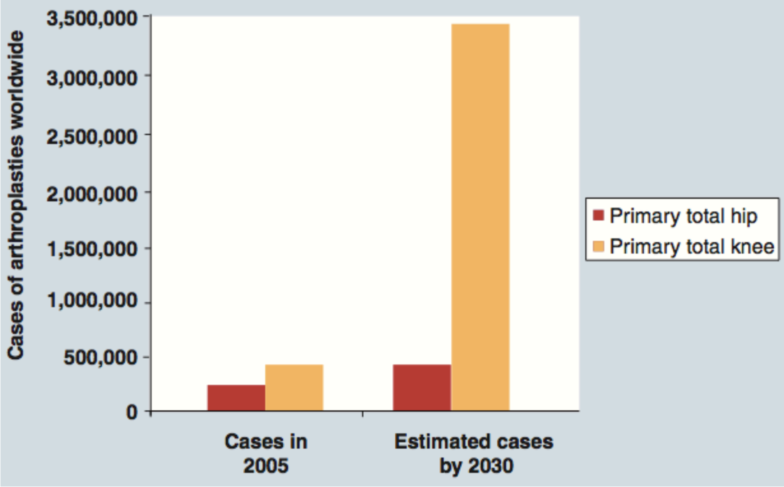

Figure 1.3. Projections of the worldwide increase of arthroplasties from 2005 to 2030. Taken from [24]**.**

It seems impossible to develop biomaterial surfaces capable of preventing bacterial adhesion regardless of the aetiological agent and the physiological environment. Nonetheless, the knowledge of the most prevalent pathogens causing BAI and of their respective characteristics can be studied in order to lower the chance of bacterial colonization on the developed surfaces [18].

Members of the genus *Staphylococcus* belong to the family *Micrococcaceae* and have a Gram-positive cell wall structure. Staphylococci are characterized by round shaped cells and, similarly to all medically important cocci, they are non-flagellate, non-motile and non-spore forming. These cells tend to be arranged in grape-like clusters (microscopically the best known aspect of these bacteria after gram-staining) (Figure 1.4), although some single cells, pairs and short chains are also seen. *Staphylococcus* spp. grow either by anaerobic respiration (preferentially) or by fermentation that produces mostly lactic acid [25-28].

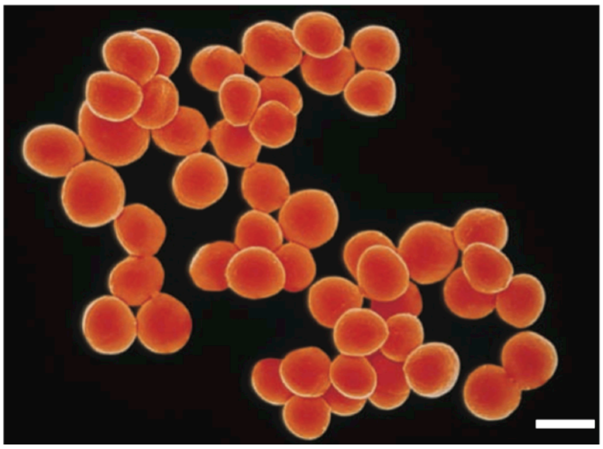

Figure 1.4. A false-color scanning electron micrograph of *S. aureus* illustrating the typical grape-like cluster of cocci. Scale bar represents 1 μm. Adapted from [29]**.**

Staphylococcus spp. can be allocated in two groups based on the ability to produce the enzyme coagulase: coagulase-positive (mainly represented by *S. aureus*) and CoNS (which includes *S. epidermidis*) [26]. CoNS are generally less virulent [30].

The most notable characteristic of the adherent staphylococci colonizing medical implants is the abundant amount of EPS that encloses and protects cells from host defences and antibiotic treatment [8,31]. This defense mechanism makes staphylococcal biofilms that form on tissues or medical devices extremely difficult to eradicate [31]. The biofilm formation of *S. aureus* is a complicated process impacted by multiple factors such as extracellular DNA (eDNA) (the main structural component in the biofilm matrix), surface-associated proteins, cell wall teichoic acids, and an intercellular polysaccharide adhesin (PIA) (also named poly-N-acetyl-glucosamine (PNAG)) (Figure 1.5) [18,31-33]. The glycocalix of the majority of biofilm-producing staphylococcal strains contains PIA [18], produced by the *ica* operon (although not all strains carry this operon) [31,34], and constituted of b-1,6-linked N-acetylglucosamine residues and an anionic portion with a lower content of non-N-acetylated D-glucosaminyl residues [35]. The increasing incidence of methicillin-resistant *S. aureus* (MRSA) has intensified efforts to discover different ways to fight these pathogens [10,31].

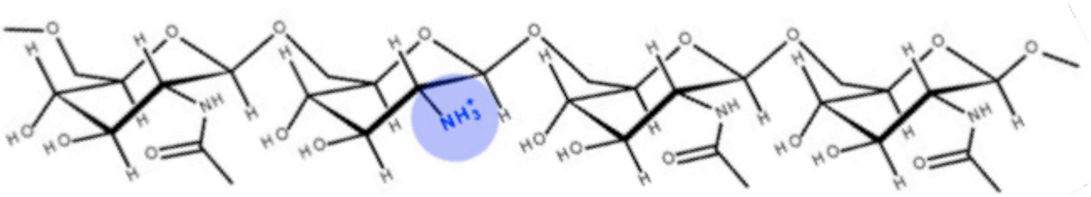

Figure 1.5. The major biofilm exopolysaccharide of staphylococci is intercellular polysaccharide adhesin (PIA) (blue: deacetylation creates free amino groups that at neutral or acid pH give the molecule a cationic character). Adapted from [36]**.**

1.2.3. Risk factors underlying the development of BAI

BAI may result in clinical complications, including death. Furthermore, BAI also increases healthcare costs caused by prolonged hospital stays and revision surgeries [4].

Focusing on the possibility of infections, the implant surgery can be considered a success when no complications for the patient arise, in the short and in the long term, or a failure, in the case of infection. In the latter case, contamination can occur in the perioperative or early postoperative stage, when microorganisms enter the wound or adhere to the implant during surgery, or in the late postoperative stage, when microorganisms infect the patient during hospitalization, or even afterwards (Figure 1.6) [4,6,37,38]. Generally, peri-/early postoperative infections are detected within a short period of time after surgery (but also can cause BAI many years after implantation, since bacteria can stay inactive on an implant surface for several years inside the human body or in adjacent tissue [37,38]), whereas the late postoperative infections represent more serious consequences for the patient and are considerably more difficult to detect and treat, since they derive from the hematogenous spreading of bacteria through blood from infections elsewhere in the human body. In such circumstances, the effective protection is only obtainable by integration of the biomaterial into host tissues and establishment of a normal host immune response at the implant site [6].

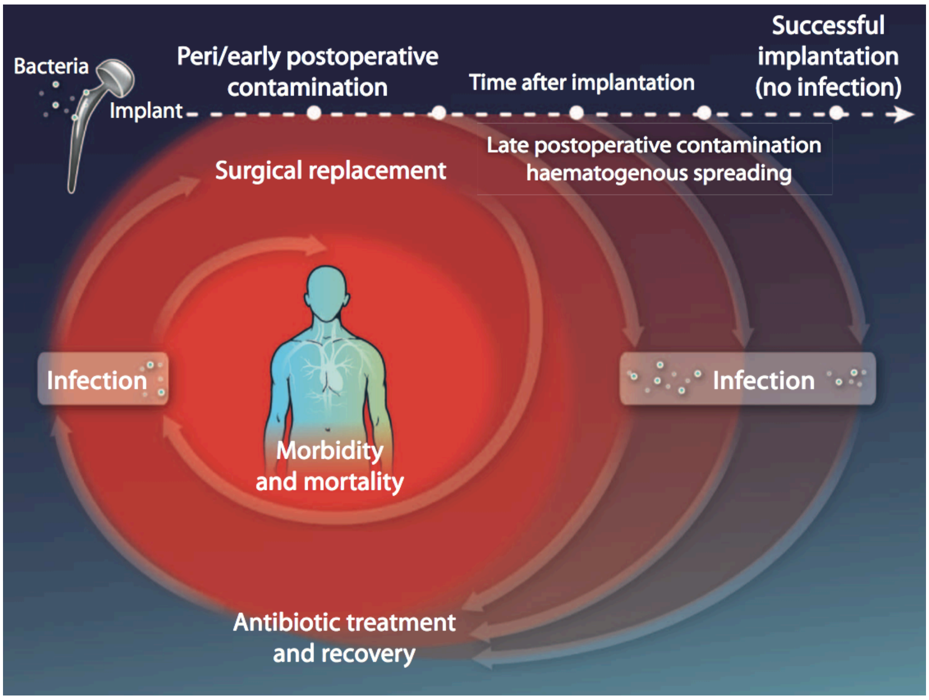
Bacteria
Implant
Peri/early postoperative contamination
Time after implantation
Successful implantation (no infection)
Late postoperative contamination haematogenous spreading
Surgical replacement
Infection
Infection
Morbidity and mortality
Antibiotic treatment and recovery

Figure 1.6. Patient-associated risk factors underlying the development of BAI. Revision surgery patients are at greater risk than primary surgery implant patients. The risk of an implant or device becoming infected hematogenously decreases with time after implant placement due to more extensive host tissue integration. Taken from [6].

Typically, biofilms are found in chronic diseases that resist host immune responses and antibiotic treatment [5,15]. Nonetheless, in BAI, no chronic disease is needed for biofilm formation [5]. Although acute (planktonic) infection generally requires only one single antimicrobial treatment to eliminate microorganisms, chronic (biofilm) infections may need sophisticated diagnostic procedures, long-term antimicrobial therapy and repetitive surgical interventions [19]. Biofilms present several characteristics that can be essential in the development of infections, such as adherent bacteria escaping routine diagnostic methods, infection persistence despite susceptibility of planktonic bacteria to the antimicrobial agent, and host defenses being unable to eradicate microorganisms, i.e. natural healing does not occur [3,5]. When an infection of an indwelling or implanted foreign body is suspected, a general decision has to be addressed; whether to remove the foreign body or to initiate calculated antimicrobial treatment [9].

Several medical interventions are currently used to treat BAI, including long-term antimicrobial strategies and combinations of antibiotics (treatment with antibiotics slows down biofilm progression by eliminating planktonic cells and interfering with biofilm metabolism) [39]. BAI is typically treated with vancomycin (frequently in combination with rifampicin) and in some cases eventually by surgical revision. Unfortunately, these interventions carry the risk of re-infection, often at a higher rate, and the development of antibiotic resistance due to changes in bacterial resistance patterns (vancomycin treatment has a reasonably high failure rate, which may compromise the result of revision surgery) [4,6,19]. Bacteria infecting a secondary implant may arise from peri-implant tissue and usually have been exposed for longer periods of time to antibiotics, possibly creating resistance or altering their adhesiveness for a new implant surface. Accordingly, after the occurrence of infections, the placement of secondary implants and devices require different methodologies to eliminate bacteria, because improper removal increases the chance of recurring infections [6,19].

It is essential to reduce the number of BAI since biofilms cause persistent infections and often the removal of the colonized implant or device is the only successful treatment option [12]. Moreover, future research should also try to develop strategies to prevent infections of secondary implants after BAI of a primary implant, due to the high incidence rate at which these infections occur [19]. According to Zimmerli *et al.*, the prerequisite for correct treatment of BAI is a balanced concept of the optimal surgical and antimicrobial therapy [5].

1.3. Biofilms

1.3.1. Biofilm formation and development

In natural environments, medical and engineered systems [40], bacteria are predominantly organized in structured communities so-called biofilms [41], the primary mode of microbial existence [16]. In fact, bacterial cells prefer to adhere, aggregate, colonize materials and grow into a mature biofilm, rather than staying planktonic [42].

Biofilms are surface-associated complexes constituted by numerous microorganisms (single or multiple species) exhibiting an altered phenotype compared to planktonic cells and are encased in a self-produced extracellular matrix [39,41,43,44]. In nature, biofilms can form a single layer or a 3-Dimensional (3-D) structure and are able to present a high level of organization [45], by working as a cooperative conglomerate [40].

Biofilm formation and development occurs on almost all surfaces [46] and is affected by many parameters related to the properties of the substratum, surrounding fluid and the cell type (Table 1.3) [25,47].

Table 1.3. Variables important in cell attachment and biofilm formation. Adapted from [25]

Properties of substratum	Properties of surrounding fluid	Properties of the cell
Texture or roughness	Flow velocity	Cell surface hydrophobicity
Hydrophobicity	pH	Fimbriae
Conditioning film	Temperature	Flagella
	Cations	Adhesion molecules

There are several reasons why the biofilm lifestyle is advantageous compared to planktonic life. Biofilms act as a barrier that prevents or reduces the contact with antimicrobials agents [47] by causing poor penetration of these agents through the surface film that covers the microbial community and also because of inactivation of the antimicrobials by the extracellular matrix [46]. For this reason, biofilms contribute to the protection of individual bacteria, providing them resistance against antibiotics, biocides or predators [41,43]. Biofilms also facilitate acquisition of nutrients and promote genetic exchange [43]. Inside the biofilm the chemical composition is highly dynamic, encouraging solute gradient formation and nutrient exchange [41], whereas a high local density provides a stable structured environment for genetic exchange events [43].

1.3.2. The life cycle of a biofilm

The identification of novel targets to prevent and control the formation of biofilms (for applications in both industry and medicine) is one of the main motivations for current efforts in trying to clearly understand the life cycle of biofilms [40].

The biofilm life cycle is highly dynamic and consists of predictable transitions (initial attachment, irreversible attachment, early development of biofilm architecture, maturation and dispersion) from single cells to complex microcolonies, the basic organizational units of a biofilm (Figure 1.7) [39,40,47].

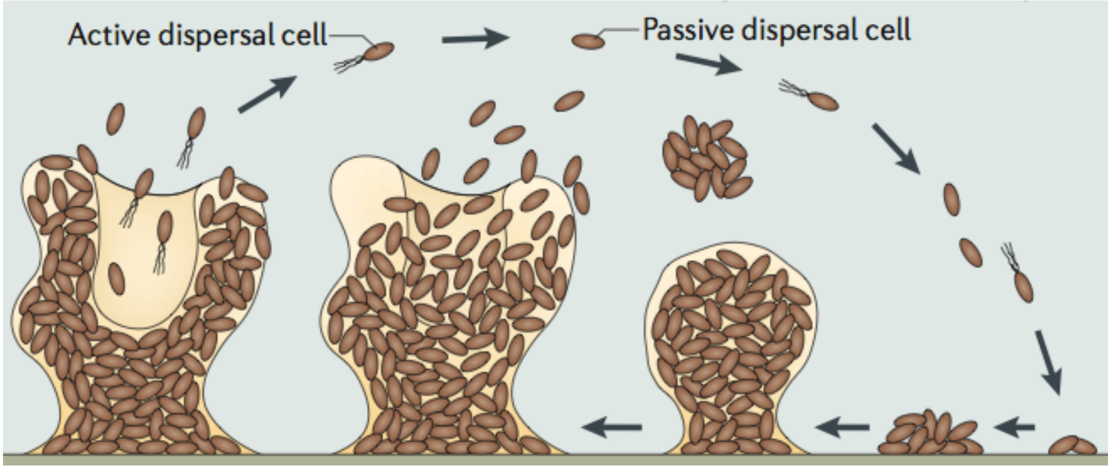

Figure 1.7. Sequential steps of biofilms development. From right to left: initial attachment, irreversible attachment, early development of biofilm architecture, maturation and dispersion. Taken from [40].

In the bacteria's initial attachment, an equilibrium between adhering and suspended cells exists. The adherent cells have a small quantity of extracellular polymeric substances (EPS) and many are able of autonomous movement. In this stage, adhesion is reversible (the bacteria are poorly connected to the surface) as the attached cells are not yet pledged to the differentiation process that leads to biofilm formation [39,47]. As mentioned, frequently, the first step comprises surface conditioning, characterized by the formation or accumulation of an organic layer responsible for neutralizing the excess charge and free energy of the surface, in order to permit adhesion [39,48].

In irreversible attachment, permanent bonding between the bacterial cells and the surface occurs in the presence of EPS [47] which is produced due to stimulation of membrane-bound sensory proteins of the cells. Subsequently, the development of cell-to-cell bridges cements the cells to the surface [39].

The simultaneous accumulation and growth of microorganisms results in microcolony formation. During this phase, recruitment and entrapment of planktonic cells from the adjacent medium takes place as a result of cell-to-cell communication, also referred to as quorum sensing [48]. Microcolonies are advantageous because they provide interspecies exchange and mutual end-product removal [39,47].

Biofilm maturation corresponds to the development into an organized and complex structure (the biofilm shape depends on the stress to which it is exposed and the source of nutrients [48]). At this stage, attached bacteria grow and divide under sessile conditions into mixed complex-enclosed microcolonies dispersed with highly permeable water channels carrying nutrients and waste products [39,47]. These channels form the primitive circulatory system for maintaining homeostasis inside the biofilm [48].

Finally, the dispersion (also known as detachment or dissolution) from the mature biofilm is a process [39] that allows the cells (differentiated and highly motile cells [40]) to revert into their planktonic form. The cells are able to migrate to new surfaces, attach and mature into new 3-D communities, including microcolonies [40]. Several strategies have been suggested regarding how biofilm bacteria disseminate into other areas for further surface colonization [39]. In the case of active dispersal, the production of specific dispersal cells is an active and highly regulated response. On the other hand, in the passive dispersal, the scattering is the result of cell release and erosion from the biofilm [40]. There are several causes of biofilm detachment such as external perturbation, internal biofilm processes and starvation [47,48]. Dispersal becomes especially important when deterioration of the local habitat quality inside the biofilm occurs [41]. In that sense, this phase is considered crucial for the preservation of biofilm sustainability [49]. Ideally, bacteria should adjust their behavior according to the current environmental context, depending on the ability to recognize and reply to environmental signals in a timely manner [41].

Despite the vast amount of information about biofilms, there is still a great lack of detailed knowledge regarding crucial steps in the formation of biofilms, such as biofilm structuring, detachment and the production of persistent cells (a small subpopulation of dormant cells that are multi-drug tolerant and resist to antibiotic treatment [13,50]) [48,49]. This type of cells are partly responsible for antibiotics resistance and, consequently, their understanding is essential for directing further research towards the development of effective strategies against biofilm development [48].

1.3.3. Biofilm structure: Extracellular polymeric substances matrix

1.3.3.1. Definition, composition and spatial distribution

Biofilms are largely comprised of microbial cells and EPS (50% to 90% of the total organic carbon of biofilms), which is present both outside of the cells and in the interior of microbial aggregates [51]. Some commonly found constituents of EPS are water (biofilms are extremely hydrated, with fluid-filled channel running throughout the biofilm), exopolysaccharides [48], proteins, deoxyribonucleic acid (DNA) and ribonucleic acid (RNA) (Table 1.4) [25].

Table 1.4. Components of biofilms. Adapted from [25]

Component	Percentage of matrix
Water	> 97 %
Microbial cells	2 % - 5 % (many species)
Exopolysaccharides	1 % - 2 %
Proteins	< 1% - 2 %
DNA and RNA	< 1 % - 2 %

There is no biofilm without an EPS matrix, [32] which usually consists of a complex mixture of exopolysaccharides, proteins, eDNA, amyloid fibres, bacteriophages and other macromolecules (Figure 1.8). The EPS also incorporates large amounts of water [3,40,41,52]. The nature of EPS depends on the growth conditions, medium and substrates [34]. EPS is essentially the result of high-molecular-weight secretions from microorganisms and the products of cellular lysis and hydrolysis of macromolecules, although some organic matters from wastewater can also be adsorbed onto the EPS matrix [51].

According to several studies, the distribution of various EPS components is heterogeneous and depends on the microbial aggregate type, structure and origin [51]. In fact, the EPS of biofilms is generally not uniform but may vary spatially and temporally. Additionally, different organisms produce differing amounts of EPS and those amounts increase with the biofilm aging [3]. The spatial distribution of EPS is usually studied using confocal laser scanning microscopy (CLSM) or fluorescent microscopy (after EPS is stained by fluorescent dyes or lectins) [51].

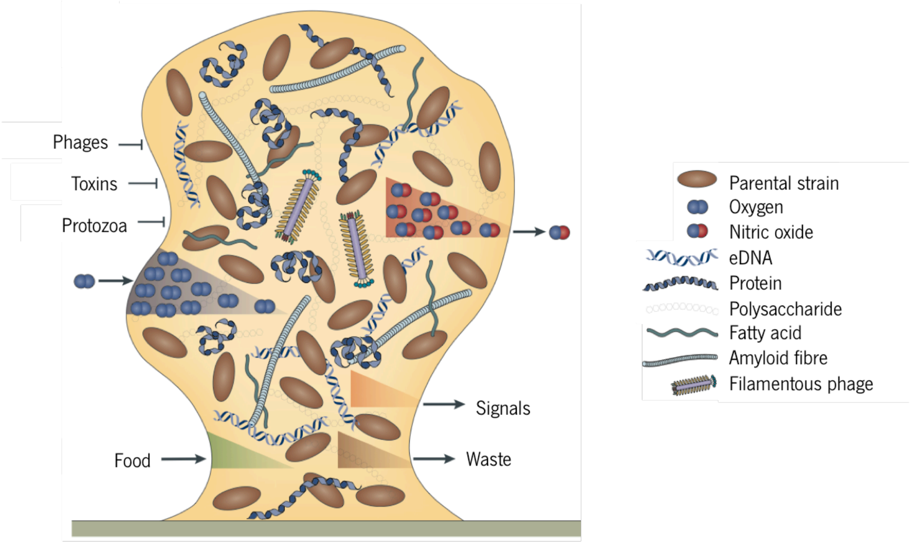

Figure 1.8. The complex structure of bacterial biofilms. Microcolonies in the mature biofilm are characterized by an EPS matrix typically constituted by exopolysaccharides, proteins, eDNA, amyloid fibres, bacteriophages and other macromolecules. Adapted from [40]**.**

1.3.3.2. Functionality

The uniqueness of the matrix constituents, the chemical diversity and adaptability of the EPS matrix are significant factors that assist the different bacterial species and strains to ensure the satisfaction of their own particular needs [53]. Each matrix component has specific functions (not all are exactly known) contributing to the maintenance of the biofilm health [12].

Some of the most important functions of the EPS matrix are related to the stabilization of the biofilm structure, protection of the bacterial community, nutrients gathering and facilitation of the exchange of genetic information. In addition, the EPS matrix also creates gradients within the biofilm, for instance oxygen and nutrients dispersing inwards, and waste products, as well as signals such as nitric oxide diffusing outwards (Figure 1.8) [40,52,54]. Briefly, the EPS matrix offers the scaffold for adhesion to a surface and cohesion between cells [54]. The EPS matrix also works as a shield offering resistance against predators and chemical toxins [3,39,40]. The EPS matrix can impede the access of some components of the host immune system, such as macrophages, which display partial penetration into the matrix and "frustrated phagocytosis". The matrix retains nutrients and several biologically active molecules (such as cell communication signals) in order to immobilize the bacteria. In addition, the EPS matrix may simulate an external digestion system, collecting valuable enzymes that can degrade various matrix constituents, as well as any nutrients or other substrates (after the degradation, the products are close to the cells, facilitating uptake), and also promotes the recycling of lysed cell components [40,54].

1.3.3.3. Extracellular DNA

1.3.3.3.1. Origin

When a cell dies, the genetic coding material or DNA contained within the cell can sometimes survive intact in a protected environment for many years [55]. When the bacterial DNA is not contained within the cell anymore, it is referred to as eDNA. This eDNA is present on the bacterial cell surfaces, becoming an integral part of the matrix and of the biofilm mode of life and it is not different from chromosomal DNA [32,46,55].

The amount and localization of eDNA in biofilms varies considerably among different species and may be very different even between related species [32]. In addition, eDNA concentration in biofilms differs substantially over time during the biofilm development [56]. In some cases, it is the most abundant matrix polymer in the biofilm [54]. Studies have shown that eDNA accumulates in the late exponential growth phase of planktonic batch cultures [56].

The mechanism of eDNA production seems to differ between species [32] and is still under debate [46], but it is believed that eDNA is released due to various mechanisms such as controlled lysis of subpopulations of bacterial cells (considered the main origin of eDNA in the mature biofilm matrix [54]) prompted by prophages, enzymes, lytic proteins and metabolites or by physical and chemical approaches, but also via active release by bacterial membrane vesicles [57]. However, it should be noted that the source of eDNA in a biofilm matrix may even be partly human (as happens for biofilms isolated from the lungs of cystic fibrosis patients) [54].

1.3.3.3.2. Role

Biofilm development is profoundly influenced by the presence of several chemical structures on bacterial cell surfaces [57].

These days, the importance of eDNA in biofilm formation is unquestionable [54], however, initially, eDNA was assumed as a product with no functions besides carrying genetic information [56]. Present at the bacterial cell surface [58], eDNA plays an essential role in several stages of biofilm formation, determines biofilm architecture [46], provides mechanical stability to biofilms, protects bacterial cells in biofilms from physical stress, antibiotics and detergents [34,57,59] and could be a significant source of organic nutrients in the environment whilst disseminating genes amongst different microorganisms [55].

The role of eDNA in biofilm formation has mostly been studied in clinically important strains [56]. The development and stability of *S. aureus* biofilms relies on eDNA secretion. For example, in order to cause dispersion of the biofilm, *S. aureus* produces enzymes that degrade the eDNA [40]. In addition, during biofilm formation, the removal of eDNA or blocking of eDNA production causes a decrease in *S. aureus* adhesion. The removal of eDNA also affects the initial adhesion of *S. epidermidis, S. aureus* and *Streptococcus mutans* to glass. Both biofilm adhesion and biofilm aggregation are negatively affected after eDNA removal in *S. mutans, S. epidermidis, P. aeruginosa and E. coli* [58].

The adhesion of single bacterial cells to a surface consists of two distinct phases, both of them influenced by the presence or absence of eDNA on the cell surface. First, the bacterial cells come into contact with surfaces according to their physico-chemical properties; then, the adhesins anchor the cells more firmly to the surface through specific interactions. In the first phase, the eDNA adsorbs to the surface of single bacterial cells in long loop structures that extend from the surface of the cell to a distance sufficient to bridge the weak repulsive forces that separates the cell from the substratum. Secondly, eDNA on the cell surface mediates acid-base interactions that are favorable for the adhesion of cells to the substratum [54,57].

Most cells are negatively charged, including bacteria. Thus, adsorption of cations such as Ca^{2+} on the cell surface decreases electrostatic repulsion, aiding adhesion and aggregation [60]. eDNA, as a negatively charged molecule (due to the phosphates in the deoxyribose backbone [61]), presents the ability to bind cations via electrostatic interactions (similarly to chelators such as ethylenediamine tetraacetic acid (EDTA) [61,62]). Hence, in the presence of Ca^{2+}, eDNA and cells further adhere and aggregate (Figure 1.9.A) and Figure 1.9.B)). In contrast, removal of the eDNA leads to disruption of the biofilm matrix, since the acid-base interactions (present in the interactions between cells [59]) and ionic-bridging are negatively affected and subsequently bacterial cell-to-cell interactions decrease (Figure 1.9.C) and Figure 1.9.D)) [57].

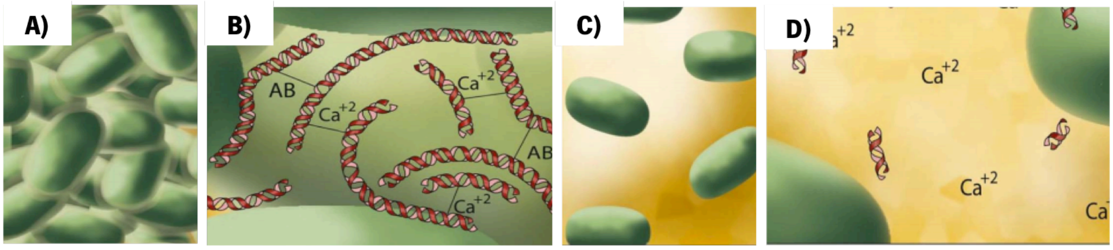

Figure 1.9. Removal of eDNA influences acid-base interactions (named AB) B,D) and Ca^{2+} mediated cationic bridging between bacterial cells and consequently A,C) bacterial aggregation. Adapted from [57].

Adhered eDNA on hydrophobic or low energy surfaces plays an influential role in promoting aggregation by repelling water and attracting adjacent bacteria. In the biofilm matrix, eDNA is the longest molecule [58] and binds with various biopolymers (polysaccharides and proteins – such as Beta toxin in the matrix of *S. aureus* biofilms and integrin host factor (IHF) in the biofilm matrix of numerous of the α-proteobacteria and γ-proteobacteria) and metabolites (phenazines – such as pyocyanin, a molecule produced by *P. aeruginosa*) [42, 57,59], providing structural integrity and stability (Figure 1.10.A), Figure 1.10.B), Figure 1.10.D) and Figure 1.10.F)) [57].

The importance of eDNA for structural stability is typically demonstrated by disintegration of biofilms after DNase treatment [54]. In addition, some studies have also shown that adding DNA to bacterial cultures can stimulate biofilm formation. In some biofilms, eDNA also plays a role in modulating biofilm dispersal while ensuring that the existing biofilm structure remains intact [34,54,59,63].

It is noteworthy that the importance of eDNA to the structural stability (specifically for cellular aggregation) of the biofilm can not necessarily be judged from the relative abundance of eDNA in the EPS matrix. For instance, eDNA is essential for biofilm formation of *S. aureus* and *S. epidermidis*, though present in larger quantities in the biofilms matrix formed by *S. aureus* [54].

eDNA also guides motility in biofilms through unspecific and specific interactions [54]. For instance, an extensive range of Gram negative bacteria presents Type IV pili (like *P. aeruginosa*), that bind to eDNA, playing a role in both bacterial adhesion and eDNA-guided motility (Figure 1.10.C)) [54,59].

Substantial proportions of most bacterial genomes consist of horizontally acquired genes. Horizontal gene transfer is a vital source of new genetic material for bacterial evolution and enhances the biofilms efficiency. In fact, this sharing of genetic material leads to beneficial adaptations such as antibiotic resistance (even though this is not necessarily genetic, it can also be the result of the diversity of metabolic states among the cells in the biofilm) or pathogenicity. Horizontal gene transfer is facilitated by a biofilm lifestyle, which is characterized by the existence of a mixed population at high bacterial density. The lysis of a subpopulation of cells during biofilm formation appears to be a common occurrence and the eDNA liberated by these events is available for horizontal gene transfer to competent cells in the environment [54, 64,65].

According to Schooling *et al.* [66], eDNA interacts with biofilm-derived membrane vesicles (MV) (found within the matrices of Gram negative and mixed biofilms) forming mobile complexes, DNA-MV, able to affect cell adhesion and possibly involved in transfer of genetic information (Figure 1.10.E)).

eDNA plays a direct role in protection against host defense systems, by chelating cationic antimicrobial peptides produced by the immune system [54]. In addition, eDNA also plays an indirect role in antimicrobial resistance by triggering expression of genes leading to elevated antibiotic resistance due to the lack of some divalent cations (such as Mg^{2+}) [54,57].

eDNA also influences the viscoelastic properties of biofilms, increasing the viscosity and, subsequently, the "sticky" character of biofilm matrix/slime. In this sense, the release of eDNA (at sub-inhibitory concentrations, since DNA is toxic at high concentrations [61]) promotes mechanical strength and protection of biofilms from biocides, grazing and shear stress [57,63,65].

Ultimately, eDNA can work both in favor and against infecting bacteria. In fact, too much eDNA can strip Ca^{2+} and Mg^{2+} from the bacterial surface, leading to cell lysis caused by membrane disruption. Besides that, eDNA can alert the mammalian immune system to the existence of invading microorganisms, since the host organism is able to differentiate between self-produced DNA and bacterial DNA [54].

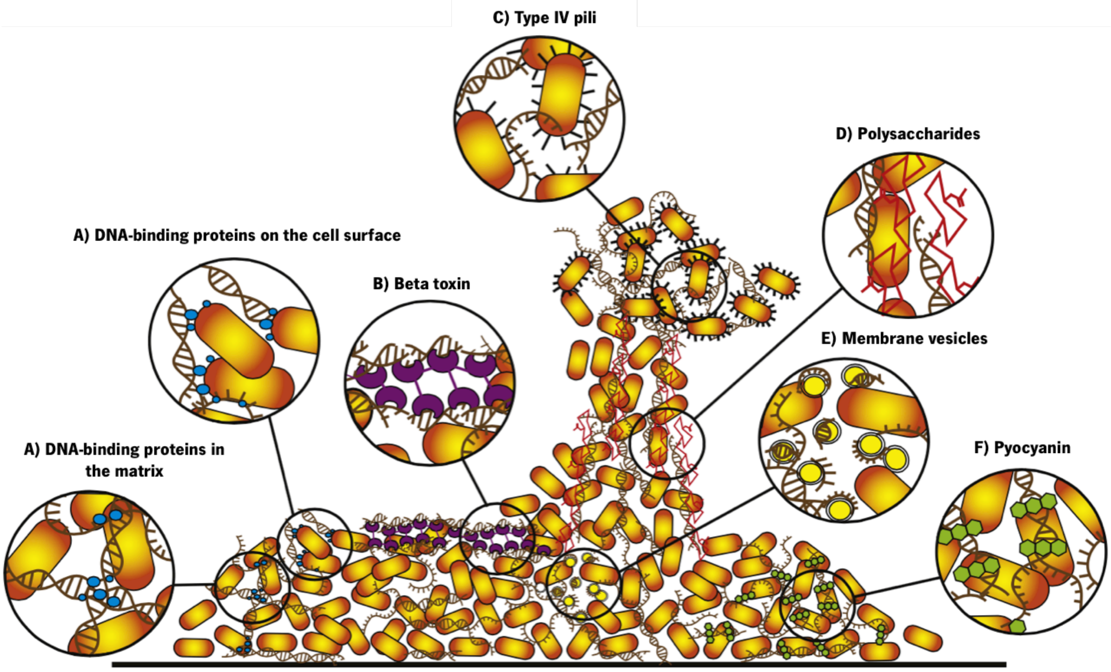
C) Type IV pili
D) Polysaccharides
A) DNA-binding proteins on the cell surface
B) Beta toxin
E) Membrane vesicles
A) DNA-binding proteins in the matrix
F) Pyocyanin

Figure 1.10. Interactions between eDNA and other matrix components. Adapted from [59].

1.4. Anti-biofilm strategies

In contemporary medicine, biofilm-related infections have become an increasingly prevalent problem [67], since most bacterial infections in human are correlated with biofilms [68]. In order to decrease the occurrence of these infections, factors that disrupt biofilm structure, lead to biofilm growth inhibition or biofilm eradication have been the topic of intense attention [67]. These factors may be physical, biological or chemical and influence the biofilm structure via various mechanisms and with different efficiencies [67,69].

Anti-biofilm strategies can be categorized in four main working mechanisms; prevention, which includes the bioengineering approaches that consist of altering the biomaterials used in medical devices to make them resistant to biofilm formation [70]; weakening; disruption; and last; direct killing (Figure 1.11). However, the general consensus is that a combination of these strategies will probably be most efficient [13]. In fact, an ideal anti-biofilm strategy should involve multidisciplinary approaches or combinations thereof, to prevent the initial adhesion step and disintegrate any of the pre-formed biofilm. Realistically, there is no universal anti-biofilm method and some of the selection criteria are costs, site of application, delivery at site, dosing, frequency of application, specificity, contact time, biofilm stage and heterogeneity, residual effect, nature of biofilm (static or dynamic) and safety guidelines (if any) [69].

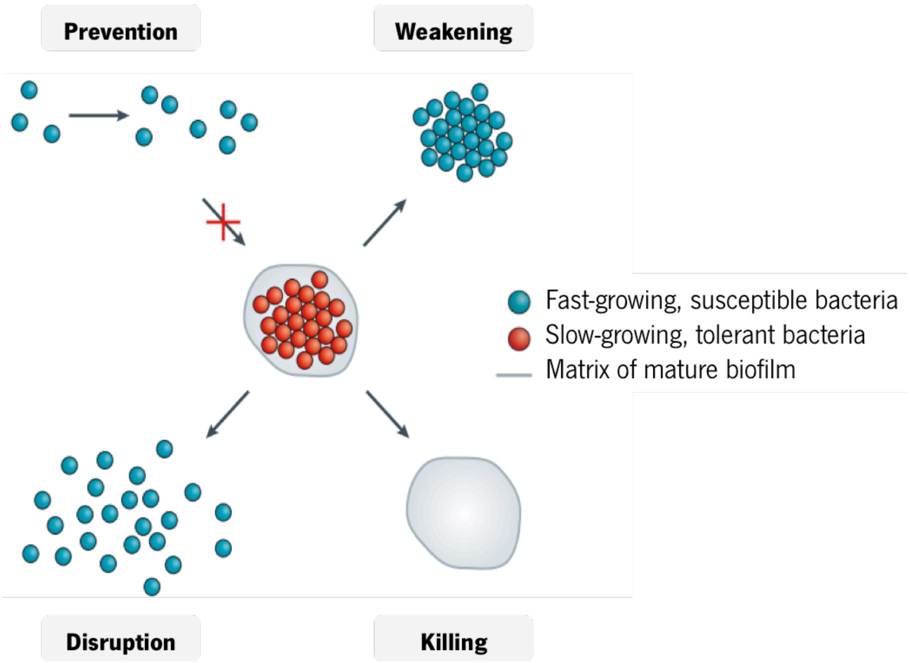
Prevention
Weakening
Fast-growing, susceptible bacteria
Slow-growing, tolerant bacteria
Matrix of mature biofilm
Disruption
Killing

Figure 1.11. Anti-biofilm strategies. Adapted from [13]**.**

1.4.2. Biofilm prevention

The ideal defense against infection is prevention. By preventing initial adhesion, not only host defenses are more efficient in the phagocytosis of bacteria, but also antibiotics show optimal efficacy [13]. However, the presence of a foreign body on the infection site produces a slight inflammation, making it almost impossible to detect the initial bacteria. Thus, when the inflammatory process is identified, the biofilm structure is already mature and difficult to eradicate [13,68]. Accordingly, preventive strategies are only suitable in the prophylactic setting [13].

Nowadays, preventive strategies are already applied in catheters and orthopedic implants with variable success rates [13,39]. The selection of the approach depends on whether the implant is easily accessible in the body or not. In the first situation, surfaces can be treated with ultraviolet (UV) light and then sterilized non-invasively. On the other hand, if surfaces are not reachable, hypothetic targets to prevent biofilm formation include flagella, pili, eDNA, polysaccharides and surface properties involved in the initial attachment of bacterial cells. The prevention of biofilm formation can be achieved using different methods, for example through inhibition of specific regulatory pathways for the production of the aforementioned elements or application of enzymes that degrade the components of EPS matrix or use of neutralizing antibodies addressed at these molecules [13].

The development of anti-infective biomaterials has become a primary strategy to prevent the occurrence of infections in medical devices [18]. Improving biomaterial anti-biofilm properties remains the most effective and promising strategy to prevent the morbidity and mortality associated with biofilm infections. In order to make biomaterial surfaces resistant to biofilm formation it is possible to coat the surface with bactericidal/bacteriostatic substances such as antibiotics, heavy metal silver and furanones [70]. Evidently, the substances added to superficial coatings should be selected to provide a broad activity against the microorganisms commonly found in the target application area [71]. PLGA, for instance, has generated a pronounced interest due to their favourable properties, easy formulation into different devices for carrying a variety of drug classes and also proteins and peptides [72], while it already has been approved by the Food and Drug Administration (FDA) for drug delivery [73]. One of the shortcomings of the bactericidal surfaces is that they could be covered by macromolecules and dead microorganisms, therefore losing their antimicrobial function [13,70].

The number of bacteria that may adhere on biomaterial surfaces is greatly influenced by the physicochemical properties of the biomaterial. So, altering the surface properties of indwelling medical devices is one of the main focuses to prevent or decrease biofilm infections. The surface properties of biomaterials or medical devices can be changed by coating application, such as heparin coatings, trimethylsilane plasma nanocoatings and polymer brush coatings (the most studied ones being made from poly(ethylene oxide) (PEO)), or surface modification such as surface hydrophobicity and texture, to create the desired anti-adhesion characteristics without altering the bulk properties of materials [16,39,70].

In spite of the extensive offer of new materials to reduce the susceptibility of medical devices, the information available on their respective clinical effectiveness is often unclear and recurrently preclinical studies provide the only supporting data. Additionally, existing clinical studies are frequently poorly structured and show questionable or inconsistent results [18].

1.4.3. Biofilm weakening

If biofilm formation cannot be prevented, another method is to defuse bacteria inside the biofilm. It is necessary to highlight that many of these strategies are species-specific or even strain-specific. Furthermore, all efforts (both *in vitro* and *in vivo*) to determine the efficiency of biofilm-weakening compounds have been achieved using drugs acting on immature and developing biofilms [13].

Many bacterial species possess well-characterized virulence factors, such as rhamnolipids for *P. aeruginosa,* alpha-haemolysin for *S. aureus* and β-lactamase for both species. By developing specific antibodies or compounds that bind to the virulence factor, the pathogen might lose its virulence and can be more easily eradicated by the host defence system or antibiotics. This method presents some drawbacks, such as the possibility of stimulating immunopathology since only single virulence factors are targeted (there is a increased inflammation due to an immune-complex-mediated reaction), and it is likely to only be effective in the initial stages of infection, since these factors are lost during adaptation [13].

As iron is a critical factor in the struggle between the pathogen and the host and has been shown to be an important signalling factor in biofilm formation (for *P. aeruginosa*), antimicrobial approaches that target bacterial iron metabolism are being developed. In fact, some of these antimicrobial substances have already been tested and showed good anti-biofilm activity against *P. aeruginosa in vitro* [13].

Among the main mechanisms leading to biofilm maturation (of bacteria or fungi) are quorum sensing (QS) signals [68,74]. QS has been shown to regulate the expression of numerous virulence factors in both Gram-negative (related to the stabilization of biofilms) and Gram-positive bacteria (linked to the destabilization of biofilms). QS inhibitors (QSIs) are distinct from conventional antibiotics since they do not focus on the growth and on the elementary life processes of bacteria, but on the reduction of bacterial virulence. Therefore, possible development of bacterial resistance to QSIs is expected to be lower and these drugs are likely to be efficient against bacteria that are already resistant to conventional antibiotics. Additionally, several QSIs contribute to the increase of bacterial susceptibility to conventional antibiotics. Despite it being demonstrated that QSIs work equivalently well on both planktonic bacteria and bacteria in biofilms, they are typically species-specific [13].

Potential future strategies for weakening biofilms will probably involve the control of gene regulation networks by cyclic diguanosine-5'-monophosphateor (c-di-GMP) or small RNAs (sRNAs) (a class of regulatory biomolecules abundant in many bacterial species) inhibitors, as both signalling pathways act in a synchronized way on the same targets with the purpose of stimulating biofilm formation [13].

Finally, the association of chelators of divalent cations such as citrate or EDTA and biocides has also been proposed, based on their ability to destabilize biofilm matrix [74].

1.4.4. Biofilm disruption

Disrupting the EPS matrix can weaken and disperse biofilms [70]. In fact, the disruption of the biofilm reverses the physical tolerance of the bacteria within the biofilm, forcing the bacterial cells (or part of them) to live in the planktonic state (Figure 1.12) [75].

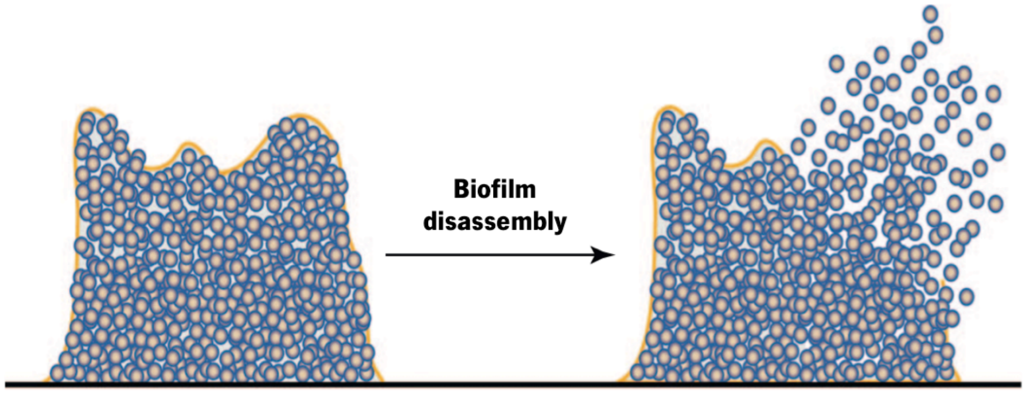

Figure 1.12. Schematic illustration of the biofilm disassembly. Taken from [75]**.**

In the planktonic state, the bacteria are significantly less resistant to antimicrobial substances (most of the currently used drugs have been developed and optimized to kill planktonic microorganisms [74]) and phagocytosis by polymorphonuclear leukocytes [13].

If the surface is not accessible, as in the case of implants, biofilm disruption by ultrasound treatment is one of the possibilities being studied. However, there are some disadvantages in such approaches, namely that biofilm disruption can lead to spreading of the infection (hence the important of antibiotic prophylaxis), and the ultraviolet light or ultrasound waves are absorbed by the host tissue mitigating the effect of these strategies and may have a destructive effect on host tissues [13].

Another method to encourage biofilm dispersal is by decreasing the c-di-GMP levels [13]. This molecule is responsible for the transformation from the motile to the sessile state of microbial cells towards the establishment of biofilms [68]. In this sense, diminishing c-di-GMP levels (controlling c-di-GMP signalling pathways in bacteria) offers a new alternative to clinically manage biofilm formation and dispersal [13,68].

Direct dispersal of biofilms can also be accomplished by decreasing the adhesiveness of bacteria. Elements that cause disruption of the exopolysaccharide of bacterial biofilms (such as the alginate oligomer (oligoG) that binds to a bacterial surface, inducing microbial aggregation, decreasing microbial motility and swarming, and consequently affecting biofilm disruption [76]) are good possibilities [13,74].

Lastly, it is important to emphasize that up to this moment, biofilm dispersal strategies (except when disrupting enzymes are applied) have only been tested *in vitro* [13].

1.4.4.1. Biofilm disruption enzymes

Since it has been postulated that the EPS matrix may contribute to the resistance of biofilm cells to antimicrobials, it would follow that targeting the EPS would aid in the design of infection targeting strategies [39]. The biofilm matrix is an excellent target for anti-biofilm treatments, due to the fact that the biofilm matrix is highly exposed to the environment (which is not as much the case for bacterial cells therein) and also because the biofilm structure is intrinsically porous [54]. As bacterial lyses in biofilms is common (Figure 1.13), one possible strategy to disrupt the biofilm structure could be achieved via the degradation of individual biofilm compounds by their own enzymes (potential therapeutic agents) [67,77].

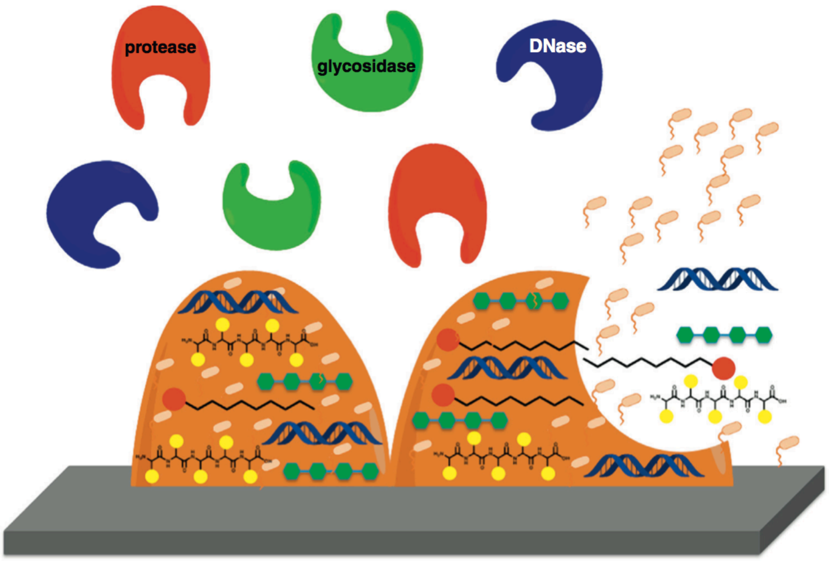

Figure 1.13. Schematic representation of several matrix-degrading enzymes used for biofilm inhibition and dispersal. Taken from [77]**.**

Strategies using enzymatic degradation of matrix components have been identified as efficient ways to disperse biofilms [74]. The mechanism of biofilm dispersal is an intrinsic phenomenon employed by several bacterial species. DNase thermonuclease, glycoside hydrolase dispersin B and alginate lyase are some examples of enzymes produced by *S. aureus*, *Aggregatibacter actinomycetemcomitans* and *P. aeruginosa*, respectively, with the goal of initiating active dispersion of the biofilm, ensuring bacterial survival and disease transmission [77]. In this context, various enzymes have been studied aiming at biofilm disruption (Table 1.5).

Table 1.5. Biofilm-disrupting enzymes

Enzyme	**Target in the biofilm matrix**	**Bacteria in which the treatment is effective**	
		in vitro	***in vivo***
Dispersin B	PNAG [75,78]	*S. aureus* (growing biofilms), *S. epidermidis* [31,77], *E. coli*, *Yersinia pestis* [77], *P. fluorescencens* [13]	*S. aureus* (combined with triclosan) [77]
Alginate lyase	Alginate [77]	*P. aeruginosa* [77]	*P. aeruginosa* (coadministered with amikacin [77] or gentamicin [13])
Lysostaphin	Pentaglycine bridges [75,79]	*S. aureus*, *S. epidermidis*, *MRSA* [67]	MRSA (in the presence of nafcillin) [67]
Serratopeptidase (SPEP)	Ami4b autolysin, internalin B, and ActA [80]	*L. monocytogenes* [80]	*P. aeruginosa* and S. *epidermidis* (combined with ofloxacin), *Listeria monocytogenes* [77]

DNase	eDNA [77]	**NucB:** *Bacillus subtilis, E. coli, Micrococcus luteus* [77] **Nuc:** *S. aureus* [77,81], *H. influenza, Klebsiella pneumonia, P. aeruginosa*, *Acinetobacter baumannii,* [81] *Streptococcus pyogenes* [67]	
DNase 1L2	eDNA	*S. aureus, P. aeruginosa* [67]	
Recombinant human DNase I (rhDNase I)	eDNA [77]	*S. aureus*, *S. epidermidis*, *Streptococcus pneumoniae, P. aeruginosa* [77]	*P. aeruginosa* (rhDNase I) [77]
Protease Esp	Unknown [75]	*S. aureus* [77,82]	*S. aureus* [77]
Proteinase K	Biofilm-associated protein	*S. aureus* [77]	
α - Amylases	α-1,4-glicosidic bond in glycogen, starch, maltooligosaccharides [83]	*S. aureus* [67,81], *V. cholerae, P. aeruginosa* [81]	
Lactonase	Acylated homoserine lactones (AHLs) [84]	*P. aeruginosa* [67]	

However, it is necessary to emphasize that enzyme-based approaches have some limitations mostly regarding their restricted spectrum of action, the effectiveness of the individual mechanisms that is highly dependent on the matrix composition of the strain in question [85] and the risk of immunization against these molecules [74]. In addition, the *in vivo* efficacy of this method is not well established and treating hosts with proteins could cause inflammatory and allergic reactions, which could affect the enzymes therapeutic potential [70].

1.4.4.1.1. eDNA as a target in biofilm treatment

The recognition of the role of eDNA in providing mechanical stability to biofilms (Figure 1.14.A)) makes this molecule an attractive target for new approaches to anti-biofilm treatments [12,55]. As stated before, eDNA is an important component of the EPS matrix [70,77] and the use of nucleases as an anti-biofilm strategy has been explored against various bacterial strains [77]. Interestingly, some bacteria already use this strategy themselves, for example, *Bacillus licheniformis* releases a self-produced extracellular DNase in order to disperse the biofilms of its competitors [54].

DNase I is an endonuclease that digests DNA through the hydrolysis of the phosphodiester bonds [59,86]. The enzyme activity is strictly dependent on Ca^{2+} (stabilizes two disulfide bridges in the DNase I) and is activated by Mg^{2+} or Mn^{2+} ions [86-88].

Degradation of eDNA by DNase I disrupts the EPS matrix of adhering bacteria at the biomaterial-bacteria interface, hence interfering with the first phase of biofilm formation (initial adhesion) and preventing formation of a mature biofilm (Figure 1.14.B)) [12,58]. When a bacterium adheres to a surface, degradation of the eDNA leads to disintegration of the EPS formed during growth of the adhering bacteria, leaving them incapable to evolve into a structurally stable biofilm. Additionally, the presence of DNase I at the bacterial-substratum interface interferes with the aggregation of bacteria and cell-cell interactions at the substratum surface, since eDNA is an essential component in both processes [58]. Therefore, biofilms formed in the presence of DNase exhibit reduced biomass resulting from a reduced number and size of microcolonies within the biofilm, and exhibit decreased antibiotic tolerance [77]. Consequently, the therapeutic potential of biofilm dispersing enzymes, particularly DNase, is of increasing research interest. Not only does DNase treatment have the potential to dissolve bacterial biofilms, but pre-treatment with DNase has been demonstrated to sensitize some biofilms to eradication by topical antiseptics, as well as enhancing the effect of antibiotic treatments by altering the biofilm structure to allow increased penetration of antibiotics. The dispersion of the biofilm by applying DNase could be useful to the prevention of biofouling in several systems [54].

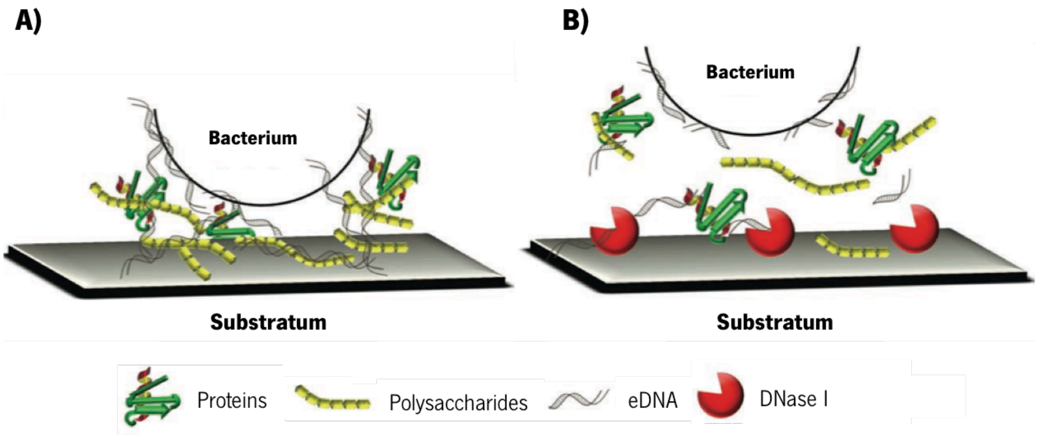

Figure 1.14. Mechanism of biofilm dispersal caused by DNase I. A) eDNA acting as a bridge between a bacterial cell surface and various biopolymers in EPS. B) Disruption of EPS by DNase I coating attacking the eDNA component of the EPS, preventing bacterial adhesion to the substratum surface. Adapted from [58]**.**

1.4.5. Biofilm Killing

The most straightforward anti-biofilm strategy is the direct killing of pathogens. For example, ethanol or hydrochloric acid are used as topical therapy of biofilms on intravenous catheters [13].

Gallium nitrate is approved by the FDA for scanning in medical diagnostics and is an investigational agent that treats biofilm infections by directly killing bacteria, more precisely *P. aeruginosa* (*in vitro* and *in vivo* using animal models). If efficient, this antibacterial agent could be extremely useful in patients with cystic fibrosis, decreasing the density of sputum [13].

Bacteriophages are viruses that are able to infect and replicate within bacteria, killing both antibiotic-sensitive and antibiotic-resistant bacteria (host bacterial cell). Some phages also produce enzymes that degrade the biofilm matrix, inducing the dispersion of the biofilm [13,68].

1.4.6. Combined strategies

Occasionally, for the efficient treatment of biofilm-related infections, a combination of different strategies is necessary.

Essentially all biofilm dispersal approaches will need to have simultaneous antibiotic treatment to eradicate the planktonic bacterial cells that are released after dispersion in order to avoid the spread of infection to other parts of the body [13], the return of these cells to the biomaterials surface and the following development of new biofilms. For instance, in the case of dispersal by bacteriophages, the process could be improved by combining bacteriophages with antibacterial drugs [13,68]. Furthermore, the combination of DNase I with certain antibiotics (such as azithromycin, rifampin, levooxacin, ampicillin and cefotaxime) increases the bacterial susceptibility [67].

Since several studies showed that antibiotic monotherapy is considerably less effective against biofilms infections [68], another possibility to facilitate the effective eradication of biofilms is the combination of high concentrations of antibiotics during a proper period of time in the infection site. Preferably, the used antimicrobial agents should be sensitive, well-penetrating in profounder levels of biofilms and preserve their activity in these locations [13,68]. In addition, the route of antibiotics administration could also be mixed. Coupling of systemic and topical antibiotic treatments can present superior results in patients with biofilm infections suitable for topical treatment of high doses of antibiotics [68].

Mechanisms exploiting external metabolic and chemical stimuli, combined with antibiotics or engineered bacteriophages are being proposed for treating persistent cells [13].

Lastly, weakening of the EPS matrix by phage-encoded depolymerases might also increase the effects of antimicrobial drugs [13].

Chapter 2

Materials and methods

2.1. Particle preparation

2.1.1. Particle formulations and dimension

Inulin-DNase I mixed (with a ratio of 4:1) and single powders of inulin and DNase I were produced by dissolving DNase I (from bovine pancreas, purity ≥ 86%, 400 Kunitz units/mg, Sigma Aldrich, St. Louis, MO, USA) and inulin (with a degree of polymerization of 23, Sensus, Roosendaal, The Netherlands) in water up to a total concentration of 5 mg/ml. The solutions were spray-dried using a B-90 spray-dryer (Büchi Labortechnik AG, Flawil, Switzerland) in combination with a B-296 dehumidifier and a two-fluid nozzle. The inlet air temperature was set at 80 °C, the aspirator at 150 l/min, liquid feed flow at 1 ml/min and atomizing air flow at 600 l_n hr^{-1}.

The particle size distribution of the spray dried trehalose was measured by laser diffraction analysis (HELOS, Sympatec, Clausthal-Zellerfeld, Germany). Measurements were performed using a HELOS laser diffraction sensor with an R1 (0.1/0.18-35 μm) lens, and a RODOS for powder dispersion (Sympatec GmbH, Clausthal-Zellerfeld, Germany) at 3 bar. Laser diffraction data was analyzed with the Fraunhofer method.

2.2. Surface coating

2.2.1. Titanium substrate preparation

Before applying the different PLGA coatings to the titanium surface (1.50 cm × 1.50 cm × 0.10 cm, Goodfellow Cambridge Ltd., Cambridge, United Kingdom), the titanium substrata were sonicated using a 35 kHz ultrasonic bath (Transsonic TP 690-A, Elma®, Germany) for 3 min in 2% RBS35 (Omnilabo International B.V., Breda, The Netherlands). Then, in order to eliminate any traces of the alkaline cleaning agent, titanium plates were rinsed several times with ultrapure water (18.2 MΩ cm^{-1}, Arium®, 611 DI, Sartorius, Göttingen, Germany), followed by methanol (Sigma-Aldrich, purity ≥ 99.93%, Venezuela) and again ultrapure water. After multiple usage of titanium substrata, the procedure described above was preceded by additional cleaning that consisted of sonication in a 35 kHz ultrasonic bath for 3 min in acetone (VWR, BDH, Prolabo®) and polishing the surface manually with a water-based monocrystaline diamond suspension (MetaDi® 1 μm, Buehler, Lake Bluff, USA) for approximately 30 s in a basic lapping with a polishing cloth.

2.2.2. Coating of the titanium substrata

The polymer used to incorporate the different particle formulations was PLGA (PURASORB® PDLG 5002, Corbion, Diemen, The Netherlands) with a copolymer ratio of 50:50 [lactide-to-glycolide], an inherent viscosity of 0.2 and an average molecular weight (M_{wb}) of 17 kDa.

PLGA was dissolved (10% w/v) in acetonitrile (EMPLURA®, purity ≥ 99%, Merck KGaA, Darmstadt, Germany) under continuous agitation at 250 rpm overnight, followed by the addition of the different particle formulations (section 2.1.1.) (1% w/v). After 3 h, 100 µl of the suspension was applied to the titanium substrata, which were then left to dry overnight at room temperature. In the case of titanium substrata coated with only PLGA, the PLGA solution in acetonitrile was directly applied to the surface (Figure 2.1). Coated substrata were stored at room temperature and used within a maximum time period of 5 d.

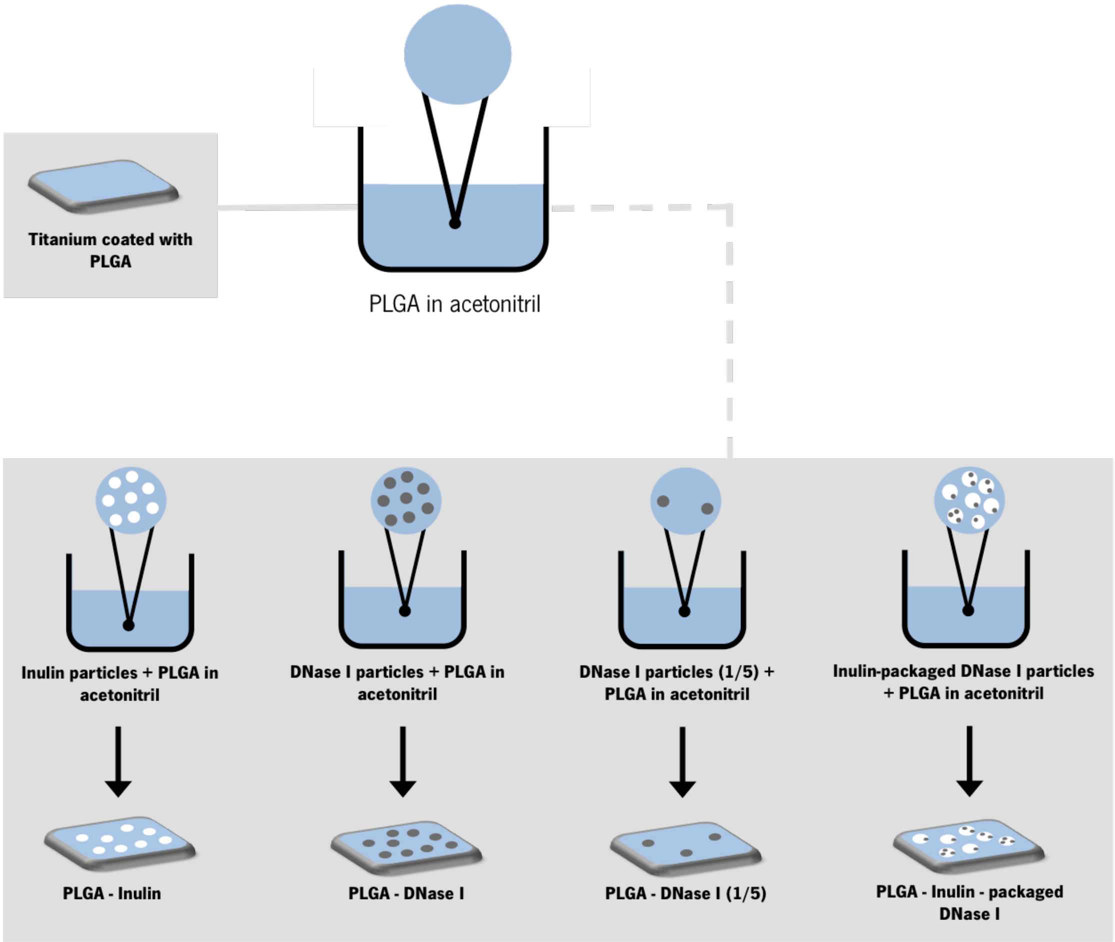
Titanium coated with PLGA
PLGA in acetonitril
Inulin particles + PLGA in acetonitril
DNase I particles + PLGA in acetonitril
DNase I particles (1/5) + PLGA in acetonitril
Inulin-packaged DNase I particles + PLGA in acetonitril
PLGA - Inulin
PLGA - DNase I
PLGA - DNase I (1/5)
PLGA - Inulin - packaged DNase I

Figure 2.1. Schematic representation of the procedure used to coat each titanium substrata (only PLGA, PLGA-DNase I, PLGA-DNase I (1/5) and PLGA-inulin packaged DNase I).

In quantitative terms, each coating consisted of 4.4 mg PLGA/cm^2, containing 0.44 mg of particles/cm^2 (for the PLGA-inulin and PLGA-DNase I coatings) or 0.088 mg of DNase I/cm^2 (for the PLGA-DNase I (1/5) coating). PLGA-inulin packaged DNase I contained 0.352 mg of inulin/cm^2 and the same amount of DNase I as the PLGA-DNase I (1/5) coating.

2.2.3. Coatings roughness and thickness

The roughness of the uncoated titanium surface and each PLGA coatings (section 2.2.2.) was determined using white light interferometry (Proscan 2000, Scantron Industrial Products Ltd., Taunton, Somerset, UK). The samples were placed in a holder and mounted on the profilometer with the use of double-sided sticky tape. The sample was put below the laser to obtain height images in three dimensions of an area of 4 mm^2. The height was measured in this area every 2 µm. The average roughness (Ra), obtained from the acquired images, indicates the average distance of the roughness profile to the centre plane of the profile.

To determine the thickness of the different PLGA coatings (section 2.2.2.), a cut was made in each coating, exposing the underlying titanium surface, and the depth of the cuts was measured (difference in height between the surface of the PLGA coating and the titanium surface).

All measurements were performed in triplicate on random locations of independently prepared coatings.

2.2.4. Coatings degradation time

In order to determine the degradation time of each PLGA coating (section 2.2.2.), samples were placed in 7 ml of a phosphate-buffered saline (PBS) (150 mM NaCl, 5 mM K_2HPO_4, 5 mM KH_2PO_4, pH 7.0) solution in a 6-well polystyrene plate (Cellstar®, Greiner Bio-One, Netherlands), incubated at 37 °C and 60 rpm (New Brunswick Scientific CO., INC. Edison, New Jersey, USA).

Pictures (Canon, lens 28-35mm, Japan) of the various PLGA coatings were taken every 7 d, until no residue of the coating could be macroscopically observed.

2.3. DNase I release kinetics

2.3.1. DNase I calibration curve

A standard curve was constructed using several solutions of DNase I with known concentrations, ranging from 0 μg/ml (reference) to 150 μg/ml, in PBS. The absorbance (Abs) was measured using a Nanodrop® spectrophotometer (ND-1000, NanoDrop Technologies, Inc., Wilmington, DE) at 595 nm, after mixing 100 μl of each solution with 100 μl of Bradford reagent (Sigma Aldrich, USA) and vortexing. Demineralized water was used as blank.

2.3.2. Inulin calibration curve

A calibration curve of the absorbance of inulin solutions with known concentrations was constructed, ranging from 0 μg/ml (reference) to 100 μg/ml inulin, in PBS. To measure the absorbance, 1 ml of each solution was mixed with 2 ml anthrone reagent (Sigma Aldrich) (commonly used to determine carbohydrate concentrations [51,89]), prepared at a concentration of 1 mg/ml in sulfuric acid (H_2SO_4, 95-97%, Merck KGaA, Darmstadt, Germany), and vortexed. After letting the mixture cool down for 30 min, it was transferred to a plastic cuvette and the absorbance at 630 nm was measured (Smart SpecTM 3000, Bio-Rad, Hercules, Ca, USA).

2.3.3. DNase I release kinetics

In order to determine the release kinetics of DNase I from the protective PLGA coating, titanium substrata coated with PLGA-DNase I or PLGA-inulin packaged DNase I, were placed in a 12-well polystyrene plate (Cellstar®, Greiner Bio-One, Netherlands) submersed in 2 ml PBS and incubated at 37 °C and 60 rpm.

At several time points (1 h, 4 h, 8 h, 24 h, 48 h, 72 h, 96 h and 120 h), the PBS was completely removed, stored and then replaced for the same amount of fresh PBS. Afterwards, the amount of released DNase I was measured using spectrophotometry. Briefly, 100 μl PBS was mixed with 100 μl Bradford reagent and the absorbance was measured using a NanoDrop® spectrophotometer at 595 nm, after vortexing each sample. PBS without DNase I was used as a reference and demineralized water was used as blank. Whenever needed, samples were diluted 2 times in PBS and the absorbance was measured again.

The calibration curve (section 2.3.2.) was used to determine the amount of DNase I released by the different samples.

The analysis was based on the results of three experiments using titanium with separately prepared PLGA-DNase I or PLGA-inulin packaged DNase I coatings.

2.3.4. Inulin release kinetics

In the case of the titanium coated with PLGA-inulin packaged DNase I, the amount of inulin released was determined using the anthrone assay. Anthrone reagent was freshly prepared for each measurement at a concentration of 1 mg/ml in sulfuric acid and the absorbance for each sample was measured as described in 2.3.2. Whenever necessary, samples were diluted 2 times in PBS and measured again.

The calibration curve was used to determine the concentration of inulin released by the samples.

2.3.5. Scanning electron microscopy

To study the coating structure and degradation in more detail, images were collected using scanning electron microscopy (SEM) (Phenom Pure Desktop SEM, PhenomWorld, Eindhoven, the Netherlands). Before image collection, the titanium samples coated with PLGA-DNase I or PLGA-inulin packaged DNase I after 1 h and 120 h of immersion in PBS were washed with ultrapure water and after drying, were placed on the top of double-sided sticky carbon tape on metal disks, followed by sputtercoating with approximately 10 nm gold/palladium (SC7620 Mini Sputter Coater, Quorum Technologies Ltd, United Kingdom).

2.3.6. Initial burst release

To control the initial burst release of DNase I two different approaches were used as described below. The DNase I release kinetics for both strategies were determined as previously described (section 2.3.3).

The first approach consisted in applying an extra layer of only PLGA (prepared under the same conditions as described in 2.2.2.) over already coated titanium substrata with PLGA-DNase I (Figure 2.A)) or PLGA-inulin packaged DNase I (Figure 2.B)).

The second approach consisted of increasing the thickness of the PLGA coating. To this extend, coatings of PLGA-DNase I or PLGA-inulin packaged DNase I were applied using 200 µl (instead of 100 µl) of the respective solutions of PLGA, (section 2.2.2) diluted two times (in order to keep the same amount of DNase I or inulin and DNase I, respectively, as used before).

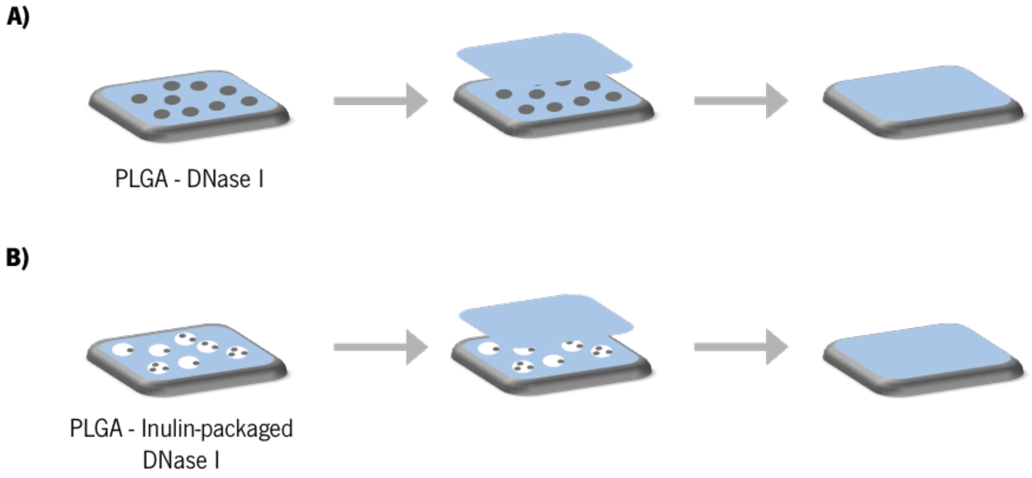

Figure 2.2. Schematic illustration of the procedure used to avoid the initial burst release of DNase I from titanium coated with A) PLGA-DNase I and B) PLGA-inulin packaged DNase I (first approach).

2.4. Bacterial culture and harvesting

2.4.1. Bacterial strains

Two clinical isolates of *S. aureus* were used in this study, *S. aureus* ATCC 12600 and *S. aureus* Newman D2C (also known as *S. aureus* ATCC 25904). Both strains were supplied by the American Type Culture Collection (ATCC, Manassas, USA). The first strain (ATCC 12600) was isolated from pleural fluid, while the second strain (Newman D2C) was obtained in 1952 from a human infection (a case of secondarily infected tubercular osteomyelitis in a men [90]) and has been used in animal models of staphylococcal disease due to its vigorous virulence phenotype [10].

S. aureus ATCC 12600 and *S. aureus* Newman D2C were selected as representatives of the genera staphylococcus for their capacity to develop biofilms with an EPS matrix [53], and more importantly, because they are common colonizers of biomaterials and biomedical device surfaces.

To generate a green fluorescent protein (GFP) expressing *S. aureus* ATCC 12600 and *S. aureus* Newman D2C, the pMV158GFP [91] containing optimized GFP, under the control of the constitutively expressed MalP promotor [92], was introduced into competent bacterial cells by electroporation, as described by Li et al. [93]. The selection of subsequent transformants was performed on tryptone soya broth (TSB) (OXOID, Basingstoke, UK) agar (bactoagar, BD Le Pont de Claix, France) plates containing 10 μg/ml of tetracycline (hydrochloride, purity ≥ 95%, Sigma). *S. aureus* ATCC 12600 and *S. aureus* Newman D2C containing the pMV158GFP (*S. aureus* ATCC 12600^{GFP} and *S. aureus* Newman^{GFP}, respectively) showed constitutive GFP expression, thus allowing an easy quantification of adhesion numbers and biofilm formation without additional staining [12].

Both strains were stored in 7% dimethyl sulfoxide (DMSO) at -80 °C.

2.4.2. Growth conditions

From a frozen stock, staphylococci were cultured overnight aerobically at 37 °C on TSB agar plates containing 10 μg/ml tetracycline in aerobic conditions. For pre-cultures, three single colonies were inoculated in 10 ml TSB containing 10 μg/ml tetracycline and incubated at 37 °C for 24 h (conditions routinely used in the growth of *S. aureus* strains). Main cultures were grown by diluting the pre-cultures in 200 ml of TSB in absence of antibiotics, which were then allowed to grow for 16 h at 37 °C prior to harvesting.

2.4.3. Bacterial harvesting

Bacteria were harvested by centrifugation at 5000 × g for 5 min at 10 °C (Beckman Coulter®, JLA – 16.250, USA) and washed twice in 10 mL PBS, before being resuspended in 10 mL of PBS and sonicated at 30 W (Vibra Cell model 375, Sonics and Materials Inc., Danbury, CT, USA) for 3 × 10 s in order to obtain single cells, i.e. to break existing aggregates. Sonication was performed discontinuously (with 30 s breaks in between) while being cooled in an ice-water bath to avoid excessive heat development.

Bacterial densities were determined using a Bürker-Türk hemocytometer and an Olympus light microscope with × 40 magnification (Olympus Co., Tokyo, Japan). Suspensions were diluted to 3×10^{8} bacteria/ml in PBS for all experiments.

2.5. Initial bacterial adhesion and biofilm growth

2.5.1. Initial bacterial adhesion

For initial adhesion experiments, 5 ml of bacterial suspension supplemented with 1 mM $CaCl_2.2H_2O$ (BOOM, purity ≥ 99%, Germany) and 10 mM $MgCl_2.6H_2O$ (Sigma-Aldrich, purity ≥ 99%) was added to the various substrata in 6-well polystyrene cell suspension culture plates and incubated at 37 °C and 60 rpm under aerobic conditions for 1 h.

After 1 h, samples were rinsed in PBS (in order to remove non-adherent and/or loosely bound bacterial cells on the titanium surface – since loosely bound cells possibly interfere with microscopy imaging), placed into new 6-well plates with 5 ml PBS and analyzed using fluorescence microscopy (Leica DM4000B, Leica Microsystems GmbH, Heidelberg, Germany). Images were taken at three randomly chosen locations on each substrate using a 40 × water immersion objective using filter sets only for GFP.

The total number of adhering bacteria was determined using ImageJ (a Java-based image processing program developed at the National Institutes of Health (NIH)).

All experiments were performed in triplicate with separately grown cultures.

2.5.2. Biofilm growth

Biofilm growth was started after 1 h of initial bacterial adhesion. To this end, samples were removed from bacterial suspensions, non-adhering cells were removed by rinsing with PBS and placed into new 6-well plates containing 5 ml TSB, supplemented with 1 mM $CaCl_2.2H_2O$, 10 mM $MgCl_2.6H_2O$ and 10 μg/ml tetracycline. Next, samples were incubated for 24 h, 72 h or 120 h at 37 °C and 60 rpm under aerobic conditions. Every 24 h, samples were removed and placed into new 6-well plates containing fresh TSB and the same supplements as mentioned above and were then incubated under the same conditions until the desired incubation time was reached.

Biofilms grown on bare titanium and protective PLGA coatings were evaluated using both confocal laser scanning microscopy (CLSM) (Leica DMRXE TCS-SP2; Leica Microsystems Heidelberg GmbH, Heidelberg, Germany), as well as optical coherence tomography (OCT) (Telesto-II 1300, Thorlabs, Newton, NJ, USA). The use of OCT was necessary to rule out possible interference of DNase I with the fluorescence signal [12]. Again, all experiments were performed in triplicate with separately grown cultures.

After the incubation period, biofilm samples were carefully transferred to new 6-well plates containing 5 ml PBS and examined by CLSM and by OCT, in this order.

Using CLSM, optical cross-sections of the biofilms were taken at three random locations of each surface with a 40 × ultra-long-working-distance objective (a water immersion lens). A Matlab (The MathWorks, Natick, MA, USA) based analysis program used for quantification of 3-dimensional (3D) biofilm structures, COMSTAT, was used to calculate the biovolumes of the image stacks [94,95]. 3-D images were constructed employing Icy, an open community platform for bioimage informatics.

The images obtained using OCT were analyzed only qualitatively and processed using Fiji, an image-processing package based on ImageJ.

2.6. U-2 OS adhesion and XTT assay using U-2 OS

2.6.1. U-2 OS cell line

The occurrence of potential adverse effects of the various PLGA coatings on mammalian cells was evaluated using U-2 OS osteoblast-like cells (ATCC number: HTB-96; obtained from LGC standards, Wesel, Germany), an immortalized human cell line derived from osteosarcoma cells.

2.6.2. Growth conditions

U-2 OS cells were routinely cultured in low-glucose Dulbecco's Modified Eagle's medium (DMEM) (Gibco, Life Technologies), supplemented with 10% fetal bovine serum (FBS) and 0.2 mM ascorbic acid-2-phosphate (AA2P) (DMEM+FBS). Cells were maintained at 37 °C in a humidified atmosphere with 5% CO_2 and passaged at 95% confluence using trypsin/ethylenediaminetetraacetic (EDTA) (Gibco, Life Technologies). Harvested cells were counted using a Bürker-Türk haemocytometer and subsequently diluted to a concentration of 4.3×10^4 cells per ml in growth medium and incubated at 37 °C and 5% CO_2 during 24 h in 6-well polystyrene plates with 5 ml of cell suspension. Subsequently, the 2,3-bis(2-methoxy-4-nitro-5-sulfophenyl)-2H-tetrazolium-5-carboxanilide (XTT) assay (AppliChem) and the cell adhesion assay were performed (Figure 2.3).

Note that prior to all cell experiments all substrata were sterilized by placing them in 70 % ethanol for 10 s.

2.6.3. XTT assay

After 24 h incubation at 37 °C and 5% CO_2, titanium samples were placed in a 12-well plate and covered with 2 ml of fresh DMEM+FBS. The medium in the 6-well plate in which the U-2 OS cells were incubated was replaced by 3 ml of new DMEM as well. Then, the XTT assay was performed using the U-2 OS cells above the substrata and the U-2 OS cells adhered to each well of the 6-well plate (cells surrounding the material) according to the procedure from AppliChem [96].

First, a reaction solution was prepared by adding 0.1 ml of activation solution to 5 ml of XTT reagent. Next, 130 μl of the reaction solution was added to each well (6 wells containing the titanium substrata and 6 wells where the titanium substrata were incubated) and incubated at 37 °C and 5% CO_2 for 3 h in the dark. The cell metabolism reduces the XTT tetrazolium salt to XTT formazan by mitochondrial dehydrogenases, thus resulting in a colorimetric change. The amount of water-soluble product generated from XTT is proportional to the number of metabolically active cells and was measured in a 96-microplate reader at 485 nm (Fluostar OPTIMA, BMG Labtech) using 200 μl of each sample in duplicate [97]. In order to measure the reference absorbance (i.e. to measure non-specific readings) the absorbance of the samples was measured again at a wavelength of 690 nm and these values were subtracted from the 485 nm measurement.

The XTT assay was performed three times with separately grown U-2 OS cells and different batches of coated samples.

2.6.4. Cell adhesion assay

After the XTT assay, substrata were prepared for immuno-cytochemical staining by fixation in 3.7% paraformaldehyde (Sigma Chemical Co.) in cytoskeleton stabilization buffer (0.1 M Pipes, 1 mM ethylene glycol tetra acetic acid (EGTA), 4% (w/v) polyethylene glycol 8000, pH 6.9) and subsequent treatment with 0.5% Triton-X100 (Sigma, St. Louis, MO, USA) for 3 min.

The fixated U-2 OS cells were stained using tetramethylrhodamine (TRITC)-Phalloidin (Sigma Chemical Co.) for quantitative analysis. To this end, after rinsing with PBS, substrata were incubated in 1 ml PBS containing 2 μg/ml TRITC-Phalloidin and 4 μg/ml DAPI (4,6-diamidino-2-phenylindole,Sigma Chemical Co.) for 30 min in the dark.

Before being examined using fluorescence microscopy (using a 40 × water immersion objective and filter sets for TRITC-Phalloidin and DAPI), substrata were washed 4 times with PBS to remove any excess of dye. Images (three images on random locations) were taken and the number of adhering cells per cm^2 on each sample was determined by counting the number of blue-stained nuclei.

The cell adhesion assay was performed three times with independently grown U-2 OS cells and different batches of coated samples.

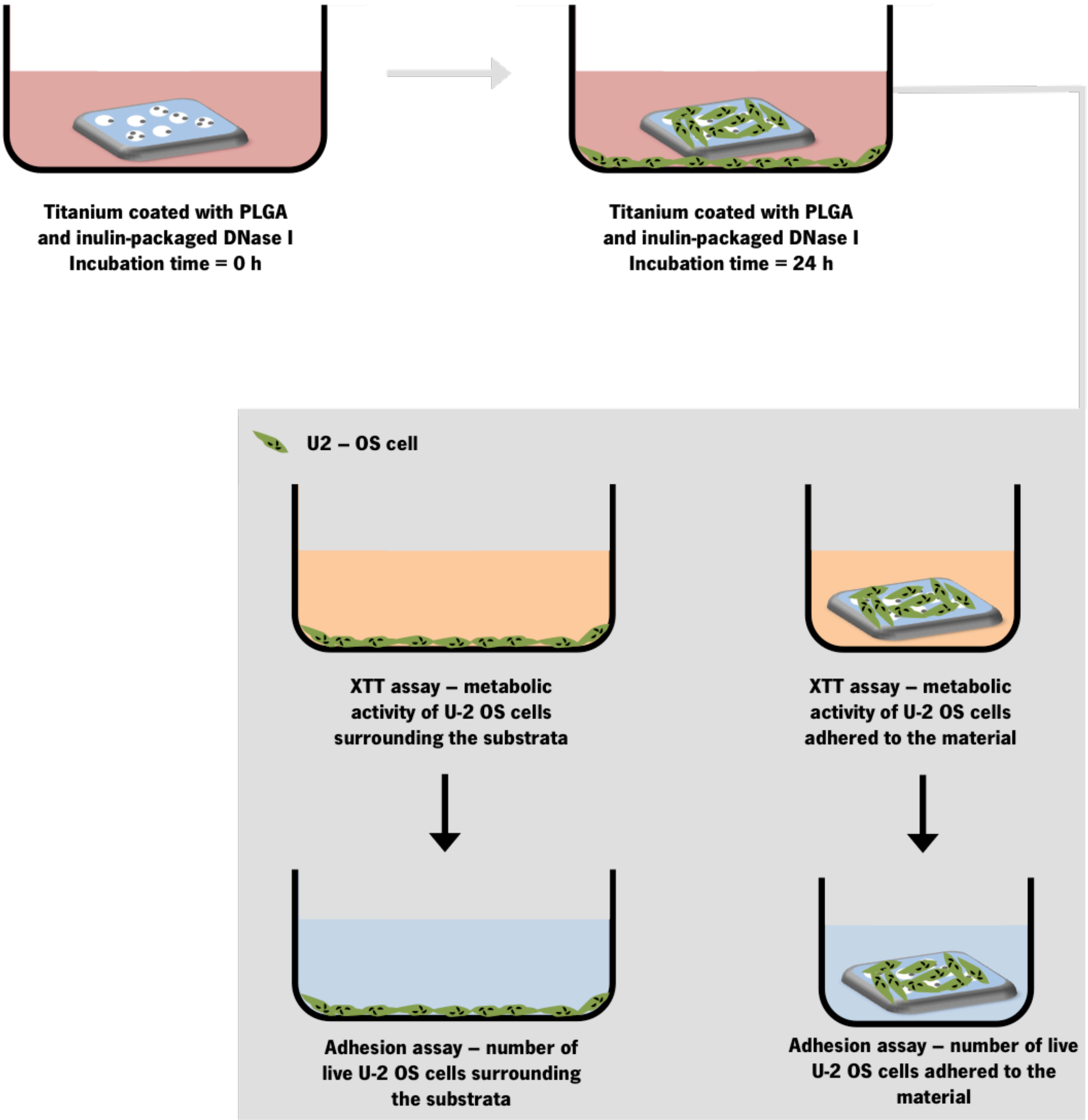
Titanium coated with PLGA
and inulin-packaged DNase I
Incubation time = 0 h
Titanium coated with PLGA
and inulin-packaged DNase I
Incubation time = 24 h
U2 – OS cell
XTT assay – metabolic
activity of U-2 OS cells
surrounding the substrata
XTT assay – metabolic
activity of U-2 OS cells
adhered to the material
Adhesion assay – number of
live U-2 OS cells surrounding
the substrata
Adhesion assay – number of live
U-2 OS cells adhered to the
material

Figure 2.3. Schematic representation of the procedure used to analyse the metabolic activity of U-2 OS cells around the material and cells adhered to the material (XTT assay), as well as the number of live cells in both cases (cell adhesion assay).

2.7. Pilot experiment: effect of gentamicin when combined with the PLGA coatings containing either DNase I or inulin-packaged DNase I

2.7.1. Minimum inhibitory concentration and minimum bactericidal concentration

The minimum inhibitory concentration (MIC) and the minimum bactericidal concentration (MBC) of gentamicin were determined using a modified broth macrodilution method, as described by the Clinical and Laboratory Standards Institute (CLSI) guidelines [98].

Planktonic cells of *S. aureus* ATCC 12600^{GFP} and *S. aureus* Newman D2C^{GFP} were obtained as described before (section 2.4.1., 2.4.2. – pre-cultures without tetracycline – and 2.4.3). The final concentration of bacteria in each broth macrodilution tube was 5×10^5 colony-forming units (CFU)/ml in TSB. Serial two fold dilutions of gentamicin (ranging from 0.125 µg/ml to 64 µg/ml) were used. The MIC was defined as the lowest concentration of gentamicin that inhibits visible growth in a broth culture after 24 h (instead of 16 to 18 h, as recommended by CLSI). Tubes were incubated at 37 °C for 24 h under static conditions. Control tubes contained no antibiotic.

The MBC was described as the lowest concentration of gentamicin that results in $\geq$ 99.9% killing of bacterial cells in the inoculum and was obtained by subculturing 100 µl suspension from each tube, in which the MIC assay showed no apparent growth, onto TSB agar plates. Agar plates were incubated for 24 h and 37 °C and visually inspected.

MIC and MBC values were determined in duplicate using separately grown bacteria.

2.7.2. Biofilm susceptibility to gentamicin

To test whether the approach caused increased antibiotic (in this case, gentamicin) susceptibility, two different strategies were used to treat biofilms grown on PLGA-DNase I and PLGA-inulin packaged DNase I coatings: 24 h of total biofilm growth, of which 9h without gentamicin and 15 h with gentamicin MIC; *versus* 48 h of total biofilm growth, of which 24 h without gentamicin and 24 h in the presence of the gentamicin MIC. Biofilm growth was initiated using the same experimental procedure as described before for both staphylococcal strains (section 2.4. and section 2.5.) (tetracycline was not added to the pre-cultures or when the medium was renewed).

After the incubation period, biofilm formation on the samples (titanium, PLGA-DNase I and PLGA-inulin packaged DNase I) was visualized by CLSM, after staining for 30 min in the dark at room temperature with a LIVE/DEAD BacLight Bacterial Viability Kit (Life Technologies®, GmbH, Darmstadt, Germany). The biovolumes of dead and live cells were determined as described before, using MATLAB.

2.8. Statistics

Statistical analysis was performed using Excel and Statistical Package for the Social Sciences ((SPSS), Inc., Chicago, IL) software version 22.0 for Mac. All experiments, except for the particle size determination by laser diffraction (section 2.2.1), degradation time of the coatings (section 2.2.4.) and experiments involving gentamicin (section 2.6.), were performed in triplicate, the data averaged and the standard deviations calculated. Bacterial adhesion, biofilm formation and mammalian cell adhesion data followed a normal distribution (Shapiro-Wilk test, $p<0.05$). Statistical significance of differences between the several coatings studied was determined using a one-way Analysis of Variance (ANOVA) followed Tukey's HSD post hoc test and a p-value of <0.05 was considered significant.

Chapter 3

Results

3.1. Particle preparation

3.1.1. Particle dimension

Spray-drying of inulin, DNase I or inulin DNase I mixtures, resulted in particles with a mean diameter of approximately 1 μm (Table 3.1 and Appendices – Figure A.3, Figure A.4 and Figure A.5). Inulin appeared to be partly crystallized (as indicated by the high x_{90} value), most likely due to wetting during storage. Nevertheless, particle size was consistent amongst the different constituents.

Table 3.1. Geometric mean diameter (μm) of inulin, DNase I and inulin-DNase I (ratio 4:1) particles and SPAN values of dry powders ± standard deviations (SD) over two measurements calculated automatically by the laser diffraction software. SPAN is the width of distribution based on the x_{10}, x_{50} and x_{90} quantile

Particles	x_{10} (μm)	x_{50} (μm)	x_{90} (μm)	SPAN
Inulin	0.62 ± 0.00	1.21 ± 0.01	106.25 ± 7.67	87.30
DNase I	0.61 ± 0.00	1.11 ± 0.01	2.32 ± 0.06	1.54
Inulin - DNase I	0.62 ± 0.00	1.16 ± 0.01	2.47 ± 0.02	1.59

3.2. Surface coating

3.2.1. Coating roughness and thickness

The surface roughness of uncoated titanium substrata (Figure 3.1.A)) was approximately 0.58 ± 0.17 μm. Thickness of PLGA coatings increased when these contained particles of DNase I, doubling the total thickness of the coating when compared to sole PLGA. PLGA-Inulin and PLGA-DNase I (1/5) coatings presented higher values of Ra (Figure 3.1.B,C,D,E,F), thus indicating a rougher surface (Table 3.2).

Table 3.2. Average roughness (Ra) (μm) and thickness (μm) of the various coatings applied on the titanium surface. Values are expressed as means ± SD over three experiments with separately prepared coatings. *Indicates significant differences in Ra and thickness compared to the titanium surface coated with only PLGA ($p<0.05$)

Coating	Ra (μm)	Thickness (μm)
PLGA	1.88 ± 0.41	5.96 ± 1.29
PLGA - Inulin	5.10 ± 0.80*	7.70 ± 2.50
PLGA - DNase I	4.77 ± 1.87	10.59 ± 3.23*
PLGA - DNase I (1/5)	7.23 ± 3.41*	11.95 ± 4.14*
PLGA - Inulin - packaged DNase I	4.13 ± 1.22	10.11 ± 2.06*

Ai)

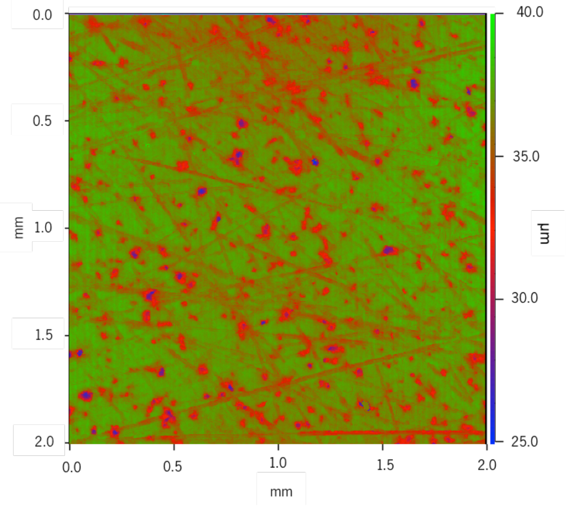

Aii)

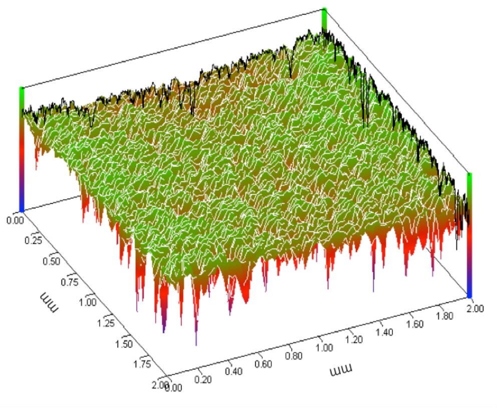

Bi)

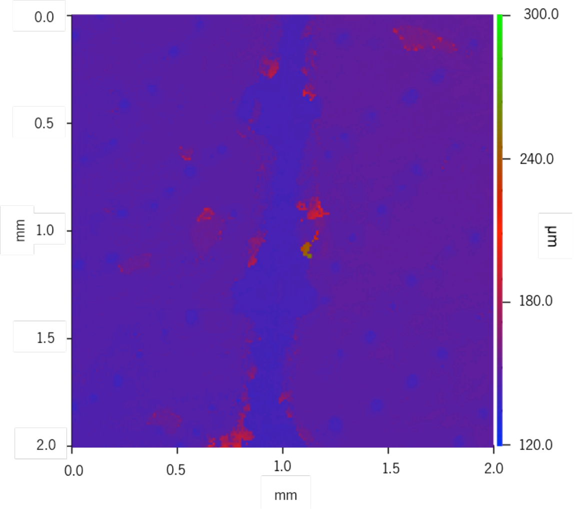

Bii)

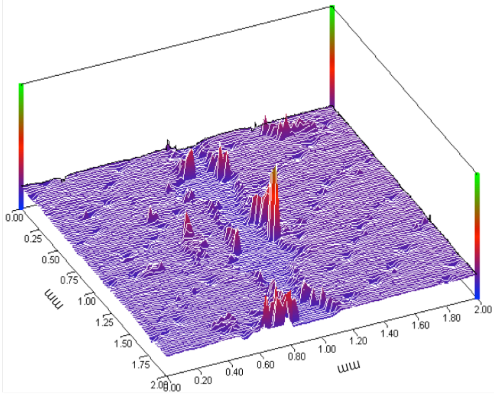

Ci)

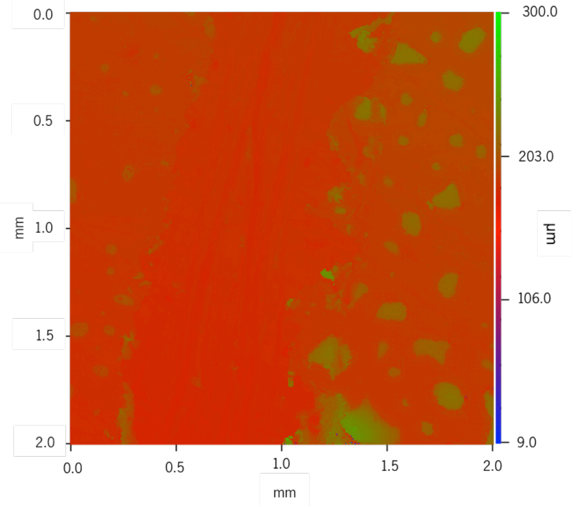

Cii)

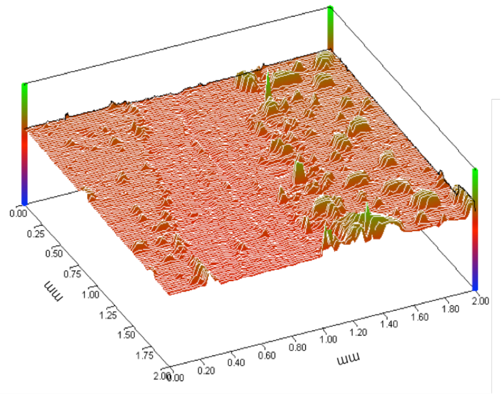

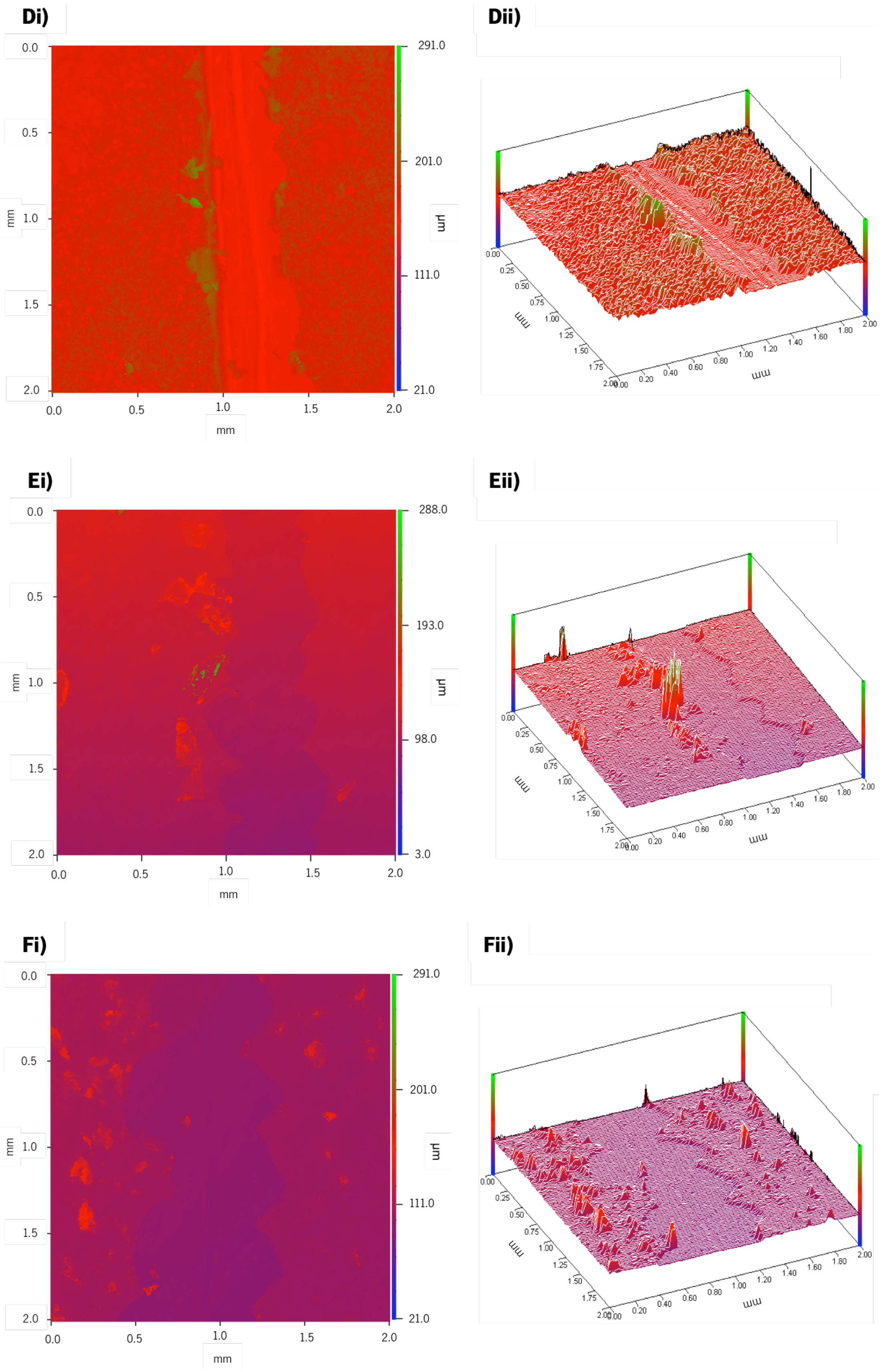

Figure 3.1. Height map generated through white light interferometry in i) 2-Dimensional (2-D) and ii) 3-D for A) uncoated titanium surface; B) PLGA; C) PLGA-Inulin; D) PLGA-DNase I; E) PLGA-DNase (1/5); and F) PLGA-inulin-packaged DNase I. Total area is 2 mm × 2 mm and colours are artificially generated to yield a height map.

3.2.2. Coating degradation

Degradation times of the various coatings in PBS revealed that coatings containing DNase I particles exhibit a longer degradation time when compared to sole PLGA and PLGA-inulin. Coatings without DNase I degraded within 40 d, while coatings containing DNase I were still present after 70 d (Table 3.3 and Figure 3.2).

Table 3.3. Degradation time (d) in PBS solution of the various coatings applied on titanium surfaces

Coating	Degradation time (d)
PLGA	38
PLGA - inulin	40
PLGA - DNase I	77
PLGA - DNase I (1/5)	84
PLGA - inulin packaged DNase I	105

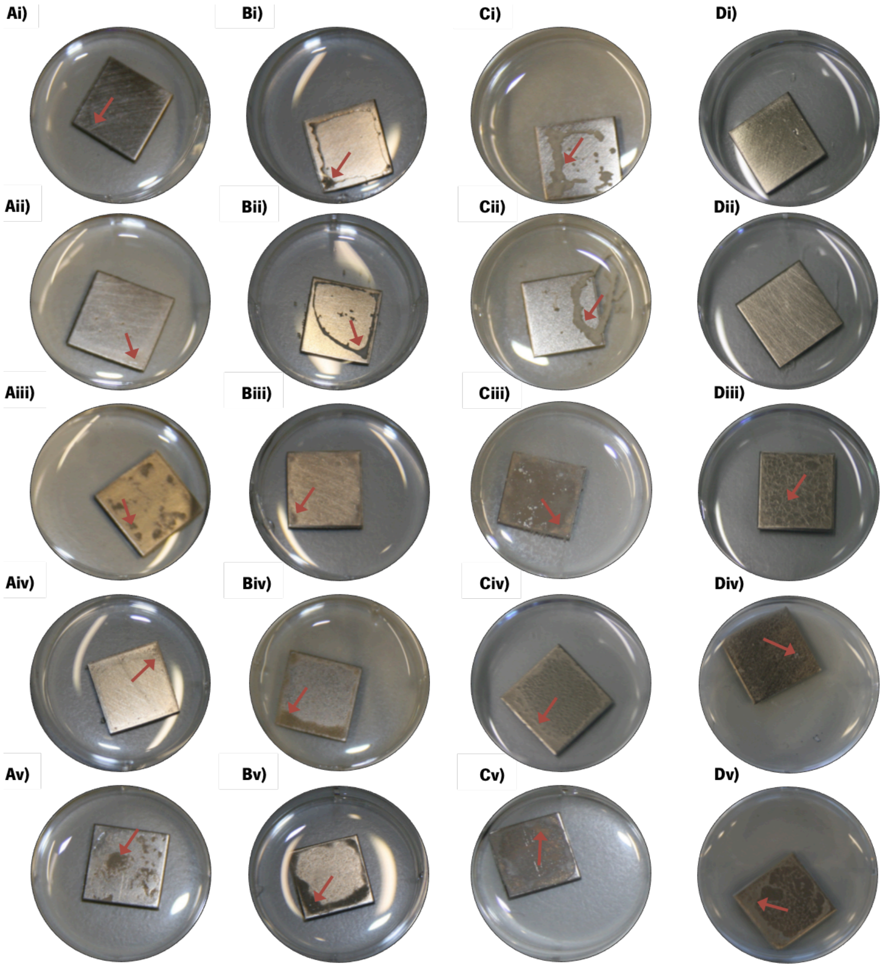

Figure 3.2. Pictures of the different PLGA coatings: i) PLGA; ii) PLGA-inulin; iii) PLGA-DNase I; iv) PLGA-DNase I (1/5); and v) PLGA-inulin packaged DNase I after A) 0 d, B) 14 d, C) 35 d and D) 56 d of immersion on a PBS solution. The red arrows point to some points of the surface where the coating is still present.

3.3. Release kinetics

3.3.1. DNase I and inulin release kinetics

PLGA-protected coatings containing only DNase I particles (PLGA-DNase I) or inulin-packaged DNase I particles showed a burst release of DNase I (Figure 3.3.A)) or DNase I and inulin (Figure 3.4.A)), respectively, within the first h of exposure to PBS, after which the release continued at a slower rate. More accurately, approximately 47% and 40% of the total content of DNase I incorporated in the coatings of PLGA-DNase I (total DNase I contents was 1000 μg) and PLGA-inulin packaged DNase I (total DNase I content was 200 μg) were released in the first 1 h. Note that the ratio of inulin over DNase I released was 4:1 on average, in line with the ratio of inulin over DNase I incorporated during particle preparation (section 2.2.2.). When assuming that particles of DNase I or inulin-packaged DNase I retained in the corresponding PLGA coating do not suffer degradation, after 120 h coatings of PLGA-DNase I and PLGA-inulin packaged DNase I still contain around 22% and 10% respectively, of the initial amount of DNase I incorporated.

Regarding the surface topography of the PLGA-DNase I and PLGA-inulin packaged DNase I coatings after immersion in PBS for 1 h and for 120 h, it was observed that the degradation transformed the coating from relatively smooth after 1 h in PBS to a surface covered with holes after 120 h in PBS. The observed holes in the coatings of PLGA-DNase I (Figure 3.3.B)) and PLGA-inulin packaged DNase I (Figure 3.4.B)) were caused by the release of the DNase I and DNase I-inulin particles, respectively.

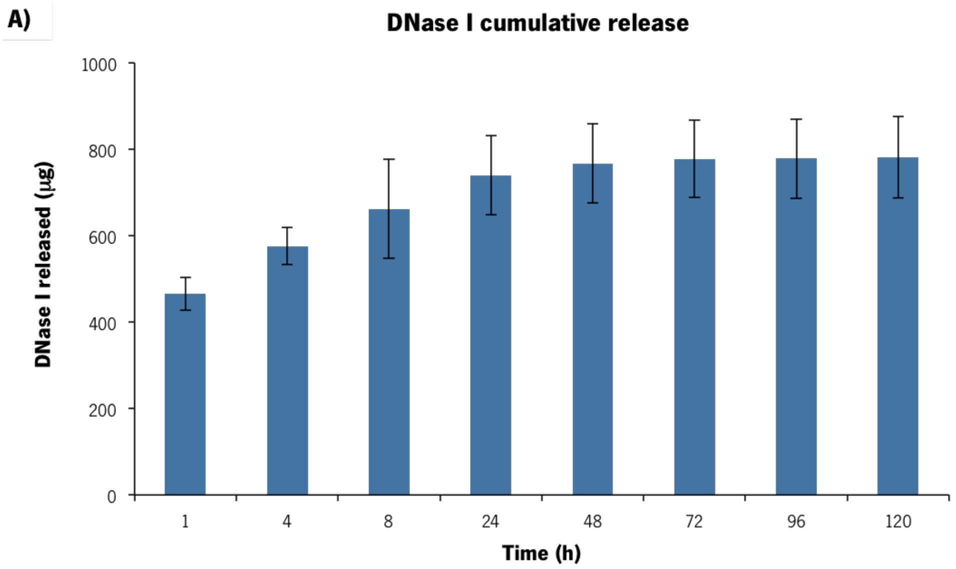

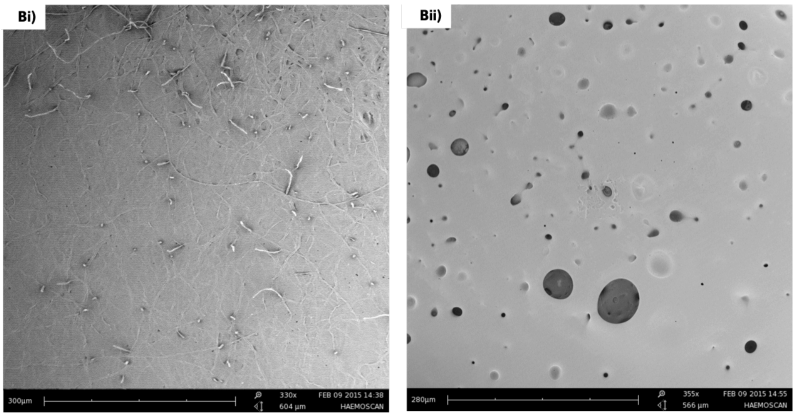

Figure 3.3. Release of DNase I from PLGA-DNase I. A) Cumulative amounts of DNase I released (µg) from PLGA-DNase I immersed in PBS for different periods of time (h) obtained specphotometrically, using the calibration curve presented in Figure B.1. Error bars indicate SD over three experiments with separately prepared coatings. B) SEM images of the PLGA-DNase I coating after immersion in PBS for i) 1 h (scale bar represents 604 µm) and ii) 120 h (scale bar represents 566 µm).

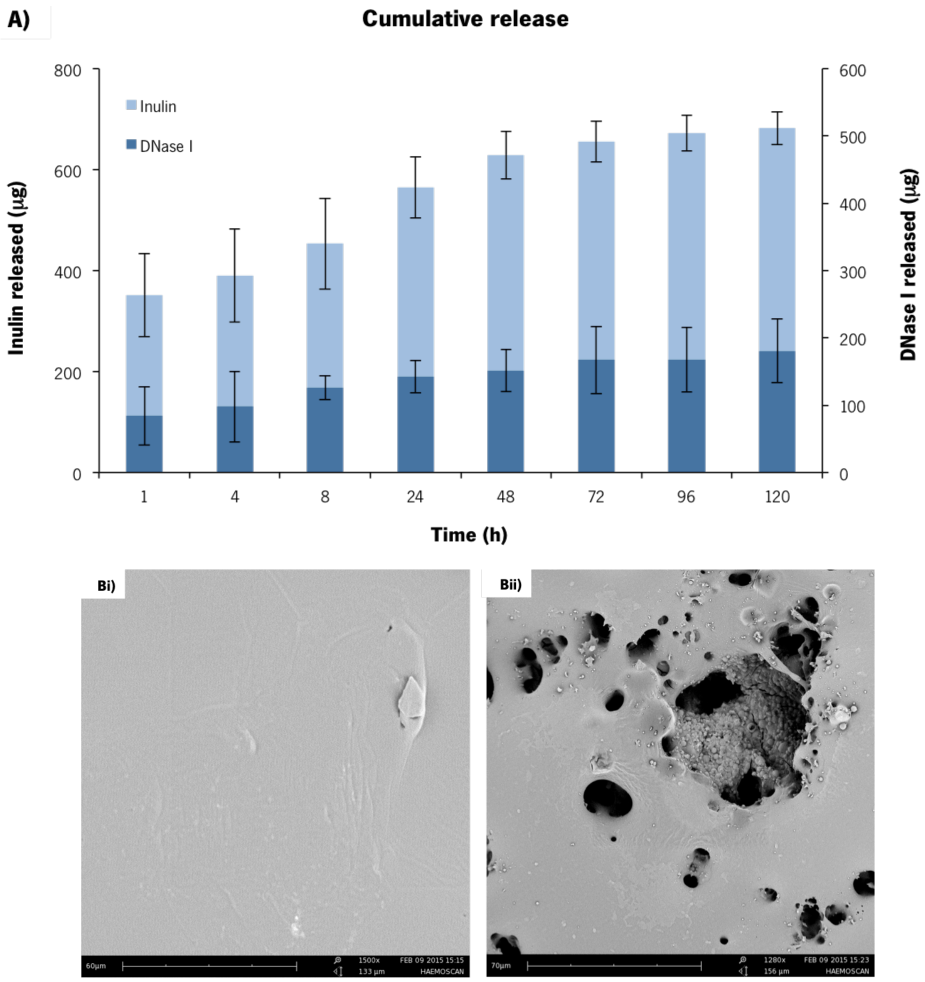

Figure 3.4. Release of DNase I and inulin from PLGA-inulin packaged DNase I. A) Cumulative amounts of DNase I and inulin released (µg) from PLGA-inulin-packaged DNase I immersed in PBS for different periods of time (h) obtained spectrophotometrically, using the calibration curve presented in Figure B.2. Error bars indicate SD over three experiments with separately prepared coatings. B) SEM images of the PLGA-inulin packaged DNase I coating after immersion in PBS during i) 1 h (scale bar represents 133 µm) and ii) 120 h (scale bar represents 156 µm).

3.3.2. Initial burst release

In order to prevent the initial burst release of DNase I, an extra layer of PLGA was added on top of the previously described coatings or, in another approach, the thickness of the PLGA layer for PLGA-DNase I and PLGA-Inulin-packaged DNase I coatings was increased. Both methods were effective in the case of PLGA-DNase I, reducing the initial release of DNase I by 90% and 70% in the first h (Figure 3.5.A). However, for the PLGA-Inulin-packaged DNase I coating, the deposition of an extra PLGA layer decreased the amount of DNase I released within four hours, while increasing the thickness of the coating did not significantly change the release kinetics (Figure 3.5.B).

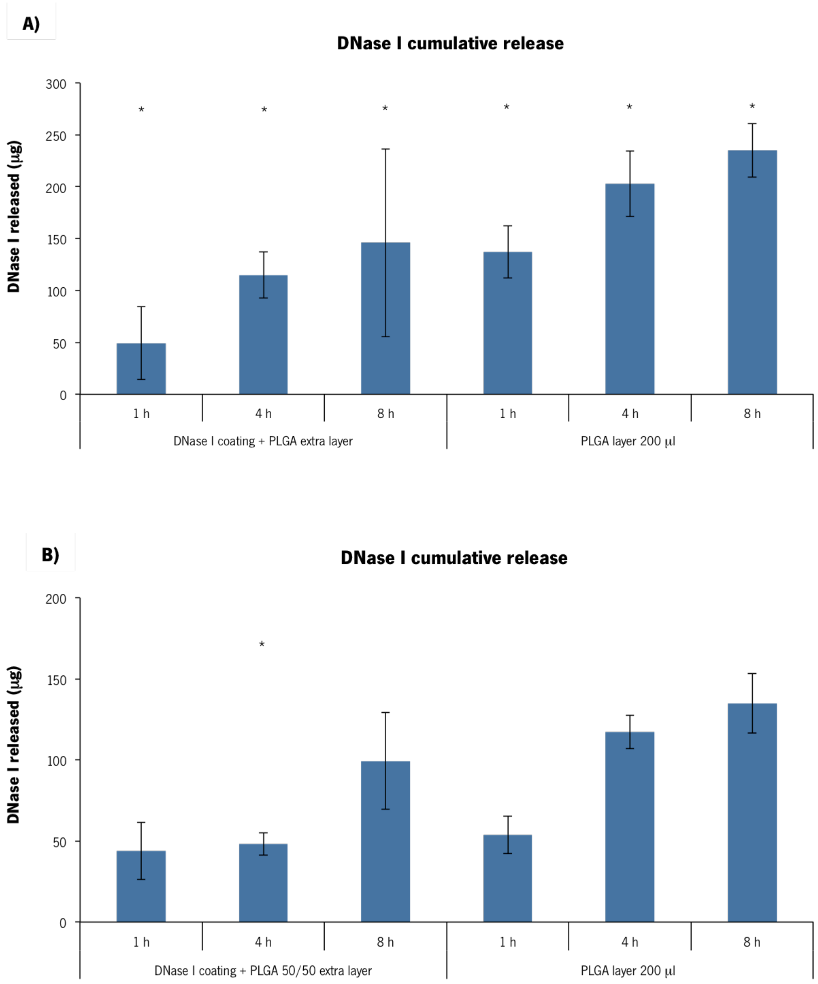

Figure 3.5. Cumulative amount of DNase I released (µg) from A) PLGA-DNase I and B) PLGA-Inulin-packaged DNase I (after immersion in PBS for 1 h, 4 h and 8 h) coatings with an extra layer of PLGA on the top of the first coating or after increasing the thickness of the PLGA layer. The values were obtained spectrophotometrically using the calibration curve for DNase I (Figure B.1). Error bars indicate SD over three experiments with separately prepared coatings. *Indicate significant differences in the amount of DNase I released when compared to the quantity of DNase I released in the release kinetics (Figure 3.3.A) for the PLGA-DNase I coating or Figure 3.4.A) for the PLGA-Inulin-packaged DNase I coating) at the same time point ($p<0.05$).

3.4. Initial bacterial adhesion and biofilm growth

3.4.1. Initial bacterial adhesion

Fluorescence microscopy images indicated that bacterial adhesion was greatly reduced by the release of DNase I from PLGA coatings for both *S. aureus* 12600^{GFP} (Figure 3.6.A)) and *S. aureus* Newman $D2C^{GFP}$ (Figure 3.6.B)).

The number of initially adhering staphylococci on titanium substrata was not affected by applying a coating consisting of only PLGA, or PLGA containing inulin particles. Addition of particles containing DNase I to the PLGA coating significantly reduced staphylococcal adhesion, regardless of whether particles consisted of only DNase I (PLGA-DNase I and PLGA-DNase I (1/5)) or inulin-packaged DNase I (PLGA-inulin packaged DNase I) (Figure 3.7). Note that bacterial adhesion is considered the first step in biofilm formation, therefore it is believed to be one of the most important targets to prevent the development of bacterial biofilms.

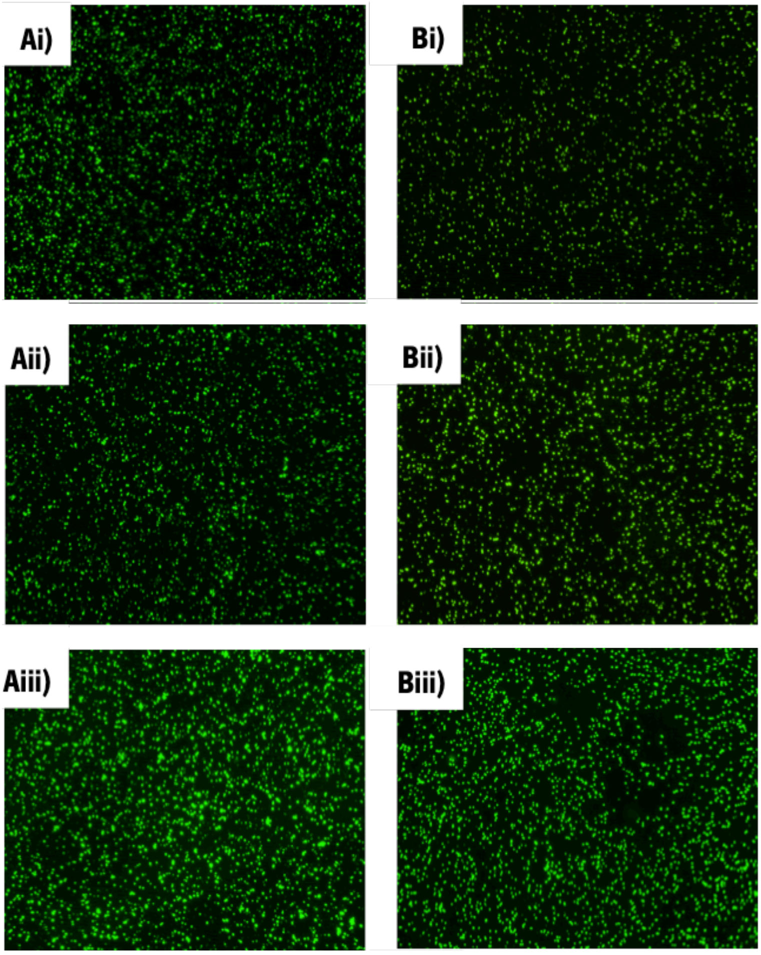

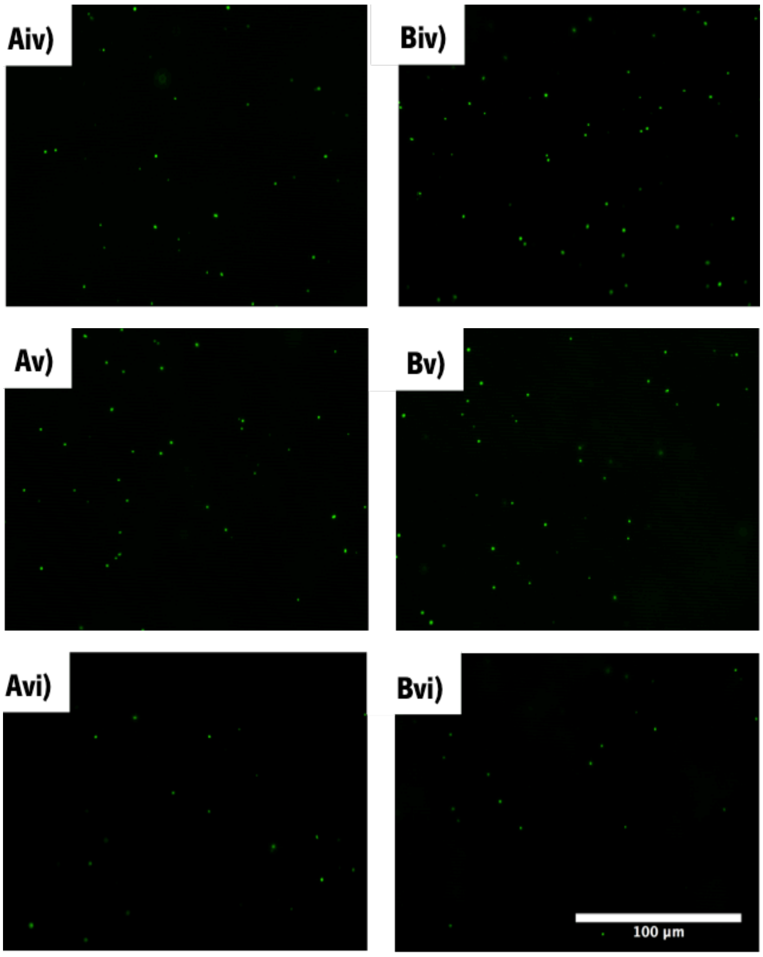

Figure 3.6. Fluorescence microscopy images of A) *S. aureus* ATCC 12600^{GFP} and B) *S. aureus* Newman D2C^{GFP} adhesion after 1 h in PBS to i) titanium surfaces and the various coatings: ii) PLGA; iii) PLGA-inulin; iv) PLGA-DNase I; v) PLGA-DNase I (1/5); and vi) PLGA-inulin-packaged DNase I. Scale bar denotes 100 μm.

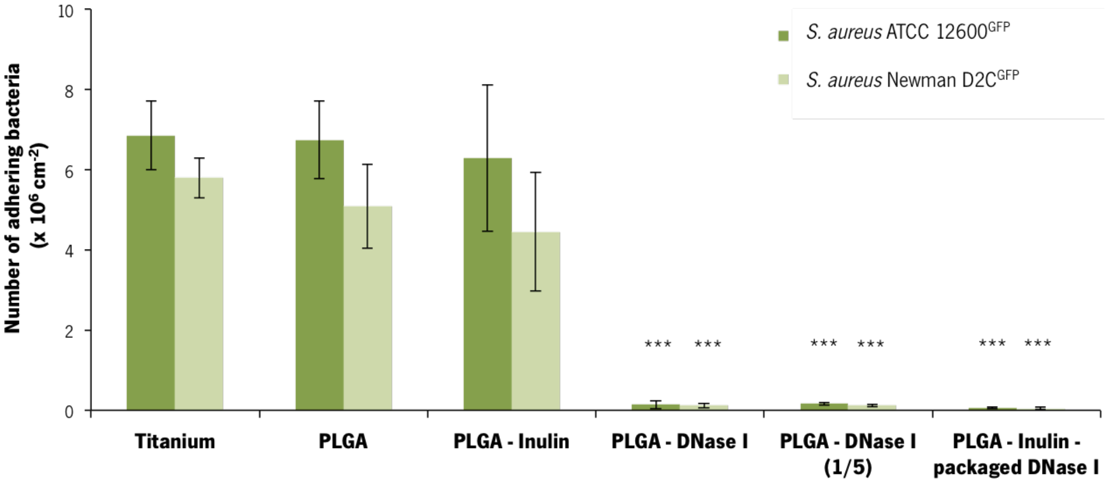

Figure 3.7. Number of adhering *S. aureus* ATCC 12600^{GFP} and *S. aureus* Newman D2C^{GFP} (x 10^6 cm^{-2}) after 1 h adhesion in PBS to titanium surfaces and the various coatings. Error bars represent the SD over three experiments with separately grown bacteria. *Indicates significant differences in the numbers of adhering bacteria, within the same strain, compared to titanium and coatings not containing DNase I ($p<0.05$).

3.4.2. Biofilm growth

CLSM 3-D reconstructed images of staphylococcal biofilms grown for 24 h (Figure 3.8.A) and Figure 3.9.A)), show abundant biofilm formation on bare titanium and coatings without DNase I particles, while the presence of DNase I particles in coatings keeps biofilm formation limited. In fact, the biovolume of both *S. aureus* ATCC 12600^{GFP} and *S. aureus* Newman D2C^{GFP} biofilms significantly decreased for the PLGA-DNase I and PLGA-Inulin packaged DNase I when compared with the biovolume for titanium and PLGA coatings without DNase I particles (Figure 3.10.A)). Increasing the growth time of biofilms to 72 h (Figure 3.8.B), Figure 3.9.B) and Figure 3.10.B)) and 120 h (Figure 3.8.C) and Figure 3.9.C) and Figure 3.10.C)) showed the same abundant biofilm formation on coated surfaces lacking DNase I, whereas coatings containing DNase I and inulin-packaged DNase I remained able to inhibit biofilm formation. However, an increase in biofilm formation over this time periods was observed for coatings containing only one-fifth of the DNase I.

The inulin-packaging of DNase I yielded much stronger reductions in biovolume for both staphylococcus strains, indicating that DNase I activity is better preserved by inulin-packaging than by exclusively protecting it in PLGA. This effect is amplified by the amount of DNase I being five-fold lower in inulin-packaged DNase I coatings, compared to PLGA-DNase I coating, due to the absence of inulin. In fact, as mentioned, the PLGA coating with the same amount of DNase I as the quantity present in the coating of PLGA-inulin packaging DNase I, the PLGA-DNase I (1/5) coating loses effectiveness over time, i.e. there is an increase in the biovolume in both *S. aureus* ATCC 12600^{GFP} and *S. aureus* Newman D2C^{GFP}.

Non-fluorescence-based OCT (Figure 3.11) images of staphylococcal biofilms grown for 72 h confirmed the results obtained by CLSM. Abundant biofilm formation was visible on bare titanium uncoated and coatings with only PLGA, PLGA inulin particles and coatings with a concentration of DNase I particles five times lower than the other coating with only DNase I particles. Biofilm formation is nearly absent on PLGA-DNase I and PLGA-inulin-packaged DNase I coatings.

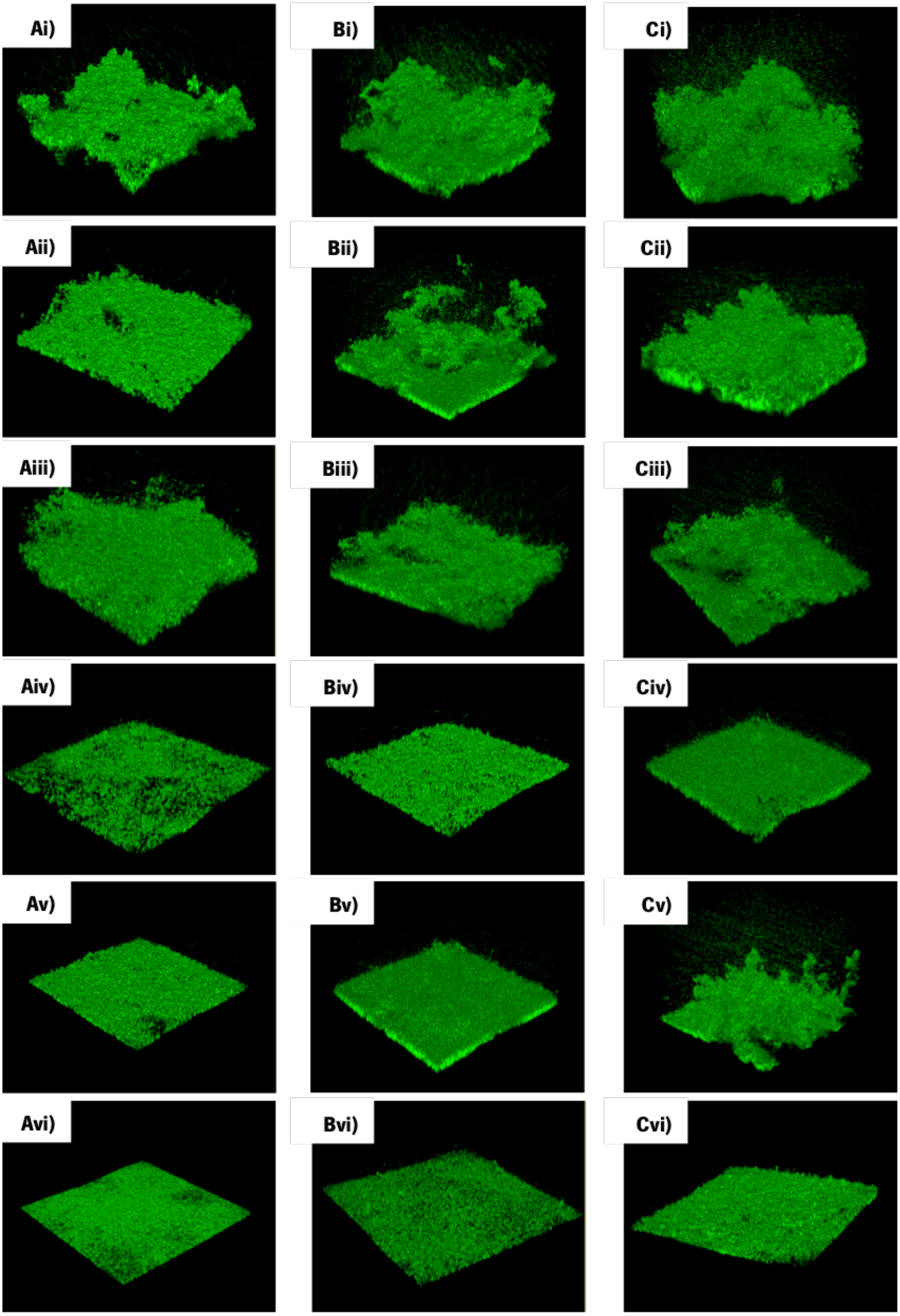
Ai)
Bi)
Ci)
Aii)
Bii)
Cii)
Aiii)
Biii)
Ciii)
Aiv)
Biv)
Civ)
Av)
Bv)
Cv)
Avi)
Bvi)
Cvi)

Figure 3.8. Confocal Laser Scanning Microscopy (CLSM) 3-D images of A) 24 h, B) 72 h and C) 120 h old biofilms of *S. aureus* ATCC 12600^{GFP} on i) titanium surfaces and various coatings: ii) PLGA; iii) PLGA-inulin; iv) PLGA-DNase I; v) PLGA-DNase I (1/5) and vi) PLGA-inulin-packaged DNase I. The base of the biofilm is 375 x 375 µm.

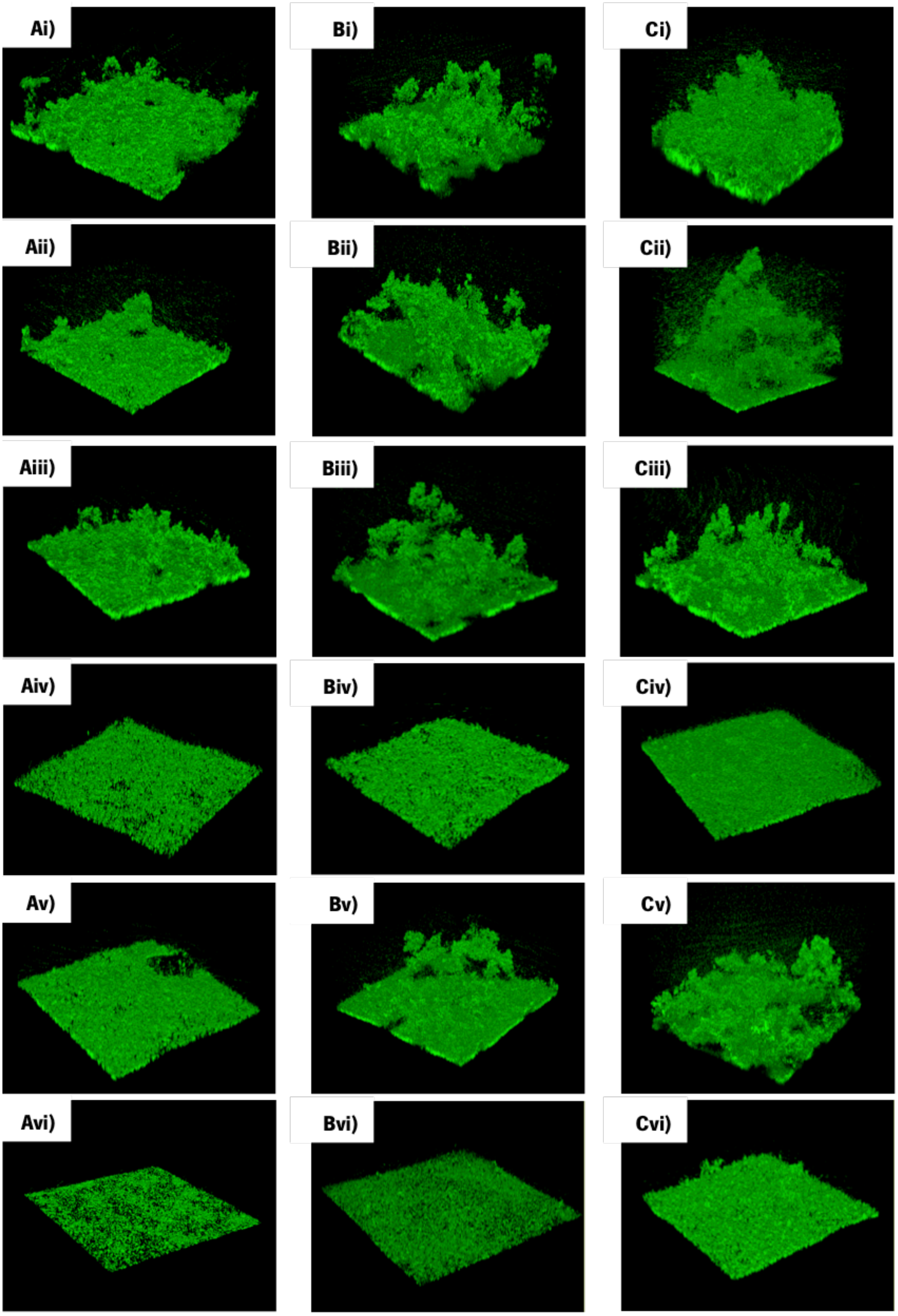
Ai)
Bi)
Ci)
Aii)
Bii)
Cii)
Aiii)
Biii)
Ciii)
Aiv)
Biv)
Civ)
Av)
Bv)
Cv)
Avi)
Bvi)
Cvi)

Figure 3.9. Confocal Laser Scanning Microscopy (CLSM) 3-D images of A) 24 h, B) 72 h and C) 120 h old biofilms of *S. aureus* Newman D2C^{GFP} on i) titanium surfaces and various coatings: ii) PLGA; iii) PLGA-inulin; iv) PLGA-DNase I; v) PLGA-DNase I (1/5) and vi) PLGA-inulin-packaged DNase I. The base of the biofilm is 375 x 375 μm.

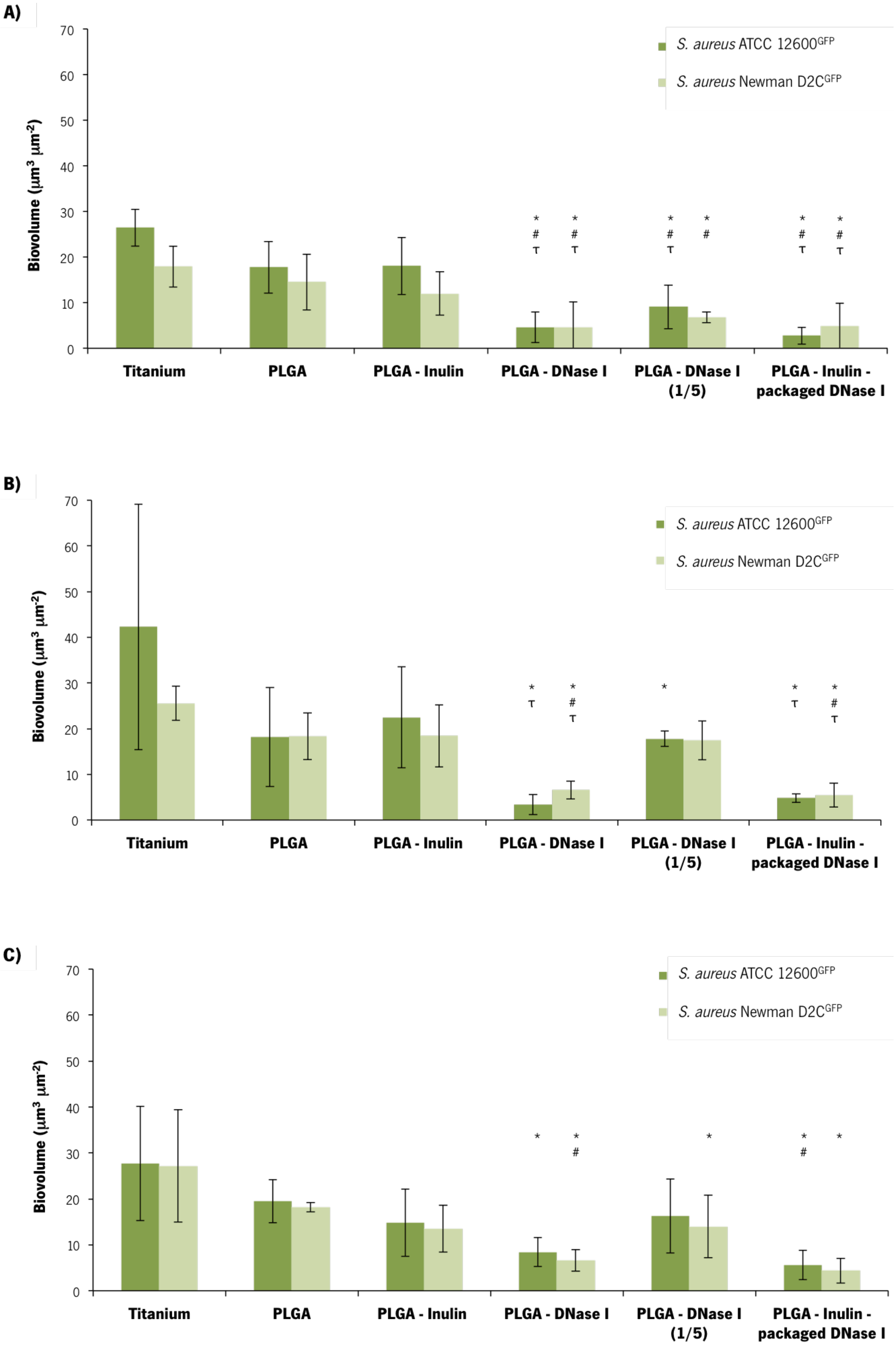

Figure 3.10. Average biovolumes ($\mu m^3\ \mu m^{-2}$) of A) 24 h, B) 72 h and C) 120 h old biofilms of *S. aureus* ATCC 12600^{GFP} and *S. aureus* Newman D2C^{GFP} grown in TSB on titanium surfaces and on the various coatings. Error bars represent SD over three experiments with separately grown bacteria and different batches of coated samples. *, # and τ indicate significant differences in the biovolumes, within the same strain, compared to titanium, PLGA and PLGA-Inulin, respectively ($p<0.05$).

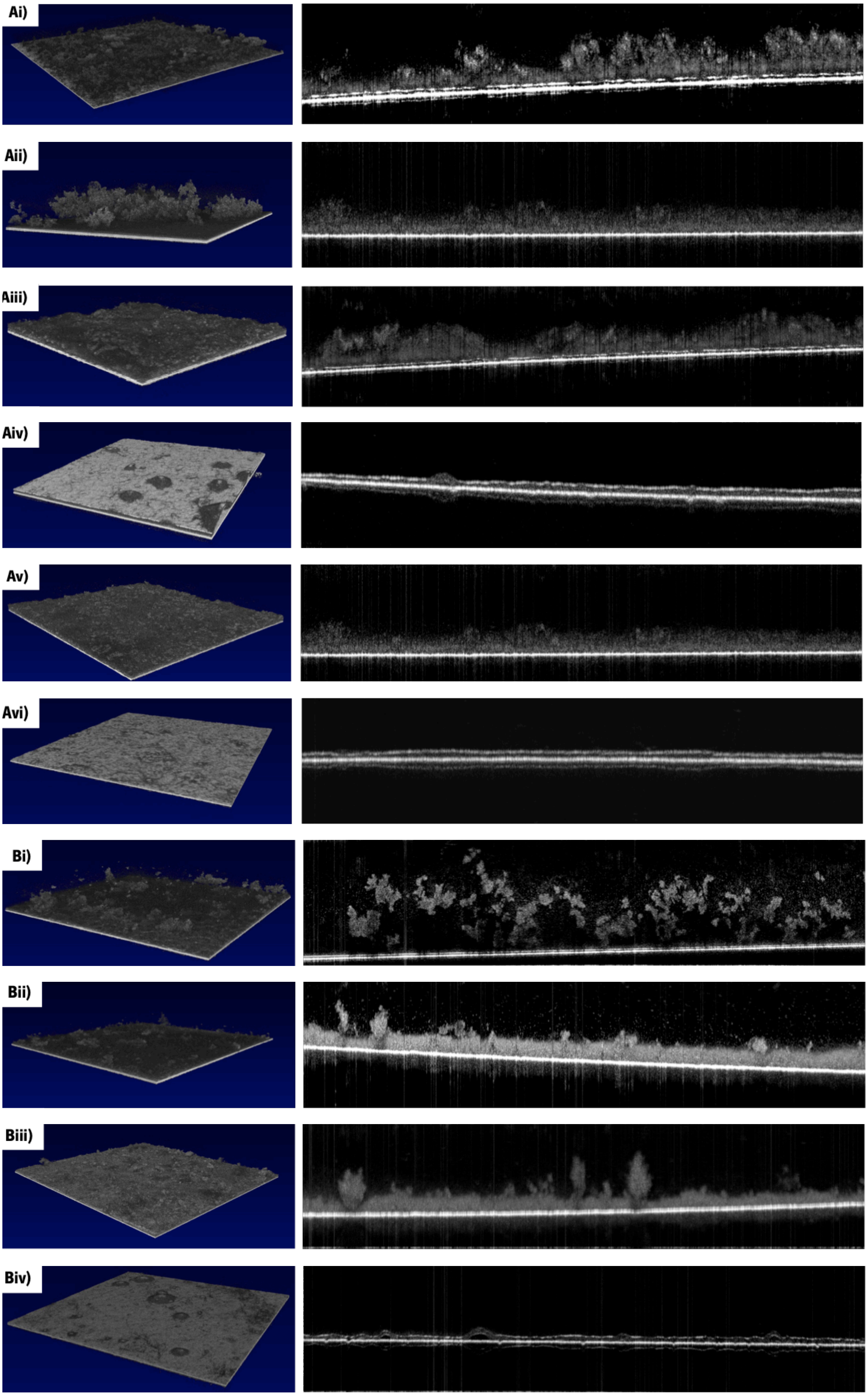
Ai)
Aii)
Aiii)
Aiv)
Av)
Avi)
Bi)
Bii)
Biii)
Biv)

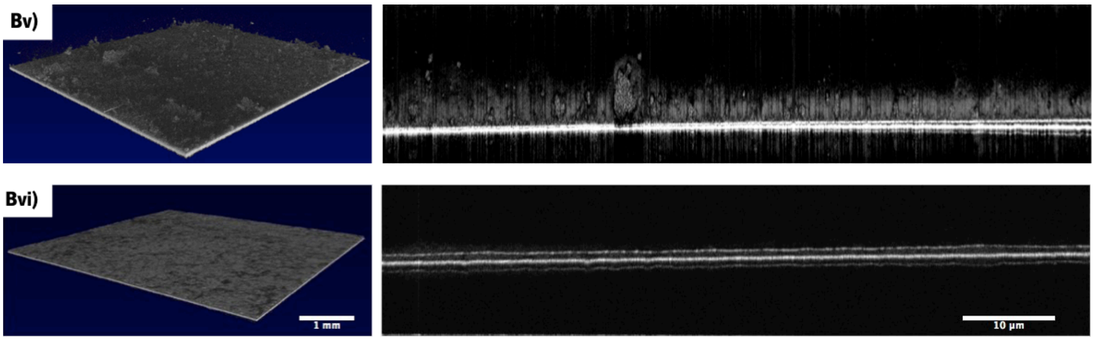

Figure 3.11. In-situ optical coherence tomography (OCT) observations of biofilm formation. 3-D (top) (scale bar represents 1 mm) and side (bottom) (scale bar represents 10 µm) views of A) *S. aureus* ATCC 12600^{GF} and B) *S. aureus* Newman D2C^{GF} biofilms 72 h old obtained using non-fluorescence-based, optical coherence tomography on i) titanium surfaces and various coatings: ii) PLGA; iii) PLGA-inulin; iv) PLGA-DNase I; v) PLGA-DNase I (1/5) and vi) PLGA-inulin-packaged DNase I.

3.5. XTT assay and cell adhesion assay using U-2 OS

3.5.1. XTT assay

Cells growing on top of PLGA coatings and on the surface of the wells surrounding each titanium substrata showed similar metabolic activity when compared to cells in the presence of bare titanium. Additionally, no significant differences between the metabolic activity of U-2 OS cells in the well and cells in the material, i.e. coated substrata, were observed (Figure 3.12).

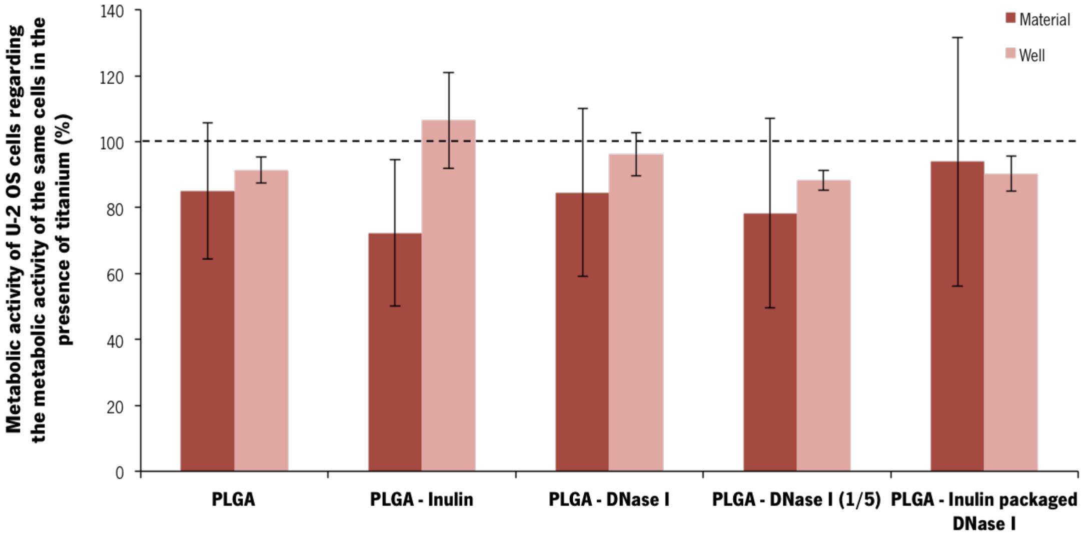

Figure 3.12. Metabolic activity of the U-2 OS cells (%) in each coated substrata (material) and on the surrounding substrata (well) compared to the U-2 OS cell in the same conditions but in the presence of titanium (dashed line). Error bars represent SD over three experiments with separately grown U-2 OS cells and different batches of coated samples.

3.5.2. Cell adhesion assay

Besides the influence on metabolic activity, coatings were assessed for their influence on the adhesion and proliferation of human osteosarcoma U-2 OS cells. None of the coatings showed a negative effect on the adhesion and proliferation of U-2 OS cells after 24 h of incubation. Cells adhered to all substrata and formed a confluent layer within 24 h (Figure 3.13). Additionally, no significant differences in the number of adhering cells were observed between any of the coatings and the titanium, and between the coatings and the wells in which incubation of the cells was performed (Figure 3.14).

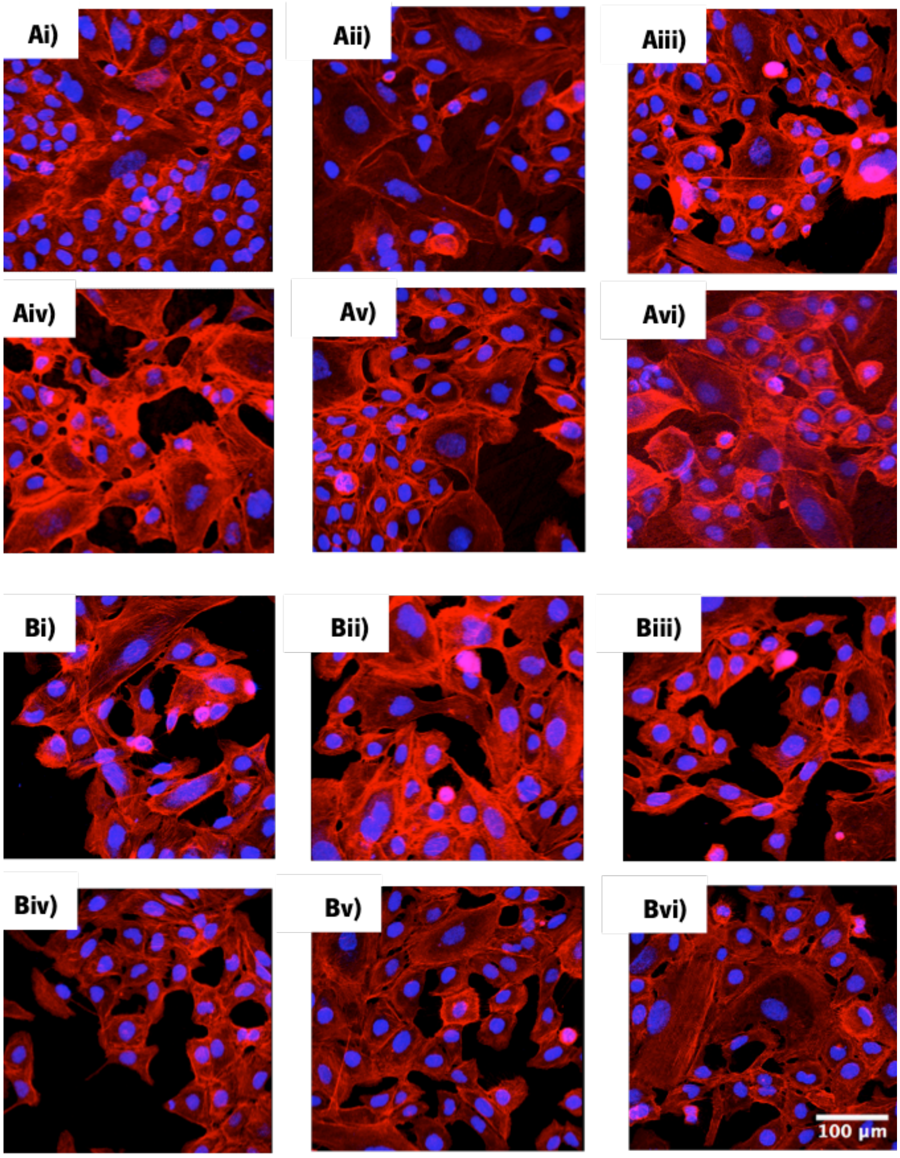

Figure 3.13. Confocal Laser Scanning Microscopy (CLSM) images of adhering U-2 OS cells after 24 h of growth on A) each one of the substrata: i) titanium surfaces; ii) PLGA; iii) PLGA-inulin; iv) PLGA-DNase I; v) PLGA-DNase I (1/5); and vi) PLGA-inulin-packaged DNase I and B) the surface of the well surrounding each one of the substrata mentioned. Scale bar denotes 100 µm.

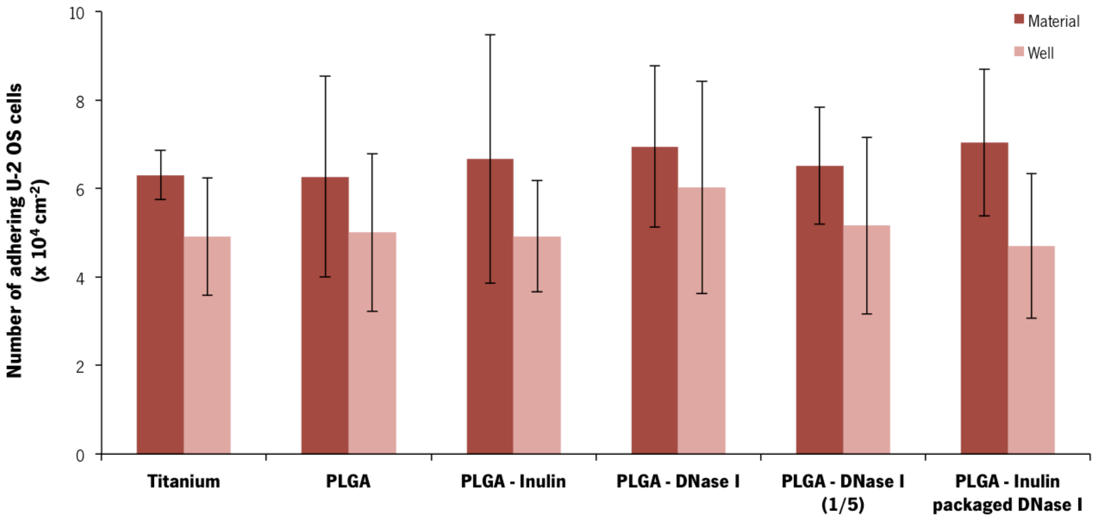

Figure 3.14. Number of adhering U-2 OS cells (x 10^4 cm^{-2}) after 24 h of growth on titanium surfaces and the various coatings and the surface of the well surrounding each one of the substrata. Error bars represent SD over three experiments with separately grown U-2 OS cells and different batches of coated samples.

3.6. Pilot experiment: effect of gentamicin when combined with the PLGA coatings containing either DNase I or inulin-packaged DNase I

3.6.1. Minimum inhibitory concentration and minimum bactericidal concentration

In order to determine the susceptibility of planktonic staphylococci to gentamicin, the MIC and MBC for both *S. aureus* ATCC 12600^{GFP} and *S. aureus* Newman D2C^{GFP} were determined by macrodilution (Table 3.4). To evaluate the influence of PLGA-DNase I and PLGA-inulin packaged DNase I coatings (chosen by their efficacy in preventing the biofilm formation (section 3.4.2.)) on the susceptibility to gentamicin by both staphylococcal strains, 8 μg/ml of gentamicin, a concentration between the MIC and the MBC, was used to treat mature biofilms.

Table 3.4. MIC (μg/ml) and MBC (μg/ml) of gentamicin for the *S. aureus* strains studied

***S. aureus* strain**	**MIC (μg/ml)**		**MBC (μg/ml)**	
ATCC 12600^{GFP}	> 4	< 8	> 8	< 16
Newman D2C^{GFP}	> 4	< 8	> 8	< 16

3.6.2. Biofilm susceptibility to gentamicin

For 24 h (15 h in the presence of gentamicin) and 48 h (24 h in the presence of gentamicin) of biofilm growth, coatings of PLGA-DNase I and PLGA-Inulin packaged DNase I increased the susceptibility of both staphylococcal strains studied (Figure 3.15 and Figure 3.17). This effect seemed to be higher for the PLGA-DNase I coating (Figure 3.16 and Figure 3.18). In addition, for the uncoated titanium the ratio biovolume live bacteria/biovolume dead bacteria is above 1, meaning more live than dead cells; which did not occur for the PLGA coatings in almost all the situations.

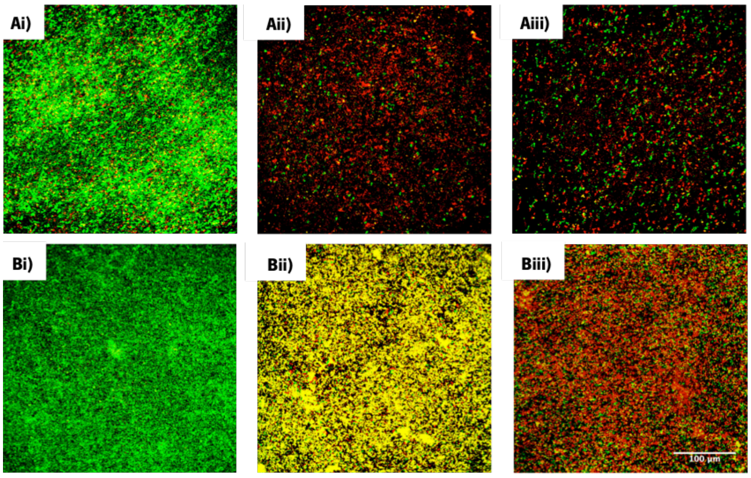

Figure 3.15. Confocal Laser Scanning Microscopy (CLSM) overlay images for 24 h old biofilm (9 h of biofilm growth without gentamicin and 15 h of biofilm growth in the presence of 8 µg/ml gentamicin) of A) *S. aureus* ATCC 12600^{GFP} and B) *S. aureus* Newman D2C^{GFP} for i) titanium; ii) PLGA-DNase I; and iii) PLGA-Inulin-packaged DNase I. Living cells fluoresced green and dead cells appeared red. Scale bar represents 100 µm.

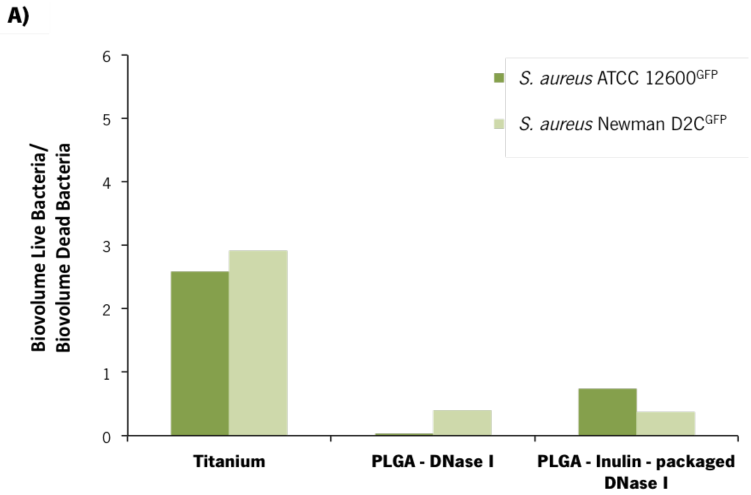

Figure 3.16. Biovolume live bacteria/biovolume dead bacteria for 24 h old biofilm (9 h of biofilm growth without gentamicin and 15 h of biofilm growth in the presence of 8 µg/ml gentamicin) for titanium, PLGA-DNase I, and PLGA-Inulin-packaged DNase I.

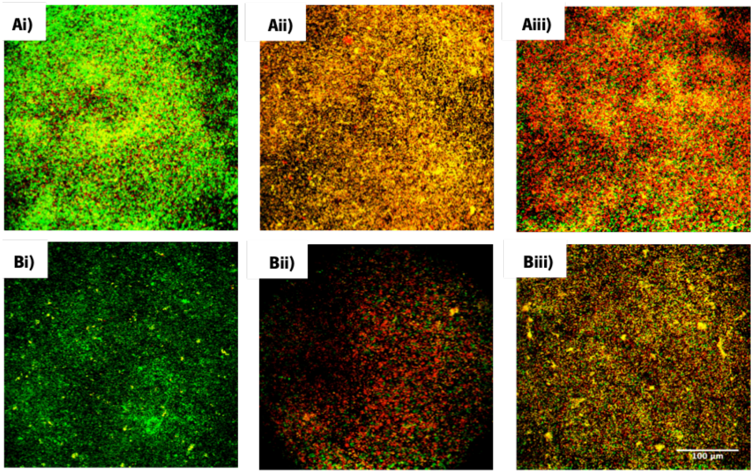

Figure 3.17. Confocal Laser Scanning Microscopy (CLSM) overlay images for 48 h old biofilm (24 h of biofilm growth without gentamicin and 24 h of biofilm growth in the presence of 8 µg/ml gentamicin) of A) *S. aureus* ATCC 12600^{GFP} and B) *S. aureus* Newman D2C^{GFP} for i) titanium; ii) PLGA-DNase I; and iii) PLGA-Inulin-packaged DNase I. Living cells fluoresced green and dead cells appeared red. Scale bar represents 100 µm.

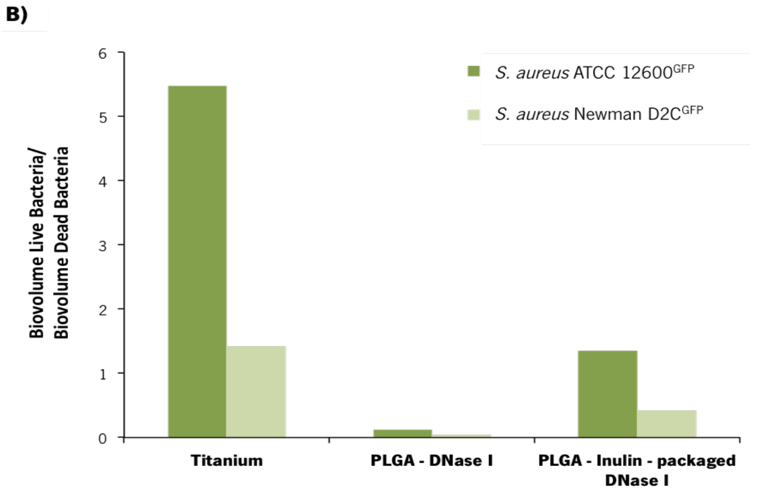

Figure 3.18. Biovolume live bacteria/biovolume dead bacteria for 48 h old biofilm (24 h of biofilm growth without gentamicin and 24 h of biofilm growth in the presence of 8 µg/ml gentamicin) for titanium, PLGA-DNase I, and PLGA-Inulin-packaged DNase I.

Chapter 4

Discussion

4.1. Particle preparation

4.1.1. Particle dimension

Frequently, the methods used to obtain proteins in the dry state from a solution are spray-drying and freeze-drying [99]. Spray-drying of inulin, DNase I or inulin-packaged DNase I, resulted in particles with a very similar size (mean diameter around 1 μm) (Table 3.1). The polydispersity, i.e. the width of the particle size distribution, of the powder was measured by the SPAN (SPAN=(particle diameter at 90% cumulative size) – (particle diameter at 10% cumulative size)/(particle diameter at 50% cumulative size)). A small SPAN, as observed for DNase I and inulin-DNase I particles, indicates a narrow size distribution [100].

Inulin DP23 formulations were successfully spray-dried, showing no coalescence during spray-drying and subsequent storage at ambient conditions [87,88]. However, the inulin appeared to have partly crystallized (as indicated by the high x_{90} value – Table 3.1), which is most often due to wetting during storage. Consequently, at the normal laser diffraction conditions, some of the agglomerated particles were not broken up by the air. This does not mean that the inulin particles will not break up when dispersed in PLGA, but it is an indication that agglomerates might be present.

Drying of pure proteins or enzymes often leads to partial or total inactivation due to damages in the tertiary structure (vital to their function and that can be affected by numerous physical – like denaturation – and chemical – such as hydrolysis – degradation mechanisms, that can eventually lead to a non-functional protein [99]). To withstand the degradation during processing and storage, stabilizing excipients such as mannitol, sucrose, trehalose and inulin are frequently used. Inulin is a sugar which helps to prevent damage of the tertiary structure of enzymes and has been used in the encapsulation of DNase I towards its use for cystic fibrosis treatment. More than 80% of the activity of DNase can be preserved during weeks of storage even at 85 °C by spray-drying this substance with inulin [12,87,88]. According to Swartjes and co-workers [12], this is essential to assure that the activity of DNase I does not get lost during the implantation of a coated biomaterial.

The preference for the ratio 1:4 of DNase I particles encapsulated in inulin was the result of a balance between having a high enough amount of DNase I to observe the effectiveness of the PLGA coatings (to prevent initial bacterial adhesion and biofilm formation for both studied *staphylococcal* strains) and, simultaneously, guarantee the stability of DNase I.

DNase I is considered a very stable protein, however, inulin protects DNase I during coating preparation since a major issue hindering the evolution of PLGA as protein drug carrier is protein stability. The organic solvents used (PLGA needs to be dissolved in a volatile solvent – such as acetonitrile) and the acidic microenvironment generated during polymer degradation are factors that most negatively affect the activity of DNase I [12,101].

4.2. Surface coating

4.2.1. Roughness and thickness of the coatings

A surface can be seen as a succession of peaks and valleys with several heights and spacings in a plane. The roughness parameter most frequently studied is the Ra (universally recognized and most used international parameter of roughness [102]), which describes the typical height variation of the surface [103], and can be measured using several equipments such as light interferometers, CLSM and atomic force microscopy (AFM). Using white light interferometry, it was concluded that the PLGA coatings displayed different roughness values, even though none of them could be considered as rough (Table 3.2). Biomedical devices usually present a smooth surface due to the commonly accepted perception that a smoother surface lowers the probability of bacterial adhesion, although some studies have suggested otherwise (it is believed that bacterial adhesion is enhanced when the features of the surface have dimensions or spacings similar to the bacterial size) [103]. The elevated Ra value of PLGA-inulin and PLGA-DNase I coatings is explained by the formation of small aggregates during application of the PLGA.

When the cut was made in the PLGA coatings (to measure the thickness), exposing the titanium surface, some parts of the coating were deposited on both sides resulting in peaks. This debris is perfectly visible in the 3-D pictures (Figure 3.1). The small thickness measured for the various PLGA coatings permit the exploitation of controlled release without substantial variations of the mechanical properties of the substrate material [104]. The thickness of PLGA coatings increased by the presence of particles doubling the total thickness of the coating when compared to only PLGA, however coating thickness was still under 15 μm (more precisely between 6 μm and 12 μm) (Table 3.2), which it was assumed as still sufficiently thin to not alter the mechanical properties of the material, thus allowing the performance of the function for which it was developed.

4.2.2. Degradation of the coatings

The variety of implants applied in the clinical setting demands the design of any future antimicrobial coating to be prudently matched to the intended application. Thereby, during the design process a number of variables must be considered, such as the duration of the coating efficacy (whether to apply in a short term implant or in a long term implant) and whether the mechanism applied should release antimicrobials (kills both microorganisms associated with the implant surface directly and susceptible pathogens in the surrounding area) or present the active component bound to the surface (the release of drug is easier to control) [105].

The PLGA coatings studied in this thesis were designed to prevent the initial bacterial adhesion and biofilm formation in orthopaedics implants, i.e. permanent implants. Therefore, the degradation rate of the coatings should be slow in order to prevent the occurrence of infections in the longest possible period of time. The degradation times of the various coatings in PBS revealed a longer degradation time for coatings containing DNase I particles, when compared to PLGA only and PLGA-inulin. In fact, coatings not containing DNase I degraded within 40 d, while remains of coatings containing DNase I were still present after 60 d (Table 3.3). The efficiency of the PLGA coatings has not been studied for such long periods of time (only for a maximum of 5 d), but their presence on the titanium surface is a good indication that they may help to combat the BAI when combined with antibiotics. Furthermore, over time, the probability of BAI decreases, since the human body considers the implant of a foreign body and forms a protective capsule of fibrous tissue around it.

According to Daghighi et al. [14], the use of degradable biomaterials (instead of non-degradable biomaterials) is an efficient strategy to reduce the risk of infection. In fact, these biomaterials are less susceptible to the occurrence of infections due to the release of anti-bacterial peptides, augmented vascularization (aids the access of immune cells to injured and infected host tissue), diminution of the local immune responses (non-degradable materials may constantly attract the attention of the immune system, leading to frustrated reactions – biodegradable materials allow the restoration of the immune system after full degradation), and also the reduction of available area of the surface for bacterial colonization during the degradation process. In this context, the combination of a non-degradable material (titanium implant) with a biodegradable coating (PLGA coating containing DNase I particles) with a long degradation time could be favorable, mitigating the probability of BAI.

4.3. Release kinetics

4.3.1. DNase I and inulin release kinetics

The release profiles of coatings containing antimicrobial compounds are often difficult to effectively control and inappropriate concentrations of antimicrobials can be released. For many of these coatings, an “initial burst” of drug release occurs, during which a significant amount of the drug is released through the early stage of the release process. This initial period of high release is typically followed by a longer period of diminishing release [105].

PLGA-DNase I and PLGA-inulin packaged DNase I coatings showed an initial burst release during the first h of placement in PBS, releasing almost 47% (Figure 3.3.A)) and 40% (Figure 3.4.A)) of the total amount of DNase I. The initial burst release can be attributed to particles within the top layer of PLGA (Figure 4.1.A)). The presence of particles at the interface of the coating leads to two events contributing to the high initial release. First, upon immersion of coated material in PBS, particles which are in direct contact with the outside environment start to dissolve and are released. Second, the release of particles directly at the interface leads to a porous outer layer through which liquid can reach other particles more quickly, leading to release of particles that were connected to the earliest dissolved particles (Figure 4.1.B)). Thus, when in contact with a PBS solution, these particles are the first to be released (unlike those particles that are in the deeper layers of polymer), causing the initial burst release. It appears that within 1 h all the particles captured in the top layer are dissolved, since after this first h the release of DNase I continued at a slower rate. After this initial phase, a diffusion-controlled release phase could be observed, which is attributed to pore-diffusion of protein. In fact, after 4 h and 120 h immersion in PBS the release of DNase I was approximately and 11.1% and 0.4% for the PLGA-DNase I coatings and 6.8% (for both time points) for the PLGA-inulin packaged DNase I. The protein that has been entrapped inside of the polymer matrix might be released in a phase controlled by polymer erosion [106]. It is throughout this latter phase that bacteria may be exposed to sub-inhibitory concentrations of antimicrobials which is favourable to the development of resistance, and therefore may reduce efficiency of the treatment [105]. However, resistance against enzymatic treatment has never been reported [12], hence it is not expected any efficiency reduction of the coatings due to the development of bacterial resistance because of the presence of a reduced amount of DNase I.

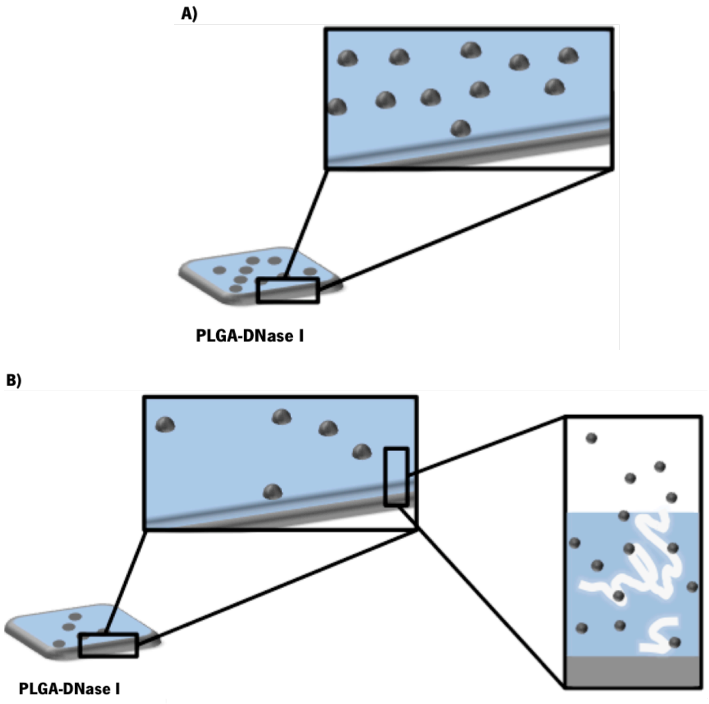

Figure 4.1. Schematic illustration of the process that led to the initial burst release of DNase I particles: A) after deposition of the coating on the titanium surface; B) after 1 h immersion in PBS. The same happens for the PLGA-inulin packaged DNase I coating.

Regarding the surface topography of the PLGA-DNase I and PLGA-inulin packaged DNase I coatings after immersion in PBS for 1 h and 120 h, it was found that degradation transformed the coating from relatively smooth and non-porous after 1 h in PBS to a surface covered with holes after 120 h in PBS. It can be speculated that the increased porosity of the coatings of PLGA-DNase I (Figure 3.3.B)) and PLGA-inulin packaged DNase I (Figure 3.4.B)) is attributed to the voids left behind by the released of DNase I and DNase I-inulin particles, respectively. Although the time points between 1 h and 120 h were not observed using SEM, it was expected that the PLGA surface for both coatings exhibited an incrementally porous surface. The formation of these pores offers transport pathway to the drug and facilitates its diffusion through the polymeric coating [107]. After 120 h immersion in PBS, the holes presented in the PLGA-DNase I coating presented a circular shape (allows a more precise control of the DNase I release over porosity), unlike the holes in the PLGA-inulin packaged DNase I coating. Conceivably, the presence of DNase I inside the inulin particles changes their shape to a bumpier one. Deposition of artefacts on the PLGA-DNase I coating, probably during its preparation, resulted in the appearance of fibers on the coating surface (Figure 3.3.B.i)). However, it is improbable that this affected the release of protein from the coating, as it most likely originated from SEM preparation procedures.

4.3.2. Prevention of the initial burst release

PLGA is a synthetic biodegradable and biocompatible copolymer, and also FDA approved for biomedical applications, including implantation [12]. PLGA is being increasingly used in sustained drug delivery applications [104] since the drug release can be achieved by different approaches [101]. Altogether, this makes PLGA an ideal candidate to protect DNase I on implant materials in order to prevent bacterial adhesion and biofilm formation, with the possibility to fine-tune its release [12]. There are three direct possibilities to adjust the degradation of, and consequently alter the release. To prevent, or lower, the initial burst release of DNase I, one can increase the coating thickness (while maintaining the same amount of enzyme), increase the polymer molecular weight (leading to slower degradation [108]), or finally, vary the ratio of poly(lactic) acid (PLA) to poly(glycolic) acid (PGA) (PLA is more hydrophobic than PGA and, therefore, lactide-rich PLGA copolymers are less hydrophilic, absorb less water, and consequently, degrade more slowly [109]).

Since the suspected cause of the initial burst release of DNase I was not directly related with the degradation of the copolymer, but with the deposition of particles on its surface, the options of using PLGA with a higher molecular weight or using higher amounts of PLA were discarded. Instead, a direct and an indirect method to increase the PLGA coating thickness were used. By either directly increasing the PLGA content, or by placing an extra layer of PLGA on the top of the regular coating, the coating thickness increased and it was hypothesized that less particles would be present at the coating interface.

The two implemented strategies to prevent the initial burst of DNase I showed to be more efficient for the PLGA-DNase I than for PLGA-inulin packaged DNase I coating. In the case of the PLGA-inulin packaged DNase I coating only the deposition of the additional layer of PLGA coating decreased the amount of DNase I released significantly at 4 h (Figure 3.5.B)). Regarding the PLGA-DNase I coating, the deposition of an extra layer of PLGA decreased the amount of DNase I released by 90%, 80% and 78% at 1 h, 4 h and 8 h, respectively (Figure 3.5.A)). This method prevents the direct contact between the DNase I particles deposited at the surface of the polymer layers and the external environment by the additionally applied PLGA layer. Accordingly, a large portion of the release of DNase I particles into the surroundings is only achievable after degradation (complete or partial) of the extra PLGA layer.

In turn, the increase of the PLGA layer thickness provided a decrease of 71% and 65% (for 4 h and 8 h) of the amount of enzyme released for the three earliest time points (Figure 3.5.A)). Even though the initial release decreased, some of the DNase I particles were still at the interface of the PLGA surface in contact with the aqueous environment, explaining the differences compared to the previous approach. Numerically analyzing, the most efficient strategy was the deposition of a PLGA extra layer; however, in practical terms a slightly higher release of DNase I in the first few hours might be preferable, since in this period of time the probability of occurrence of BAI is higher (the patient is more susceptible).

It was intended to avoid the initial burst release of DNase I, in order to prolong the period of time during which the coatings are effective, i.e. to optimize the coatings efficiency. In fact, the presence of the PLGA extra layer allows the release of the same amount of DNase I at a slower rate. The regular release of DNase I from the PLGA coating combined with an appropriate antibiotic therapy might reduce the risk of infection to satisfactory levels for a suitable period of time.

Finally, it is important to emphasize that the initial burst release is a problem, especially for highly potent drugs, since it increases the risk of serious side effects *in vivo* [106]. However, DNase I is naturally produced in the human body by the pancreas, kidneys, liver and subsequently released into body fluids, being aware of any negative effects caused by this enzyme to humans. Evidently, the absence of negative effects is considered a critical point for the further downstream translation of the DNase I coating to clinical application [58,110].

4.4. Initial bacterial adhesion and biofilm growth

The increasing understanding of how biofilms form and the role of different components involved in cell adhesion is providing valuable information for the development of complete new strategies to combat bactericidal colonization in unwanted situations [71]. According to Meng Chen and co-workers [70], the most promising methodologies currently being developed to prevent and treat infections caused by biofilms include of small molecules and matrix-targeting enzymes to inhibit or disrupt the process of biofilm formation and proliferation. The resulting anti-biofilm coatings that will be used to modify the surface of medical devices will lead to implants that are highly resistant to biofilm formation. These novel anti-biofilm tools could eventually lead to anti-biofilm treatments that are superior to the current antibiotic therapy.

Since eDNA is ubiquitous and pivotal in bacterial adhesion and biofilm formation, attacking this essential component of the EPS matrix by DNase I, has been considered a possible approach to prevent biofilm formation [58,59]. Therefore, this dissertation focused on studying of a protective biodegradable PLGA coating on titanium in which DNase I is embedded with the proposal of preventing initial bacterial adhesion and biofilm formation.

Destabilization of biofilms by removing eDNA has been documented by the addition of DNase during or after biofilm formation [59]. In this thesis, DNase I was present in the PLGA coatings, being in contact with each one of the staphylococcal strains since de initial bacterial adhesion.

All coatings with DNase I particles (PLGA-DNase I, PLGA-DNase I (1/5) and PLGA-inulin packaged DNase I) were efficient in the prevention of initial bacterial adhesion by both staphylococcal strains, while all controls without DNase I showed high numbers of bacteria adhered to the surface (Figure 3.6 and 3.7).

Analyzing the results for 24 h of biofilm formation, it may be concluded that, the outcome is similar to the obtained for the initial bacterial adhesion except for the biovolume of *S. aureus* Newman D2C^{GFP} on PLGA-DNase I (1/5) coatings which is not significantly different from the biovolume in the PLGA-inulin (Figure 3.8.A), Figure 3.9.A) and Figure 3.10.A)). Paralleling the biovolumes achieved in this work for 24 h incubation with the ones presented by Swartjes and co-workers for 20 h [12], it is reasonable to justify that the disparities are caused by the presence of tetracycline in the TSB medium used in the current study. Exposure of bacterial cells to this antibiotic (responsible for the selection of fluorescent cells) could have contributed to the lower levels of biovolumes acquired. Comparing with the previous referred study, in this work the biovolume was reduced to about 2 times for both staphylococcal strains on the titanium, PLGA and PLGA-inulin; and approximately 9 and 6 times for *S. aureus* ATCC 12600^{GFP} and 2 times for *S. aureus* Newman D2C^{GFP} for the coatings PLGA-DNase I and PLGA-inulin packaged DNase, respectively. Over time, the GFP plasmid (responsible for the bacterial fluorescence) within the bacterial strains disappears in the absence of the tetracycline in the medium, not being possible to observe the staphylococcal strains on the CLSM without any staining. However, the PLGA coatings studied are very reactive with the common stains (live and dead stains), impeding the clear visualization of the bacteria. In this sense, the tetracycline has been regularly added to the medium, guaranteeing that the bacteria with the GFP plasmid were being constantly selected and, subsequently visualized.

Regarding the results of 72 h of staphylococcal biofilm formation, the coating PLGA-DNase I (1/5) only showed efficiency in the biovolume reduction when compared to titanium and exclusively for *S. aureus* ATCC 12600^{GFP}. The scenario also changed for PLGA-DNase I and PLGA-inulin packaged DNase I, which were not able to significantly prevent biofilm formation of *S. aureus* ATCC 12600^{GFP} on their surfaces with respect to only PLGA coating (Figure 3.8.B), Figure 3.9.B) and Figure 3.10.B)). Biofilms are complex and highly dynamic structures. Consequently, when working with biofilms, there is an elevated grade of unpredictability associated. It is possible to attempt to reduce the uncertainty (for instance, performing three completely independent experiments and in each one of them choose randomly three different spots to calculate the biovolume as in this study); although, there are factors that the operator cannot control. The fluctuation in the biovolume values obtained for the PLGA coating is one of those cases.

Lastly, after 120 h of biofilm formation it is possible to conclude that both PLGA-DNase I and PLGA-inulin packaged DNase I coatings were competent in biofilm prevention when compared to titanium, but not when paralleled with the other controls, mainly with PLGA-inulin. In addition, PLGA-DNase I (1/5) was the less effective coating, not preventing the formation of biofilms not even when compared with titanium uncoated for *S. aureus* ATCC 12600^{GFP} (Figure 3.8.C), Figure 3.9.C) and Figure 3.10.C)).

For the initial adhesion, comparing the number of adhered cells to the titanium and to each one of the coatings containing DNase I particles, this parameter was reduced by approximately 50 times in the surface of PLGA-DNase I and PLGA-DNase I (1/5) and over 100 times in the surface of PLGA-inulin packaged DNase I coating, for both staphylococcal strains. Regarding the biofilm growth, comparing the biovolumes of both *S. aureus* strains biofilms 24 h, 72 h and 120 h old with the biovolumes obtained on the titanium, a substantial reduction on the surfaces with the PLGA coatings comprising DNase I particles occurred. The biovolumes showed more marked differences for the *S. aureus* ATTCC 12600^{GFP} and for the PLGA-inulin packaged DNase I coating. As a corollary, similarly to previous reported studies, packaging DNase I particles in inulin protects them during the coating process, as well as it aids increasing their shelf-life [12], since the coating PLGA-inulin packaged DNase I presents most of the times better (or at least equal) efficiency than the coating with five times more DNase I particles, PLGA-DNase I; and, also, exhibited for all the situations better efficacy than the coating with the same amount of DNase I, PLGA-DNase I (1/5).

In modern medicine, the combination of systemic antibiotic administration and local-antibiotic delivery materials is used to combat perioperative infections. Local antibiotic delivery materials, such as gentamicin-loaded bone cements used in orthopedics for the fixation of hip and knee prostheses, are only active for a maximum of 24 h [58]. The first functional DNase I coating led to a delayed biofilm formation of up to 14, which is probable enough to mitigate the risk of acute infections related with medical implants [58,59]. In this work, the coatings PLGA-DNase I and PLGA-inulin packaged DNase I possess antimicrobial activity for, at least, 120 h of growth for both studied *S. aureus*. It is expected that a timescale of 120 h is sufficiently long to prevent infections arising from bacteria introduced during the preoperative stage as it is currently done with a dose of postoperatively administered antibiotics [12].

To exclude the possibility that the presence of DNase I in the coatings was hindering the visualization of the biofilm formed by *S. aureus* strains, biofilms of 72 h old were analyzed by OCT. OCT is a non-invasive optical tomography technique, which is increasingly used in medical diagnostics, since it is able to expose spatially resolved structural information on biofilm without any staining [111]. The results from OCT are qualitative and clearly in accordance with those obtained by CLSM, coating of PLGA-DNase I and PLGA-inulin packaged DNase I effectively decreases biofilm formation for up to 120 h for both *S. aureus* ATTCC 12600^{GFP} and *S. aureus* Newman $D2C^{GFP}$ (Figure 3.11).

DNase I treatment has been used to decrease sputum viscosity (enabling better sputum clearance and reducing the risk of recurrent infections) in cystic fibrosis patients, and modern antibiotic treatment of biofilms in the lungs of cystic fibrosis patients is supplemented with rhDNase I [57-59,112]. DNase-mediated biofilm dispersal is also relevant for treating or preventing other types of biofilm infections, such as endocarditis or implant-associated infections. DNase treatment is an emergent therapy for bacterial vaginosis, a highly prevalent disorder of the vaginal microbiota for which antimicrobial treatment has a high rate of failure [59,113]. DNase may also be effective for other biomedical applications such as design of DNase I based wound care gels [57], as well as non-biomedical related applications including cleaning of food contact surfaces, wastewater treatment, seawater desalination or decreasing membrane biofouling systems employed in drinking water production, since controls the microbial attachment [54,59,114]. Obviously, the procedure that DNase treatment takes, whether a prophylactic surface coating, aerosolized mist, or a solution, must be adapted to the particular purpose [59].

A common limitation associated with the application of coatings on orthopedic implants is their fragility [115]. The conditions under which an orthopedic implant is inserted will inevitably lead to mechanical stress (causing metal scraping and consequently damaging the coating, exposing the metal surface to bacterial cells) and exposure to fluids, such as PBS or blood [12,115]. According to Swartjes and co-workers [12], the hardened PLGA provides protection against storage and handling conditions. Importantly, even in circumstances that can compromise the integrity of the PLGA coating (such as tight bone junctions), this coating remains in the place where it was applied, ensuring the protection of the implant.

Although promising, the use of DNase I to prevent biofilm formation and initial bacterial adhesion has some limitations such as the absence of eDNA in certain bacterial biofilms [59]. The variation between matrices of different species (and even strains) makes it impossible to find a unifying element to be targeted for biofilm control [34]. Some bacterial species appear to have little or no dependence on eDNA and, in rare cases, eDNA can even act as a barrier to microbial adhesion [54]. In this context, notwithstanding the strategies that target the eDNA are promising, further research must be developed in order to find more widely effective agents [59]. For this purpose it is necessary to bear in mind that the importance of the different components of the EPS matrix for the integrity of the biofilm is dependent of the growth conditions, medium and substrates [34]. In addition, the use of DNase for biofilm removal is effective, but dependent on the age of the biofilm. Probably, once the biofilm has aged past a certain point, the role of eDNA in biofilm matrix is supplemented or replaced by other matrix components. This, together with the difficult access to eDNA (possibly this element is linked to another that protects it from enzymatic degradation performed by DNase, i.e. that acts as a shield), calls the question of the efficiency of DNase treatment. In this context, it is therefore necessary to consider how eDNA can be reachable to DNase, or alternatively how its interactions with other matrix components can be weakened. Finally, production of DNase is currently expensive and consequently unacceptable for large-scale use [59] due to the glycosylation of this enzyme after translation, which impedes the use of inexpensive prokaryotic expression systems [116]. Swapping mammalian DNase to bacterial extracellular nucleases in *E. coli* expression systems could offer a route to lower production costs [59,117]. However, the effectiveness and stability of bacterial nucleases in the prevention of the biofilm formation should be assured (for example, making use of the yeast *Pichia pastoris* modified) [59].

Alternative strategies to degradation of eDNA by DNase, could be the destabilization of the interactions between eDNA and other biomolecules (in the EPS matrix or on the cell surface via the proteins that crosslink eDNA strands in the matrix – eDNA has an extensive and highly organized network) [59,118] or target components that substitute or supplement the role of eDNA in the structural stability of the mature biofilm [119]. Evidently, the first approach requires deep knowledge of these interactions, and preferentially the components should be common among bacteria (such as polysaccharides and proteins). In this sense, a broad-range enzymatic approach to weaken biofilms by enzymatic degradation of the EPS matrix should thus ultimately combine the activity of enzymes that target not only eDNA, but also polysaccharides and proteins [59]. As mentioned, examples of protein-eDNA interactions are the DNA-binding IHF (a member of the DNABII family, vital for biofilm development and stability due to its support to the structural network of eDNA [119,120]) and the Beta toxin (establishes covalent crosslinks to itself in the presence of DNA, developing the skeletal structure upon which staphylococcal biofilms are settled [121]). In addition, targeting the control mechanisms for nuclease production in bacteria encourages the production of extracellular nucleases and thereby the natural dispersal mechanism of several biofilm-forming bacteria [59]. The most vital enzymes in the degradation of the biofilm matrix and release of bacterial cells into the surrounding environment are the secreted cysteine proteases (staphopains), V8 serine protease (SspA) and Nuc. The relative significance of each enzyme will depend on the strain-specific composition of the biofilm matrix. The targets of the main proteases (V8, aureolysin (Aur), staphopains) are still not completely described, though some candidate surface proteins, like the FnBPs and ClfB, have been identified. Furthermore, the function of Nuc in biofilm dispersal has not been scrutinized in detail. The same happens with other exo-enzymes also important in dispersal mechanisms, such as hyaluronidase and lipases. In addition to the matrix-degrading mechanisms, it is probable that D-amino acids and the severe response may play a role in dispersal, but supplementary work is needed to better characterize these mechanisms. Accordingly, further work on this topic will permit developing better treatment options for biofilm-mediated diseases [85].

Based on the reported results, it is believed that the presence of DNase I in therapy will significantly decrease the initial bacterial adhesion, matrix formation and strong biofilm formation permitting the effective killing of remaining bacterial cells with the minimal use of antibacterial agents.

4.5. XTT assay and cell adhesion assay using U-2 OS cells

Interaction between the surface of implants and biological tissues is an important aspect of biomaterials research [122], determining the success of the materials implantation. In this study, two tests to determine the existence of negative effects on mammalian cells caused by contact with the developed PLGA coatings were performed. Specifically, XTT was used to measure the metabolic activity of the cells, and a cell adhesion assay was performed to test the ability of cells to adhere to the various substrata.

U-2 OS osteoblast-like cells were used because of their ease of growing, although cancer cell lines may not represent all aspects of *in vivo* cell behavior [37].

4.5.1. XTT assay

The tetrazolium salts, 3-(4,5-dimethyl-2-thiazol)-2,5-di-phenyl-2H-tetrazolium bromide (MTT) and XTT are commonly used test methods to measure cell viability and proliferation [123]. Despite both methods present equivalent sensitivity, the reduced assay time and sample handling (by eliminating the need to solubilize the formazan product prior to absorbance measurements) justify the use of XTT instead of MTT [124]. The XTT is based on the assumption that shortly after the death of the cell, inactivation of mitochondrial dehydrogenases enzymes occurs and that loss of cell viability can be measured using a tetrazolium derivative [97]. The amount of water-soluble product generated from XTT (orange formazan product) is proportional to the number of metabolically active cells, i.e. the greater the number of metabolically active cells in the well, the greater the activity of mitochondrial enzymes, and the higher the concentration of the dye formed [96,123,125].

After 24 h incubation, the metabolic activity of the U2-OS cells was measured not only of the cells adhered to the titanium uncoated substrata and each PLGA coating, but also of the cells adhered to the surface of the 6-well polystyrene plate in which substrata were incubated. The lack of general anti-fouling properties was confirmed by cell attachment and spreading, whereas biocompatibility was affirmed by comparing the metabolic activity of cells on coatings to uncoated titanium and the surface of the well plate. No significant differences between the metabolic activity of the cells attached to the polystyrene surface and the cells adhered to the different substrata were observed, indicating that cells were not impeded in their normal metabolism on the different substrata(Figure 3.12).

In the analysis of the XTT test results, the uncoated titanium material was taken as a reference. The metabolic activity of the cells adhered to these materials and to the well surrounding it was taken as 100% metabolic activity. A reference value is needed since the XTT assay is a method of comparison. Titanium was considered to be a good reference to compare metabolic activity since is a biological inert, non-toxic material and commonly used to manufacture various implants (such as hip and knee prosthesis, bone plates, screws and pins for fixation, dental implants and artificial spines, and so on) [12,126,127]. Afterwards, all the values obtained for the metabolic activity of the U2-OS cells adhered to the various PLGA coatings and to the corresponding wells where the incubation was executed have been normalized considering a basis of 100%. Accordingly, the values for the metabolic activity are all very similar with the ones for titanium, since all of them are around 100%. In addition, there are no statistically significant differences among the metabolic activity of the cells adhered to the various PLGA coatings and to the respective incubation well, indicating that the viability and proliferation of U2-OS cells were analogous in both surfaces, or in other words, the contact of the cells with the PLGA coatings do not negatively affect their viability and proliferative capacity (Figure 3.12).

4.5.2. Cell adhesion assay

The biocompatibility of both existing and novel medical devices is a crucial topic to be considered in order to determine the hypothetical toxicity resulting from body contact with a material or medical device [128]. Apart from good physicochemical and mechanical properties, the most critical condition for a biomaterial is its biocompatibility in a certain environment, coupled with the non-cytotoxicity of its degradation products [129]. The key parameters of the cell-biomaterial interaction are cell adhesion and spreading (topic not detailed in this study). It is important to understand which surface properties encourage cell adhesion, subsequent spreading and cell growth. Occasionally, surface modification or surface coating increases the capability of particular materials to support cell adhesion and/or spreading [128].

Regardless of the route of infection (peri-/early postoperative or late postoperative infections), the destiny of a biomaterial implant depends on the outcome of the “race for the surface” between efficacious tissue integration of the material implant and biofilm formation.

If tissue cells win this competition, then the biomaterial surface is entirely integrated by tissue cells and less susceptible to bacterial biofilms. Alternatively, if bacteria win the race, bacterial cells will colonize the implant surface and tissue cell functions are impeded by bacterial virulence factors and excreted toxins. Unfortunately, since microorganisms are commonly introduced on an implant surface during surgery, they have a head start in this race for the surface [37,38]. In addition, biomaterial implants are usually not completely integrated with host tissue especially when they consist of metal parts that are not easily colonized by host tissue cells or, in the case of orthopedic implants, when the repeated hinging can damage the surface exposing adhesive sites for bacteria colonization. Hence, the establishment of a robust interface with fusion between biomaterial surface and bone tissue is essential, requiring adhesion, proliferation and differentiation of tissue cells for successful implantation [37].

The presented results show complete coverage of all sample materials by U2-OS cells after 24 h incubation, indicating a rapid and complete surface coverage of mammalian cells, which crucial for the successful integration of the implant within the host tissue [37]. Additionally, good coverage of the polystyrene surface of the 6-well plate was observed. This is aligned with what expected, since the this material is specifically designed to support the adhesion and growth of mammalian cells [130]. U2-OS cells were observed firmly attached and spread, elongated in shape, whereas also rounded cells in the process of cell division were present. With the exception of few areas on the surface, full coverage by cells was reached in all cases (Figure 3.13). There were no significant differences between the number of U2-OS cells per cm^2 adhered to each substratum and to the respective well, or between the titanium and coated surfaces. Based on these results, the coatings do not exhibit toxicity towards these cells (Figure 3.14), permitting unhindered tissue integration, which is a requirement for a successful result of biomaterial associated surgery in many applications [12].

The objective of the study discussed in this subchapter was to analyze the existence of negative effects in the adhesion of U2-OS cells caused by contact with the diverse coatings. More elaborate experiments such as the race for surface between mammalian cells and bacterial cells *in vitro* have not been performed. Nevertheless, studying the behavior of U2-OS cells in the presence of *S. aureus* and perhaps even immune cells (such as macrophages) could be interesting to simulate the *in vivo* conditions, allowing more advanced evaluation of the developed coatings prior to animal experiments or human trials, than based on single studies of microbial adhesion to or mammalian cells interactions with such coatings [38].

In a study developed by Subbiahdoss and co-workers [37], it was demonstrated that despite the presence of macrophages, U2-OS cells loose the race for the surface (PMMA) in the presence of highly virulent *S. aureus* or *P. aeruginosa*, while cells can survive at least 48 h in the presence of *S. epidermidis*, regardless of the absence or presence of macrophages. Even with a complete coverage of U2-OS cells on the biomaterials surface after 24 h incubation, bacterial cells – in this case *S. aureus* ATCC 12600^{GFP} and *S. aureus* Newman D2C^{GFP} – can access the surface of the PLGA coating covering the titanium. However, as discussed in the section 4.4, it is expected that the presence of DNase I in the PLGA coating (at least in both PLGA-DNase I and PLGA-inulin packaged DNase I coatings) will prevent the initial bacterial adhesion and, subsequently the biofilm formation, allowing the colonization of the surface by tissue cells.

4.6. Pilot experiment: effect of gentamicin when combined with the PLGA coatings containing either DNase I or inulin-packaged DNase I on the staphylococcal strains

In this section, the effects of gentamicin sulphate combined with DNase I were analyzed on the growth of staphylococcal biofilms. For this purpose, firstly the MIC and MBC values of gentamicin for both *S. aureus* strains were determined and, thereafter biofilms 9 h and 24 h old (that growth in the presence of DNase I through exposure to PLGA-DNase I or PLGA-inulin packaged DNase I) were exposed to a value between the MIC and the MBC during 15 h or 24 h, respectively.

4.6.1. Minimum inhibitory concentration and minimum bactericidal concentration

Ideally, the use of antibiotics should be treated as a back-up approach in beginning infections and not as a preventive beforehand, the main point is still represented by the sterility in the surgical room and by the antiseptic operating procedures [131]. Nonetheless, any method which can hypothetically reduce adhesion of bacteria and, consequently, bacterial colonization is desired.

Gentamicin, a polycationic aminoglycoside antibiotic, is a commonly utilized antibiotic in orthopedic surgery for local treatment of infection (by means of spacers or beads) [65,132].

For instance, gentamicin is the most frequently used antibiotic for loading bone cement, because it can resist to the high temperatures reached during polymerization of the cement and also because it is effective against a wide variety of bacteria [133]. This drug can be linked to negatively-charged elements (such as residues on the external membrane of Gram-negative bacteria and RNA) due to their ionic properties. However, the ionic charges necessary for proper functioning of gentamicin may also render it less effective in the presence of bacterial biofilms. Alginate and eDNA, both negatively charged, are examples of substances that are able to bind and sequester or inhibit gentamicin [65]. The increasing resistance to gentamicin of staphylococci in bone infections [134] compels the use of different strategies to battle the biofilms.

The range of values of gentamicin MIC and MBC obtained for both staphylococcal strains studied were 4 μg/ml - 8 μg/ml and 8 μg/ml - 16 μg/ml, respectively. To study whether antibiotic susceptibility of biofilms increases when combined with DNase I treatment, the amount of gentamicin sulphate used was 8 μg/ml, a concentration of drug in-between the MIC and the MBC (Table 3.4). In immunosuppressed patients and patients with serious infections, immune defense mechanisms are suboptimal. Thus, inhibitory concentration of the drug (MIC) may not be sufficient, and obtaining bactericidal concentrations of antimicrobial agents at the infection site is essential for accomplishing the treatment. The MBC can be used for this purpose [135]. Noteworthy, it is important to emphasize that the dosage of the antibiotic differs according to the use for which the medical device is intended and an inappropriate dose may be seen as the reason of failure of the prosthesis, as it may originate the emergence of resistant bacteria [131]. Clinically, the administered dose is much higher than 8 μg/ml of gentamicin to prevent orthopaedic infections. For example, the products Palacos G and SmarSet GHV are both FDA approved as antibiotics-laden PMMA bone cement and contain 0.85 g gentamicin and 1 g gentamicin, respectively [136]. The results should be analysed taking into account this information since hypothetically, it is possible to envisage that to higher doses of antibiotics correspond to greater inhibition/elimination of microorganisms. However, the purpose of this experiment was to evaluate whether susceptibility increases and not completely kills biofilms within the analysed time window. From the results obtained it should be possible to extrapolate (for the same clinical scenario) that combining both DNase I and gentamicin the outcomes can be as effective as the ones using larger amounts of drug.

4.6.2. Biofilm susceptibility to gentamicin

The anti-adhesive coating analyzed in this thesis exerts its effect by disruption of the EPS matrix staphylococcal biofilms, weakening and dispersing biofilms [70]. The bacteria in the biofilm (or part of them) are forced to reside in their planktonic state, thereby remaining more susceptible to biocide and antibiotic action, as well as eradication by the immune system [13]. The combination of DNase I with antibiotics or biocides is an interesting opportunity for the development of more effective treatments towards bacterial infections, or development of environmentally friendly methods to combat biofilms [59]. In fact, this dispersal-mediated treatment will most likely require supplementation with antibiotic therapy responsible for killing metabolically active cells and render any remaining persistent cells vulnerable to the immune system, as dispersal alone is not sufficient for bacterial removal [85].

In most of the experiment, gentamicin sulphate solutions at the MIC (or lower limit of MBC, 8 μg/ml) combined with DNase I (present in the PLGA-DNase I and PLGA-inulin packaged DNase I coatings) were insufficient to kill staphylococci in their biofilms mode of growth (Figure 3.15 – Figure 3.18). Complete inhibition of the biofilms did not occur, which could be explained by the fact that MIC values were determined against planktonic organisms, neglecting the protective action of the biofilms [132]. However, for a biofilm 24 h old of *S. aureus* ATCC 12600^{GFP} in the presence of PLG-DNase I, there is no practically biofilm on the coating surface, i.e. the ratio of biovolume live bacteria/biovolume dead bacteria was virtually null (Figure 3.16). The same occurred for a biofilm 48 h old of *S. aureus* Newman D2C^{GFP} also in the presence of PLGA-DNase I coating (Figure 3.18). The coating PLGA-DNase I showed to be more efficient in the prevention of biofilm formation than the PLGA-inulin packaged DNase I, probably because the last coating has five times less concentration of DNase I – in contrast to that observed in section 4.4, the amount of DNase I seems to have a more prominent effect when combined with gentamicin. Additionally, it was verified that in the presence of DNase I and gentamicin, the ratios of biovolume live bacteria/biovolume dead bacteria for both *S. aureus* strains were considerably lower when compared to the ones on the titanium surface uncoated, i.e. only in the presence of gentamicin. Finally, the combination of DNase I with gentamicin seems to be less effective for *S. aureus* ATCC 12600^{GFP}, since this strain presents superior ratio of biovolume live bacteria/biovolume dead bacteria in both analyzed time points (Figure 3.16 and Figure 3.18).

It is important to note that this experiment was only performed one time (hence the SD are not present in the Figure 3.16 and Figure 3.18), whereby it should be repeated in the future to ensure the reproducibility of the obtained results.

Even though only a single pilot experiment was performed the preliminary result suggests that the combination of gentamicin with DNase I is more efficient in preventing biofilm formation for 24 h (Figure 3.10.A) and Figure 3.16). This study was not the first combining DNase I and gentamicin. For example, a study developed by Aspe and co-workers [65], showed that chemical disruption of an established *P. aeruginosa* biofilm with DNase or AlgL (separately or in combination) increased the susceptibility of the culture to gentamicin. Increased antibiotic susceptibility has also been observed with other dispersal agents such as dispersin B and proteinase K [85].

Although promising, the combination of antibiotic therapy with a dispersal agent (or, in particular, gentamicin coupled with DNase I) presents serious concerns with regards to the induced dispersal, which could result in acute infections if the antibiotic does not succeed on the eradication of the released cells (potentially leading to systemic infection). Additionally, embolism formation resulting from the release of cell clumps embedded in matrix components (generation of large detached biofilm chunks that have intrinsic resistance characteristics) could be a risk of dispersal treatments [75,85]. Sub-inhibitory concentrations of β-lactams have also been related to the induction of eDNA release and biofilm formation, which is counter-productive when coupled with a dispersal agent. Further studies are needed to address these challenges before dispersal agents are tested in a clinical setting [85].

Alternative to the technique used, antibiotics may be directly included in the biodegradable PLGA coating [12] and/or could be combined with a second antibiotic. Occurrence of gentamicin-resistant bacterial strains in prosthesis-related infections (nearly 50% of the staphylococci) has led to the development of antibiotic-loaded bone cements in which gentamicin is combined with a second antibiotic [133]. The most commonly mixed antibiotics are gentamicin and tobramycin (also an aminoglycoside) and vancomycin (a glycopeptide active mainly on gram-positive like, e.g., *S. aureus*) [131]. Therefore, a combination of antibiotics may reduce the occurrence of antibiotic resistance [133] and possibly increase the efficiency of the developed method preventing the biofilm formation.

Chapter 5

Conclusions and future perspectives

5.1. Concluding remarks

In the present work, the effect of a protective, biodegradable PLGA coating containing DNase I or inulin-packaged DNase I on bacterial adhesion and biofilm formation of two *S. aureus* strains was studied.

Coating the surfaces of the implants is one of the techniques that must be explored to prevent the adhesion of bacteria and consequent formation of biofilms. Different particles (inulin, DNase I or inulin-packaged DNase I) were obtained by spray-drying, with a very similar size, and were separately incorporated in PLGA, generating titanium coatings with smooth surfaces, reduced thickness and different degradation rates in PBS. Coatings without DNase I particles – PLGA and PLGA-inulin – presented shorter times of degradation than those with – PLGA-DNase I, PLGA-DNase I (1/5) and PLGA-inulin packaged DNase I (presented the longest degradation period). Regarding the release of DNase I particles for both PLGA-DNase I and PLGA-inulin packaged DNase I coatings, an initial burst of drug release (partially explained for the reduced thickness) occurred, followed by a longer period of gradual release. In order to optimize the efficiency of these coatings, the initial burst release was efficiently avoided placing an extra layer of PLGA on the top of the active layer, since it was prevented the contact between the active substances in the coatings and the surrounding environment, PBS.

In accordance with previous studies, it was demonstrated that eDNA is required for biofilm development, since the coating of titanium with PLGA incorporating DNase I particles (regardless of whether particles consisted of only DNase I or inulin-packaged DNase I) drastically decreases the initial bacterial adhesion *in vitro.* Additionally, the coatings PLGA-DNase I and PLGA-inulin packaged DNase I significantly reduced the biofilm formation on titanium surfaces *in vitro* for 24 h, 72 h and 120 h of biofilm growth for both staphylococcal strains. After comparing the results achieved for the coatings with the same concentration of DNase I, it is also possible to conclude that by packaging DNase I in inulin, DNase I underwent less damage during the coating process. Regarding the biocompatibility, none of the PLGA coatings tested adversely affected the capability of tissue cells to proliferate and to adhere, presenting a similar proliferation capacity and adherence to that which occurs in the uncoated titanium surfaces. Finally, the combination of DNase I (present in the PLGA-DNase I and PLGA-inulin packaged DNase I coatings) with a small amount of gentamicin (8 μg/ml) increased the bactericidal susceptibility, resulting in low biovolumes for biofilms 24 h and 48 h old.

5.2. Future perspectives

From the results obtained in this work, a number of suggestions can be proposed for future studies:

i. The presented method of protecting and packaging can be applied using other enzymes (such as lysozyme and dispersin B) that are known to be able to prevent bacterial adhesion and biofilm formation [12].

ii. Explore further opportunities for destabilizing the intermolecular interactions in the biofilm matrix, leaving it more susceptible to physical and chemical stresses. In addition, targets of V8, Aur, staphopains; and, also, the function of Nuc and D-amino acids in biofilm dispersal should be identified [85].

iii. The benefits of an extra PLGA layer on the top of the active PLGA coating that avoids the initial burst release of DNase I should be considered.

iv. The kinetics release of DNase I and inulin provided in this thesis was based on the assumption that these substances within the PLGA layer did not suffered degradation, i.e. only the DNase I and inulin particles released from the protective PLGA coating undergo degradation. In this regard, to obtain a more complete picture of what really happens with these substances inside of the polymeric layer, the activity (or loss of it) of the DNase I and inulin should be examined. This information would help to determine the amount of DNase I that should be included per particle of inulin in the PLGA-inulin coating with incorporated DNase I, for instance.

v. Implement an *in vitro* model based on the herein performed pilot experiment to determine whether the anti-biofilm treatment based on the protective PLGA coating incorporating DNase I particles increases the susceptibility to different antibiotics (such as gentamicin vancomycin, rifampicin, tobramycin) currently used clinically to prevent and/or treat infections.

vi. Test the efficiency of the PLGA-DNase I and PLGA-inulin packaged DNase I coatings with different species of bacteria, since the work provided in this thesis was limited to two staphylococcal strains presenting fluorescence due to limitations of available equipment.

vii. Finally, perform *in vivo* (animal) experiments applying the approach developed in this thesis. Notwithstanding the diversity possible in *in vitro* models currently available to identify or test anti-biofilm molecules, these models only partially reflect *in vivo* situations and for now it remains impossible to mimic the complexity of interactions between bacteria and the immune system *in vitro* [74].

References

[1] M. B. Sathyanarayanan, R. Balachandranath, Y. Genji Srinivasulu, S. K. Kannaiyan, and G. Subbiahdoss, "The Effect of Gold and Iron-Oxide Nanoparticles on Biofilm-Forming Pathogens", *ISRN Microbiol.*, pp. 1–5, 2013.

[2] J. P. Guggenbichler, O. Assadian, M. Boeswald, and A. Kramer, "Incidence and clinical implication of nosocomial infections associated with implantable biomaterials – catheters, ventilator-associated pneumonia, urinary tract infections", *GMS*, vol. 6, no. 1, pp. 1–19, 2011.

[3] R. M. Donlan, "Biofilms: Microbial Life on Surfaces," *Emerg. Infect. Dis.*, vol. 8, no. 9, pp. 881–890, 2002.

[4] M. Salwiczek, Y. Qu, J. Gardiner, R. A. Strugnell, T. Lithgow, K. M. McLean, and H. Thissen, "Emerging rules for effective antimicrobial coatings", *Trends Biotechnol.*, vol. 32, no. 2, pp. 82–90, 2014.

[5] Fintan Moriarty, S. A. J. Zaat, and H. J. Busscher, "Immunological Aspects and Antimicrobial Strategies*", Biomaterials Associated Infection,* 2013.

[6] H. J. Busscher, H. C. van der Mei, G. Subbiahdoss, P. C. Jutte, J. J. A. M. van den Dungen, S. A. J. Zaat, M. J. Schultz, and D. W. Grainger, "Biomaterial-associated infection: locating the finish line in the race for the surface", *Sci. Transl. Med.*, vol. 4, no. 153, pp. 1–10, 2012.

[7] A. K. Muszanska, M. R. Nejadnik, Y. Chen, E. R. van den Heuvel, H. J. Busscher, H. C. van der Mei, and W. Norde, "Bacterial adhesion forces with substratum surfaces and the susceptibility of biofilms to antibiotics", *Antimicrob. Agents Chemother.*, vol. 56, no. 9, pp. 4961–4964, 2012.

[8] L. Hall-Stoodley, J. W. Costerton, and P. Stoodley, "BACTERIAL BIOFILMS: FROM THE NATURAL ENVIRONMENT TO INFECTIOUS DISEASES", *Nat. Rev. Microbiol.*, vol. 2, no. 2, pp. 95–108, 2004.

[9] C. Von Eiff, B. Jansen, W. Kohnen, and K. Becker, “Infections Associated with Medical Devices: Pathogenesis, Management and Prophylaxis”, *Drugs*, vol. 65, no. 2, pp. 179–214, 2005.

[10] T. Baba, T. Bae, O. Schneewind, F. Takeuchi, and K. Hiramatsu, “Genome Sequence of *Staphylococcus aureus* Strain Newman and Comparative Analysis of Staphylococcal Genomes: Polymorphism and Evolution of Two Major Pathogenicity Islands”, *J. Bacteriol.*, vol. 190, no. 1, pp. 300–310, 2008.

[11] A. A. de S. Moreira, “Candida bracarensis virulence factors”, *Universidade do Minho,* 2013.

[12] J. J. T. M. Swartjes, P. K. Sharma, N. Grasmeijer, E. W. Frijlink, W. L. J. Hinrichs, H. C. van der Mei, and H. J. Busscher, “A protective, biodegradable PLGA-coating releasing inulin-packaged DNase I to prevent bacterial adhesion and biofilm formation”, pp. 1–20, 2013.

[13] T. Bjarnsholt, O. Ciofu, S. Molin, M. Givskov, and N. Høiby, “Applying insights from biofilm biology to drug development - can a new approach be developed?”, *Nat. Rev. Drug Discov.*, vol. 12, no. 10, pp. 791–808, 2013.

[14] S. Daghighi, J. Sjollema, H. C. van der Mei, H. J. Busscher, and E. T. J. Rochford, “Infection resistance of degradable versus non-degradable biomaterials: an assessment of the potential mechanisms”, *Biomaterials*, vol. 34, no. 33, pp. 8013–8017, 2013.

[15] L. Hall-Stoodley and P. Stoodley, “Evolving concepts in biofilm infections”, *Cell. Microbiol.*, vol. 11, no. 7, pp. 1034–1043, 2009.

[16] C. G. Roberts, “The role of biofilms in reprocessing medical devices”, *Am. J. Infect. Control*, vol. 41, no. 5, pp. 77–80, 2013.

[17] G. Reid, “Biofilms in infectious disease and on medical devices”, *Int. J. Antimicrob. Agents*, vol. 11, pp. 223–226, 1999.

[18] D. Campoccia, L. Montanaro, and C. R. Arciola, “A review of the biomaterials technologies for infection-resistant surfaces”, *Biomaterials*, vol. 34, no. 34, pp. 8533–8554, 2013.

[19] A. F. Engelsman, I. C. Saldarriaga-Fernandez, M. R. Nejadnik, G. M. van Dam, K. P. Francis, R. J. Ploeg, H. J. Busscher, and H. C. van der Mei, “The risk of biomaterial-associated infection after revision surgery due to an experimental primary implant infection”, *Biofouling*, vol. 26, no. 7, pp. 761–767, 2010.

[20] D. Campoccia, L. Montanaro, and C. R. Arciola, “The significance of infection related to orthopedic devices and issues of antibiotic resistance”, *Biomaterials*, vol. 27, no. 11, pp. 2331–2339, 2006.

[21] A. L. Casey, P. A. Lambert, and T. S. J. Elliott, “Staphylococci”, *Int. J. Antimicrob. Agents*, vol. 3, pp. 23 – 32, 2007.

[22] S. Esposito and S. Leone, “Prosthetic joint infections: microbiology, diagnosis, management and prevention”, *Int. J. Antimicrob. Agents*, vol. 32, no. 4, pp. 287–293, 2008.

[23] E. Moran, I. Byren, and B. L. Atkins, “The diagnosis and management of prosthetic joint infections”, *J. Antimicrob. Chemother.*, vol. 65, pp. 45–54, 2010.

[24] L. Montanaro, P. Speziale, D. Campoccia, S. Ravaioli, I. Cangini, G. Pietrocola, S. Giannini, and C. R. Arciola, “Scenery of Staphylococcus implant infection in orthopedics”, *Future Microbiol.*, vol. 6, pp. 1329–1349, 2011.

[25] C. R. Mahon, D. C. Lehman, and G. Manuselis, *Textbook of Diagnostic Microbiology*, Fifth Edition, Elsevier Health Sciences, pp. 754–760, 2015.

[26] G. B. Wetenschappen, F. Geneeskunde, D. Medisch, D. Wetenschappen, and L. E. Laboratoriumgeneeskunde, “ROLE OF VIRULENCE REGULATOR GENES IN *STAPHYLOCOCCUS EPIDERMIDIS* BIOFILM FORMATION”, 2009.

[27] J. J. Champoux, F. C. Neidhardt, W. L. Drew, and J. J. Plorde, *Sherris Medical Microbiology: An Introduction to Infectious Diseases*, Fourth Edition. New York: McGraw-Hill, pp. 261–262, 2004.

[28] L. G. Harris, S. J. Foster, and R. G. Richards, “AN INTRODUCTION TO *STAPHYLOCOCCUS AUREUS*, AND TECHNIQUES FOR IDENTIFYING AND QUANTIFYING *S. AUREUS* ADHESINS IN RELATION TO ADHESION TO BIOMATERIALS: REVIEW”, *Eur. Cells Mater.*, vol. 4, pp. 39–60, 2002.

[29] J. C. Pommerville, *Alcamo’s Fundamentals of Microbiology*, Ninth Edition. Boston, 2011, p. 68; 347.

[30] T. Foster, “Staphylococcus”, in *Medical Microbiology*, B. S., Ed. Texas, 1996.

[31] E. A. Izano, M. A. Amarante, W. B. Kher, and J. B. Kaplan, “Differential Roles of Poly-N-Acetylglucosamine Surface Polysaccharide and Extracellular DNA in *Staphylococcus aureus* and *Staphylococcus epidermidis* Biofilms,” *Appl. Environ. Microbiol.*, vol. 74, no. 2, pp. 470–476, 2008.

[32] H.-C. Flemming and J. Wingender, “The biofilm matrix”, *Nat. Rev. Microbiol.*, vol. 8, no. 9, pp. 623–633, 2010.

[33] L. Foulston, A. K. W. Elsholz, A. S. Defrancesco, and R. Losick, “The Extracellular Matrix of *Staphylococcus aureus* Biofilms Comprises Cytoplasmic Proteins That Associate with the Cell Surface in Response to Decreasing pH”, *MBio*, vol. 5, no. 5, pp. 1–9, 2014.

[34] D. López, H. Vlamakis, and R. Kolter, “Biofilms”, *Cold Spring Harb. Perspect. Biol.*, vol. 2, pp. 1–11, 2010.

[35] N. K. Archer, M. J. Mazaitis, J. W. Costerton, J. G. Leid, M. E. Powers, and M. E. Shirtliff, “*Staphylococcus aureus* biofilms. Properties, regulation and roles in human disease”, *Landes Biosci.*, pp. 445–459, 2011.

[36] H.-S. Joo and M. Otto, "Molecular Basis of In Vivo Biofilm Formation by Bacterial Pathogens", *Chem. Biol.*, vol. 19, no. 12, pp. 1503–1513, 2012.

[37] G. Subbiahdoss, I. C. S. Fernández, J. F. D. S. Domingues, R. Kuijer, H. C. van der Mei, and H. J. Busscher, "In vitro interactions between bacteria, osteoblast-like cells and macrophages in the pathogenesis of biomaterial-associated infections", *PLoS One*, vol. 6, no. 9, pp. 1–8, 2011.

[38] G. Subbiahdoss, R. Kuijer, H. J. Busscher, and H. C. van der Mei, "Mammalian Cell Growth versus Biofilm Formation on Biomaterials Surfaces in an In Vitro Post-operative Contamination Model", *Microbiology*, vol. 156, pp. 3073–3078, 2010.

[39] D. Lindsay and A. von Holy, "Bacterial biofilms within the clinical setting: what healthcare professionals should know", *J. Hosp. Infect.*, vol. 64, pp. 313–325, 2006.

[40] D. McDougald, S. A. Rice, N. Barraud, P. D. Steinberg, and S. Kjelleberg, "Should we stay or should we go: mechanisms and ecological consequences for biofilm dispersal", *Nat. Rev. Microbiol.*, vol. 10, no. 1, pp. 39–50, 2012.

[41] C. Berne, D. T. Kysela, and Y. V. Brun, "A bacterial extracellular DNA inhibits settling of motile progeny cells within a biofilm", *Mol. Microbiol.*, vol. 77, no. 4, pp. 815–829, 2010.

[42] T. Das, S. K. Kutty, N. Kumar, and M. Manefield, "Pyocyanin Facilitates Extracellular DNA Binding to *Pseudomonas aeruginosa* Influencing Cell Surface Properties and Aggregation", *PLoS One*, vol. 8, no. 3, pp. 1–11, 2013.

[43] J. D. Shrout, T. Tolker-Nielsen, M. Givskov, and M. R. Parsek, "The contribution of cell-cell signaling and motility to bacterial biofilm formation", *Natl. Institutes Heal.*, vol. 36, no. 5, pp. 367–373, 2012.

[44] H. Vlamakis, Y. Chai, P. Beauregard, R. Losick, and R. Kolter, "Sticking together: building a biofilm the *Bacillus subtilis* way", *Nat. Rev. Microbiol.*, vol. 11, no. 3, pp. 157–168, 2013.

[45] C. R. Kokare, S. Chakraborty, A. N. Khopade, and K. R. Mahadik, “Biofilm: Importance and applications”, *Indian J. Biotechnol.*, vol. 8, pp. 159–168, 2009.

[46] T. Das, B. P. Krom, H. C. van der Mei, H. J. Busscher, and P. K. Sharma, “DNA-mediated bacterial aggregation is dictated by acid–base interactions”, *Soft Matter*, vol. 7, no. 6, pp. 2927–2935, 2011.

[47] S. Srey, I. K. Jahid, and S.-D. Ha, “Biofilm formation in food industries: A food safety concern”, *Food Control*, vol. 31, no. 2, pp. 572–585, 2013.

[48] N. Mena Viveros, “Biofilms in Otolaryngology”, *Acta Otorrinolaringol. Española*, vol. 65, pp. 47–52, 2014.

[49] S. Periasamy, H.-S. Joo, A. C. Duong, T.-H. L. Bach, V. Y. Tan, S. S. Chatterjee, G. Y. C. Cheung, and M. Otto, “How *Staphylococcus aureus* biofilms develop their characteristic structure”, *Proc. Natl. Acad. Sci. U. S. A.*, vol. 109, no. 4, pp. 1281–1286, 2012.

[50] M. Prax and R. Bertram, “Metabolic aspects of bacterial persisters”, *Front. Cell. Infect. Microbiol.*, vol. 4, pp. 1–6, 2014.

[51] G.-P. Sheng, H.-Q. Yu, and X.-Y. Li, “Extracellular polymeric substances (EPS) of microbial aggregates in biological wastewater treatment systems: a review”, *Biotechnol. Adv.*, vol. 28, no. 6, pp. 882–894, 2010.

[52] Z. Qin, Y. Ou, L. Yang, Y. Zhu, T. Tolker-Nielsen, S. Molin, and D. Qu, “Role of autolysin-mediated DNA release in biofilm formation of *Staphylococcus epidermidis*”, *Microbiology*, vol. 153, pp. 2083–2092, 2007.

[53] B. W. Peterson and H. C. van der Mei, “A Distinguishable Role of eDNA in the Viscoelastic Relaxation of Biofilms”, *MBio*, vol. 4, no. 5, pp. 1–13, 2013.

[54] M. Okshevsky and R. L. Meyer, “The role of extracellular DNA in the establishment, maintenance and perpetuation of bacterial biofilms”, *Crit. Rev. Microbiol.*, pp. 1–11, 2013.

[55] N. S. Jakubovics, R. C. Shields, N. Rajarajan, and J. G. Burgess, “Life after death: the critical role of extracellular DNA in microbial biofilms”, *Lett. Appl. Microbiol.*, vol. 57, no. 6, pp. 467–475, 2013.

[56] L. Tang, A. Schramm, T. R. Neu, N. P. Revsbech, and R. L. Meyer, “Extracellular DNA in adhesion and biofilm formation of four environmental isolates: a quantitative study”, *FEMS Microbiol. Ecol.*, vol. 86, no. 3, pp. 394–403, 2013.

[57] T. Das, S. Sehar, L. Koop, Y. K. Wong, S. Ahmed, K. S. Siddiqui, and M. Manefield, “Influence of Calcium in Extracellular DNA Mediated Bacterial Aggregation and Biofilm Formation”, *PLoS One*, vol. 9, no. 3, pp. 1–11, 2014.

[58] J. J. T. M. Swartjes, T. Das, S. Sharifi, G. Subbiahdoss, P. K. Sharma, B. P. Krom, H. J. Busscher, and H. C. van der Mei, “A Functional DNase I Coating to Prevent Adhesion of Bacteria and the Formation of Biofilm”, *Adv. Funct. Mater.*, vol. 23, pp. 2843–2849, 2013.

[59] M. Okshevsky, V. R. Regina, and R. L. Meyer, “Extracellular DNA as a target for biofilm control”, *Curr. Opin. Biotechnol.*, vol. 33, pp. 73–80, 2015.

[60] J. B. Xavier, C. Picioreanu, S. A. Rani, M. C. M. van Loosdrecht, and P. S. Stewart, “Biofilm-control strategies based on enzymic disruption of the extracellular polymeric substance matrix - a modelling study”, *Microbiology*, vol. 151, pp. 3817–3832, 2005.

[61] H. Mulcahy, L. Charron-Mazenod, and S. Lewenza, “Extracellular DNA Chelates Cations and Induces Antibiotic Resistance in *Pseudomonas aeruginosa* Biofilms”, *PLoS Pathog.*, vol. 4, no. 11, pp. 1–12, 2008.

[62] L. Johnson, S. R. Horsman, L. Charron-Mazenod, A. L. Turnbull, H. Mulcahy, M. G. Surette, and S. Lewenza, “Extracellular DNA-induced antimicrobial peptide resistance in *Salmonella enterica* serovar Typhimurium”, *BMC Microbiol.*, vol. 13, no. 1, pp. 115–123, 2013.

[63] R. Nijland, M. J. Hall, and J. G. Burgess, "Dispersal of Biofilms by Secreted, Matrix Degrading, Bacterial DNase", *PLoS One*, vol. 5, no. 12, pp. 1–7, 2010.

[64] J. A. Otter, K. Vickery, J. T. Walker, E. deLancey Pulcini, P. Stoodley, S. D. Goldenberg, J. A. G. Salkeld, J. Chewins, S. Yezli, and J. D. Edgeworth, "Surface-attached cells, biofilms and biocide susceptibility: implications for hospital cleaning and disinfection", *J. Hosp. Infect.*, vol. 44, pp. 1–12, 2014.

[65] M. Aspe, L. Jensen, J. Melegrito, and M. Sun, "The Role of Alginate and Extracellular DNA in Biofilm-Meditated *Pseudomonas aeruginosa* Gentamicin Resistance," *J. Exp. Microbiol. Immunol.*, vol. 16, pp. 42–48, 2012.

[66] S. R. Schooling, A. Hubley, and T. J. Beveridge, "Interactions of DNA with biofilm-derived membrane vesicles", *J. Bacteriol.*, vol. 191, no. 13, pp. 4097–4102, 2009.

[67] A. Taraszkiewicz, G. Fila, M. Grinholc, and J. Nakonieczna, "Innovative Strategies to Overcome Biofilm Resistance," *Hindawi*, pp. 1–14, 2013.

[68] H. Wu, C. Moser, H.-Z. Wang, N. Høiby, and Z.-J. Song, "Strategies for combating bacterial biofilm infections," *Int. J. Oral Sci.*, vol. 7, pp. 1–7, 2015.

[69] M. Simões and F. Mergulhão, *Biofilms in Bioengineering*, New York: Nova Science Publishers, 2013, pp. 269–311.

[70] M. Chen, Q. Yu, and H. Sun, "Novel Strategies for the Prevention and Treatment of Biofilm Related Infections", *Int. J. Mol. Sci.*, vol. 14, no. 9, pp. 18488–18501, 2013.

[71] C. C. C. R. de Carvalho, "Biofilms: Recent Developments on an Old Battle", *Recent Pat. Biotechnol.*, pp. 49–57, 2007.

[72] F. Kang, G. Jiang, A. Hinderliter, P. P. DeLuca, and J. Singh, "Lysozyme Stability in Primary Emulsion for PLGA Microsphere Preparation: Effect of Recovery Methods and Stabilizing Excipients", *Pharm. Res.*, vol. 19, no. 5, pp. 629–633, 2002.

[73] R. A. Jain, “The manufacturing techniques of various drug loaded biodegradable poly (lactide-co-glycolide) (PLGA) devices”, *Biomaterials*, vol. 21, pp. 2475–2490, 2000.

[74] C. Beloin, S. Renard, J.-M. Ghigo, and D. Lebeaux, “Novel approaches to combat bacterial biofilms”, *Curr. Opin. Pharmacol.*, vol. 18, pp. 61–68, 2014.

[75] B. R. Boles and A. R. Horswill, “Staphylococcal biofilm disassembly”, *Natl. Institutes Heal.*, vol. 19, no. 9, pp. 449–455, 2012.

[76] L. C. Powell, M. F. Pritchard, C. Emanuel, E. Onsøyen, P. D. Rye, C. J. Wright, K. E. Hill, and D. W. Thomas, “A nanoscale characterization of the interaction of a novel alginate oligomer with the cell surface and motility of *Pseudomonas aeruginosa*”, *Am. J. Respir. Cell Mol. Biol.*, vol. 50, no. 3, pp. 483–492, 2014.

[77] M. S. Blackledge, R. J. Worthington, and C. Melander, “Biologically inspired strategies for combating bacterial biofilms”, *Curr. Opin. Pharmacol.*, vol. 13, no. 5, pp. 699–706, 2013.

[78] S. Jabbouri and I. Sadovskaya, “Characteristics of the biofilm matrix and its role as a possible target for the detection and eradication of *Staphylococcus epidermidis* associated with medical implant infections”, *FEMS Immunol. Med. Microbiol.*, vol. 59, no. 3, pp. 280–291, 2010.

[79] J. A. Wu, C. Kusuma, J. J. Mond, and J. F. Kokai-Kun, “Lysostaphin Disrupts *Staphylococcus aureus* and *Staphylococcus epidermidis* Biofilms on Artificial Surfaces”, *Antimicrob. Agents Chemother.*, vol. 47, no. 11, pp. 3407–3414, 2003.

[80] P. S. Ibusquiza, “Biofilm formation by *Listeria monocytogenes*. Resistance to industrial biocides and cross-response caused by adaptation to benzalkonium chloride”, 2011.

[81] W. C. M. A. Melo and J. R. Perussi, “Strategies to overcome biofilm resistance”, *Microb. Pathog. Strateg. Combat. them Sci. technlogy Educ.*, pp. 179–187, 2013.

[82] S. Sugimoto, T. Iwase, F. Sato, A. Tajima, H. Shinji, and Y. Mizunoe, “Cloning, expression and purification of extracellular serine protease Esp, a biofilm-degrading enzyme, from *Staphylococcus epidermidis*”, *J. Appl. Microbiol.*, pp. 1406–1415, 2011.

[83] R. M. van der Kaaij, X.-L. Yuan, A. Franken, A. F. J. Ram, P. J. Punt, M. J. E. C. van der Maarel, and L. Dijkhuizen, “Two Novel, Putatively Cell Wall-Associated and Glycosylphosphatidylinositol-Anchored alpha-Glucanotransferase Enzymes of *Aspergillus niger*”, *Eukaryot. Cell*, vol. 6, no. 7, pp. 1178–1188, 2007.

[84] Y. Dong, A. R. Gusti, Q. Zhang, J. Xu, and L. Zhang, “Identification of Quorum-Quenching N-Acyl Homoserine Lactonases from Bacillus Species”, *Appl. Environ. Microbiol.*, vol. 68, no. 4, pp. 1754–1759, 2002.

[85] J. L. Lister and A. R. Horswill, “*Staphylococcus aureus* biofilms: recent developments in biofilm dispersal”, *Front. Cell. Infect. Microbiol.*, vol. 4, no. December, pp. 1–9, 2014.

[86] Rn. Product Information DNase I, “Thermo Scientific: DNase I, RNase-free”, no. 3. pp. 8–11, 2012.

[87] G. S. Zijlstra, B. J. Ponsioen, S. A. Hummel, N. Sanders, W. L. J. Hinrichs, A. H. de Boer, and H. W. Frijlink, “Formulation and process development of (recombinant human) deoxyribonuclease I as a powder for inhalation”, *Pharm. Dev. Technol.*, vol. 14, no. 4, pp. 358–368, 2009.

[88] G. S. Zijlstra, B. Ponsioen, S. Hummel, N. Sanders, W. L. J. Hinrichs, A. H. De Boer, and H. W. Frijlink, “CHAPTER 5 - The preclinical development of (recombinant human) deoxyribonuclease I as a powder for inhalation”, 2009.

[89] R. Dreywood, “Qualitative Test for Carbohydrate Material”, *Ind. Eng. Chem. Anal. Ed.*, vol. 18, no. 8, p. 499, 1946.

[90] L. L. Lorenz and E. S. Duthie, “Staphylococcal Coagulase: Mode of Action and Antigenicity”, *J. Soc. Gen. Microbiol.*, no. 6, pp. 95–107, 1952.

[91] C. Nieto and M. Espinosa, “Construction of the mobilizable plasmid pMV158GFP, a derivative of pMV158 that carries the gene encoding the green fluorescent protein”, *Plasmid*, vol. 49, no. 3, pp. 281–285, 2003.

[92] J. Li, H. J. Busscher, J. J. T. M. Swartjes, Y. Chen, A. K. Harapanahalli, W. Norde, H. C. van der Mei, and J. Sjollema, “Residence-time dependent cell wall deformation of different *Staphylococcus aureus* strains on gold measured using surface-enhanced-fluorescence”, *Soft Matter*, vol. 10, pp. 7638–7646, 2014.

[93] J. Li, H. J. Busscher, H. C. van der Mei, W. Norde, B. P. Krom, and J. Sjollema, “Analysis of the contribution of sedimentation to bacterial mass transport in a parallel plate flow chamber. Part II: use of fluorescence imaging”, *Colloids Surfaces B Biointerfaces*, vol. 87, pp. 427–432, 2011.

[94] A. Heydorn, A. T. Nielsen, M. Hentzer, M. Givskov, B. K. Ersbøll, and S. Molin, “Quantification of biofilm structures by the novel computer program COMSTAT”, *Microbiology*, vol. 146, pp. 2395–2407, 2000.

[95] A. Heydorn, B. K. Ersbøll, M. Hentzer, M. R. Parsek, M. Givskov, and S. Molin, “Experimental reproducibility in flow-chamber biofilms”, *Microbiology*, vol. 146, pp. 2409–2415, 2000.

[96] AppliChem, “AppliCations No.12 - Cell Proliferation Assay XTT”, no. 12. pp. 6–9, 2010.

[97] X. Li, Z. Yan, and J. Xu, “Quantitative variation of biofilms among strains in natural populations of *Candida albicans*”, *Microbiology*, vol. 149, pp. 353–362, 2003.

[98] C. and L. S. Institute, *Performance Standards for Antimicrobial Susceptibility Testing; Seventeenth Informational Supplement*, vol. 27, 2007.

[99] J. Eriksson, *Analytical Techniques and Formulation Strategies for the Therapeutic Protein Alkaline Phosphatase*, 2004, pp. 2–52.

[100] N. Y. K. Chew and H. Chan, “Effect of Powder Polydispersity on Aerosol Generation”, *J. Pharm. Sci.*, vol. 5, no. 2, pp. 162–168, 2006.

[101] X. Wang, E. Wenk, X. Hu, G. R. Castro, L. Meinel, X. Wang, C. Li, H. Merkle, and D. L. Kaplan, “Silk coatings on PLGA and alginate microspheres for protein delivery”, *Biomaterials*, vol. 28, no. 28, pp. 4161–4169, 2007.

[102] S. I. P. Ltd., “Proscan 2000 Software Manual 2.1.0.” Somerset, England, p. 60, 2000.

[103] C. Desrousseaux, V. Sautou, S. Descamps, and O. Traoré, “Modification of the surfaces of medical devices to prevent microbial adhesion and biofilm formation”, *J. Hosp. Infect.*, vol. 85, no. 2, pp. 87–93, 2013.

[104] T. Ponnusamy, L. B. Lawson, L. C. Freytag, D. A. Blake, R. S. Ayyala, and V. T. John, “In vitro degradation and release characteristics of spin coated thin films of PLGA with a ‘breath figure’ morphology”, *Biomatter*, vol. 2, no. 2, pp. 77–86, 2012.

[105] J. J. T. M. Swartjes, “Innovative coatings for anti-bacterial surfaces”, Rijksuniversiteit Groningen, 2014.

[106] J. Shen and D. J. Burgess, “Accelerated in vitro release testing of implantable PLGA microsphere/PVA hydrogel composite coatings”, *Natl. Institutes Heal.*, vol. 422, pp. 341–348, 2012.

[107] M. Kamberi, S. Nayak, K. Myo-Min, T. P. Carter, L. Hancock, and D. Feder, “A novel accelerated in vitro release method for biodegradable coating of drug eluting stents: Insight to the drug release mechanisms”, *Eur. J. Pharm. Sci.*, vol. 37, no. 3–4, pp. 217–222, 2009.

[108] H. K. Makadia and S. J. Siegel, “Poly Lactic-co-Glycolic Acid (PLGA) as Biodegradable Controlled Drug Delivery Carrier”, *Polymers (Basel).*, vol. 3, no. 3, pp. 1377–1397, 2011.

[109] R. Dinarvand, N. Sepehri, S. Manoochehri, H. Rouhani, and F. Atyabi, “Polylactide-co-glycolide nanoparticles for controlled delivery of anticancer agents”, *Int. J. Nanomedicine*, vol. 6, pp. 877–895, 2011.

[110] D. Nadano, T. Yasuda, and K. Kishi, “Measurement of Deoxyribonuclease I Activity in Human Tissues and Body Fluids by a Single Radial Enzyme-Diffusion Method”, *Clin. Chem.*, vol. 452, pp. 448–452, 1993.

[111] C. Haisch and R. Niessner, “Visualisation of transient processes in biofilms by optical coherence tomography”, *Water Res.*, vol. 41, no. 11, pp. 2467–2472, 2007.

[112] G. S. Zijlstra, “Dry powder inhalation of biopharmaceuticals: from formulation to proof-of-concept”, 2009.

[113] S. R. Hymes, T. M. Randis, T. Y. Sun, and A. J. Ratner, “DNase inhibits *Gardnerella vaginalis* biofilms in vitro and in vivo”, *J. Infect. Dis.*, vol. 207, no. 10, pp. 1491–1497, 2013.

[114] X. Y. and L. Y., “Biological control of microbial attachment: a promising alternative for mitigating membrane biofouling”, *Appl. Microbiol. Biotechnol.*, vol. 86, no. 3, pp. 825–837, 2010.

[115] N. J. Hickok and I. M. Shapiro, “Immobilized antibiotics to prevent orthopedic implant infections”, *Natl. Institutes Heal.*, vol. 64, no. 12, pp. 1165–1176, 2013.

[116] J. Fujihara, T. Yasuda, T. Kunito, Y. Fujii, H. Takatsuka, T. Moritani, and H. Takeshita, “Two N-linked Glycosylation Sites (Asn18 and Asn106) Are Both Required for Full Enzymatic Activity, Thermal Stability, and Resistance to Proteolysis in Mammalian Deoxyribonuclease I”, *Biosci. Biotechnol. Biochem.*, vol. 72, no. 12, pp. 3197–3205, 2008.

[117] A. L. Demain and P. Vaishnav, “Production of recombinant proteins by microbes and higher organisms”, *Biotechnol. Adv.*, vol. 27, no. 3, pp. 297–306, 2009.

[118] S. Liao, M. I. Klein, K. P. Heim, Y. Fan, J. P. Bitoun, S.-J. Ahn, R. A. Burne, H. Koo, L. J. Brady, and Z. T. Wen, “*Streptococcus mutans* Extracellular DNA is Upregulated during Growth in Biofilms, Actively Released via Membrane Vesicles, and Influenced by

Components of the Protein Secretion Machinery", *J. Bacteriol.*, vol. 196, pp. 2355–2366, 2014.

[119] L. A. Novotny, A. O. Amer, E. Brockson, M, S. D. Goodman, and L. O. Bakaletz, "Structural Stability of *Burkholderia cenocepacia* Biofilms Is Reliant on eDNA Structure and Presence of a Bacterial Nucleic Acid Binding Protein", *PLoS One*, vol. 8, no. 6, pp. 1–15, 2013.

[120] S. D. Goodman, K. P. Obergfell, J. A. Jurcisek, L. A. Novotny, J. S. Downey, E. A. Ayala, N. Tjokro, B. Li, S. S. Justice, and L. O. Bakaletz, "Biofilms can be dispersed by focusing the immune system on a common family of bacterial nucleoid-associated proteins", *Mucosal Immunol.*, vol. 4, no. 6, pp. 625–637, 2011.

[121] M. J. Huseby, A. C. Kruse, J. Digre, P. L. Kohler, J. A. Vocke, E. E. Mann, K. W. Bayles, G. A. Bohach, P. M. Schlievert, D. H. Ohlendorf, and C. A. Earhart, "Beta toxin catalyzes formation of nucleoprotein matrix in staphylococcal biofilms", *Proc. Natl. Acad. Sci. U. S. A.*, vol. 107, no. 32, pp. 14407–14412, 2010.

[122] R. Fraioli, F. Rechenmacher, S. Neubauer, J. M. Manero, J. Gil, H. Kessler, and C. Mas-Moruno, "Mimicking Bone Extracellular Matrix: Integrin-Binding Peptidomimetics Enhance Osteoblast-like Cells Adhesion, Proliferation, and Differentiation on Titanium", *Colloids Surfaces B Biointerfaces*, pp. 1–10, 2015.

[123] S. Wang, H. Yu, and J. K. Wickliffe, "Limitation of the MTT and XTT assays for measuring cell viability due to superoxide formation induced by nano-scale TiO2", *Toxicol. Vitr. an Int. J. Publ. Assoc. with BIBRA*, vol. 25, no. 8, pp. 2147–2151, 2011.

[124] N. W. Roehm, G. H. Rodgers, S. M. Hatfield, and A. L. Glasebrook, "An improved colorimetric assay for cell proliferation and viability utilizing the tetrazolium salt XTT", *J. Immunol. Methods*, vol. 142, pp. 257–265, 1991.

[125] I. Litinsky, I. Golan, M. Yaron, I. Yaron, D. Caspi, and O. Elkayam, "Simvastatin Induces Apoptosis of Fibroblast-Like Synoviocytes", *Open Rheumatol. J.*, vol. 3, pp. 35–40, 2009.

[126] L. Ren and K. Yang, “Bio-functional Design for Metal Implants, a New Concept for Development of Metallic Biomaterials”, *J. Mater. Sci. Technol.*, vol. 29, no. 11, pp. 1005–1010, 2013.

[127] A. T. Sidambe, “Biocompatibility of Advanced Manufactured Titanium Implants—A Review”, *Materials (Basel).*, vol. 7, no. 12, pp. 8168–8188, 2014.

[128] T. G. van Kooten, H. T. Spijker, and H. J. Busscher, “Plasma-treated polystyrene surfaces: model surfaces for studying cell-biomaterial interactions”, *Biomaterials*, vol. 25, no. 10, pp. 1735–1747, 2004.

[129] M. E. Gomes and R. L. Reis, “Biodegradable polymers and composites in biomedical applications: from catgut to tissue engineering. Parte 1. Available systems and their properties”, *Int. Mater. Rev.*, vol. 49, no. 5, pp. 261–273, 2004.

[130] J. A. Ryan, “Corning Guide for Identifying and Correcting Common Cell Growth Problems Technical Bulletin”, pp. 1–12, 2008.

[131] A. Bistolfi, G. Massazza, E. Verné, A. Massè, D. Deledda, S. Ferraris, M. Miola, F. Galetto, and M. Crova, “Antibiotic-Loaded Cement in Orthopedic Surgery: A Review”, *ISRN Orthop.*, vol. 2011, pp. 1–8, 2011.

[132] M. Crismaru, “Mechanisms of antimicrobial actions of quaternary ammonium compounds”, 2012.

[133] G. T. Ensing, J. R. van Horn, H. C. van der Mei, H. J. Busscher, and D. Neut, “Copal bone cement is more effective in preventing biofilm formation than Palacos R-G”, *Clin. Orthop. Relat. Res.*, vol. 466, no. 6, pp. 1492–1498, 2008.

[134] O. S. Kluin, H. C. van der Mei, H. J. Busscher, and D. Neut, “A surface-eroding antibiotic delivery system based on poly-(trimethylene carbonate)”, *Biomaterials*, vol. 30, no. 27, pp. 4738–4742, 2009.

[135] C. R. Mahon, D. C. Lehman, and G. M. Jr., *Textbook of Diagnostic Microbiology*, Fifth Edition, Elsevier Health Sciences, pp. 306–307, 2014.

[136] J. S. Gogia, J. P. Meehan, P. E. Di Cesare, and A. A. Jamali, “Local Antibiotic Therapy in Osteomyelitis”, *Semin. Plast. Surg.*, vol. 23, no. 2, pp. 100–107, 2009.

Appendices

Appendix A – Particles dimension

The size distribution of inulin (Figure A.1), DNase I (Figure A.2) and inulin-packaged DNase I (ratio 4:1) (Figure A.3) particles was determined by laser diffraction.

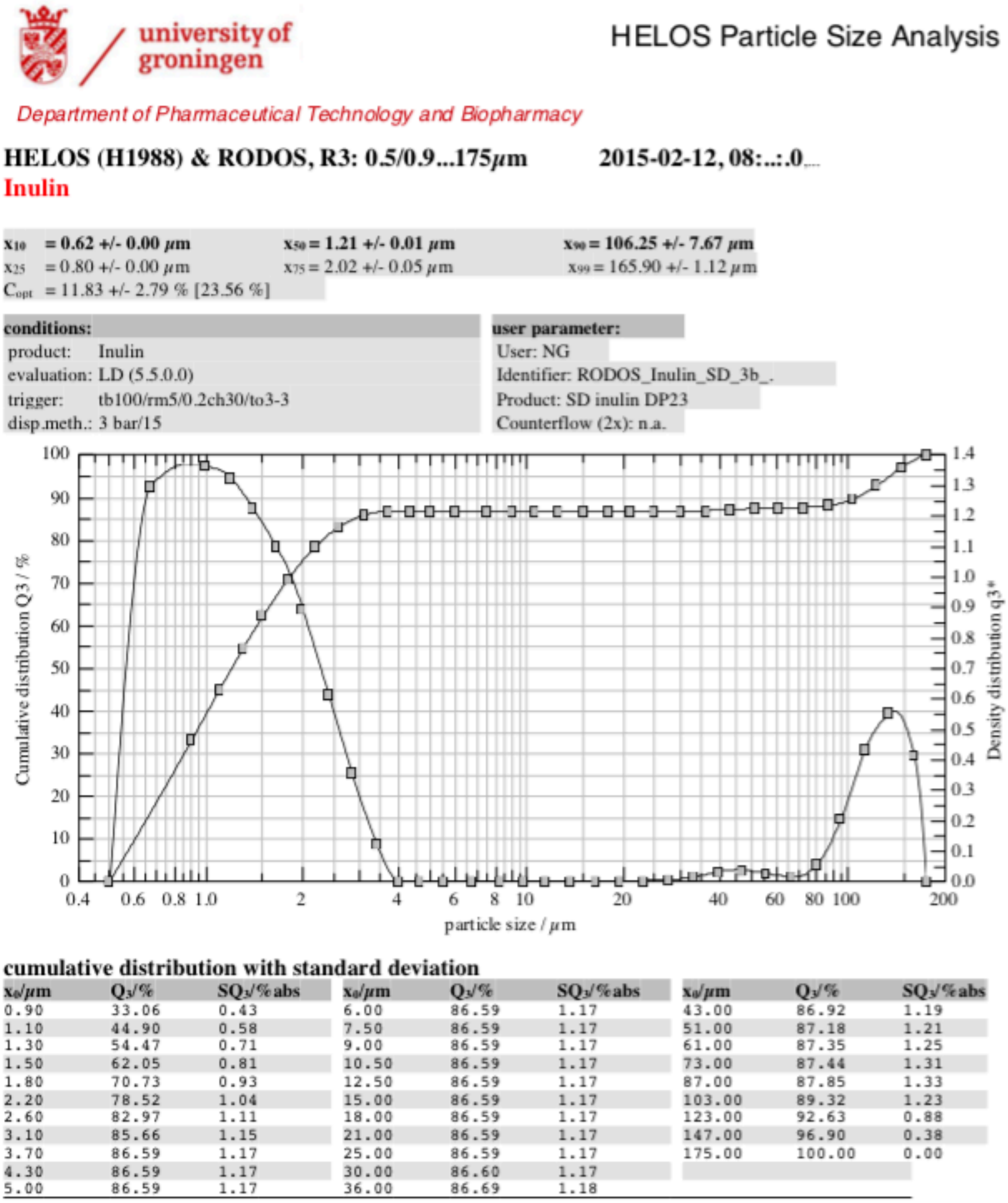

university of groningen

HELOS Particle Size Analysis

Department of Pharmaceutical Technology and Biopharmacy

HELOS (H1988) & RODOS, R3: 0.5/0.9...175μm **2015-02-12, 08:..:.0...**

Inulin

x_{10} = 0.62 +/- 0.00 μm **x_{50} = 1.21 +/- 0.01 μm** **x_{90} = 106.25 +/- 7.67 μm**
x_{25} = 0.80 +/- 0.00 μm x_{75} = 2.02 +/- 0.05 μm x_{99} = 165.90 +/- 1.12 μm
C_{opt} = 11.83 +/- 2.79 % [23.56 %]

conditions:
product: Inulin
evaluation: LD (5.5.0.0)
trigger: tb100/rm5/0.2ch30/to3-3
disp.meth.: 3 bar/15

user parameter:
User: NG
Identifier: RODOS_Inulin_SD_3b_.
Product: SD inulin DP23
Counterflow (2x): n.a.

Cumulative distribution Q3 / %
100
90
80
70
60
50
40
30
20
10
0
Density distribution q3*
1.4
1.3
1.2
1.1
1.0
0.9
0.8
0.7
0.6
0.5
0.4
0.3
0.2
0.1
0.0
0.4
0.6
0.8
1.0
2
4
6
8
10
20
40
60
80
100
200
particle size / μm

cumulative distribution with standard deviation

x_0/μm	Q_3/%	SQ_3/%abs	x_0/μm	Q_3/%	SQ_3/%abs	x_0/μm	Q_3/%	SQ_3/%abs
0.90	33.06	0.43	6.00	86.59	1.17	43.00	86.92	1.19
1.10	44.90	0.58	7.50	86.59	1.17	51.00	87.18	1.21
1.30	54.47	0.71	9.00	86.59	1.17	61.00	87.35	1.25
1.50	62.05	0.81	10.50	86.59	1.17	73.00	87.44	1.31
1.80	70.73	0.93	12.50	86.59	1.17	87.00	87.85	1.33
2.20	78.52	1.04	15.00	86.59	1.17	103.00	89.32	1.23
2.60	82.97	1.11	18.00	86.59	1.17	123.00	92.63	0.88
3.10	85.66	1.15	21.00	86.59	1.17	147.00	96.90	0.38
3.70	86.59	1.17	25.00	86.59	1.17	175.00	100.00	0.00
4.30	86.59	1.17	30.00	86.60	1.17			
5.00	86.59	1.17	36.00	86.69	1.18			

Figure A.1. Size distribution (μm) of inulin particles.

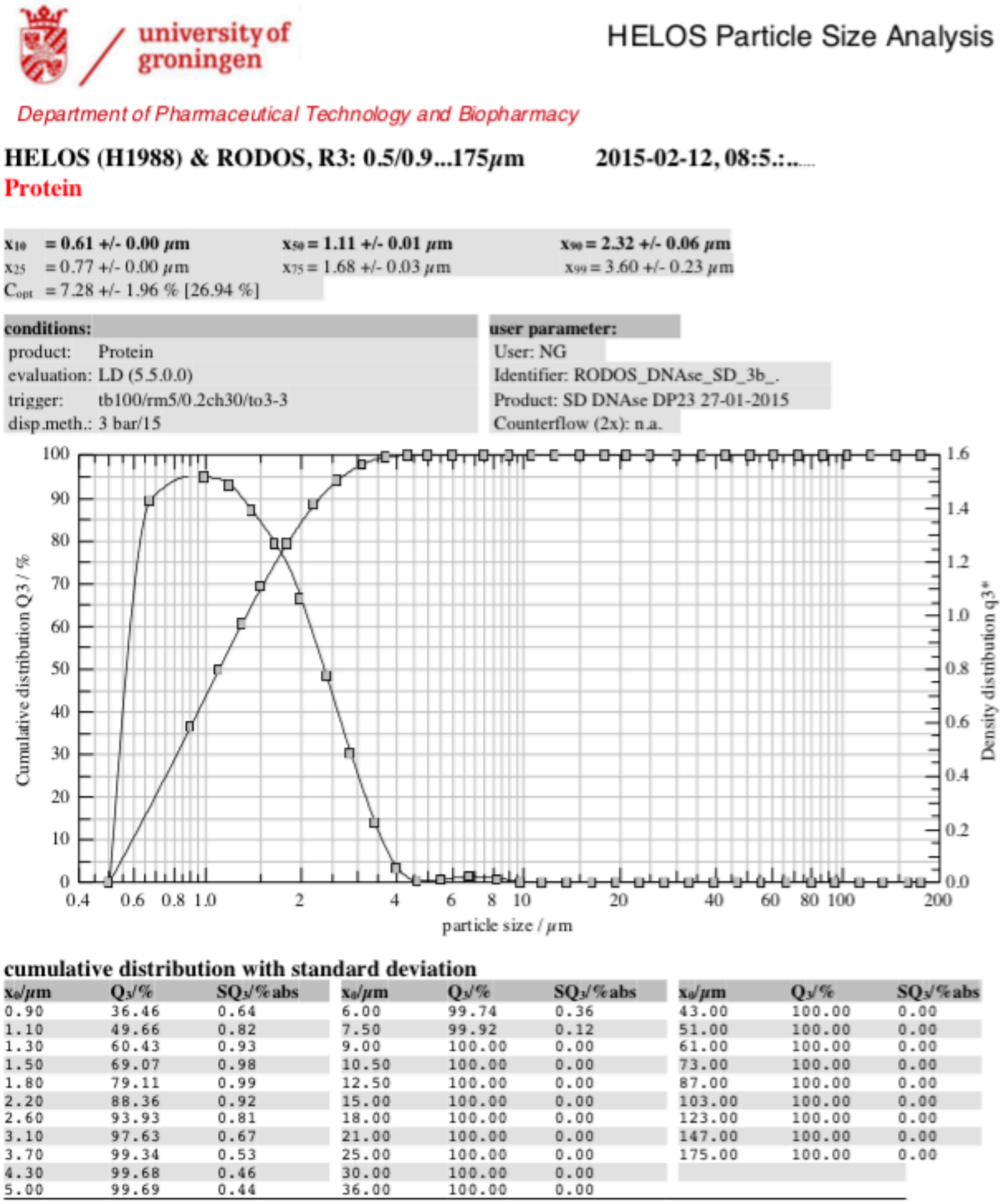

university of groningen

HELOS Particle Size Analysis

Department of Pharmaceutical Technology and Biopharmacy

HELOS (H1988) & RODOS, R3: 0.5/0.9...175µm **2015-02-12, 08:5**

Protein

x_{10} = 0.61 +/- 0.00 µm **x_{50} = 1.11 +/- 0.01 µm** **x_{90} = 2.32 +/- 0.06 µm**
x_{25} = 0.77 +/- 0.00 µm x_{75} = 1.68 +/- 0.03 µm x_{99} = 3.60 +/- 0.23 µm
C_{opt} = 7.28 +/- 1.96 % [26.94 %]

conditions:
product: Protein
evaluation: LD (5.5.0.0)
trigger: tb100/rm5/0.2ch30/to3-3
disp.meth.: 3 bar/15

user parameter:
User: NG
Identifier: RODOS_DNAse_SD_3b_.
Product: SD DNAse DP23 27-01-2015
Counterflow (2x): n.a.

Cumulative distribution Q3 / %
100
90
80
70
60
50
40
30
20
10
0
Density distribution q3*
1.6
1.4
1.2
1.0
0.8
0.6
0.4
0.2
0.0
0.4
0.6
0.8
1.0
2
4
6
8
10
20
40
60
80
100
200
particle size / µm

cumulative distribution with standard deviation

x_0/µm	Q_3/%	SQ_3/%abs	x_0/µm	Q_3/%	SQ_3/%abs	x_0/µm	Q_3/%	SQ_3/%abs
0.90	36.46	0.64	6.00	99.74	0.36	43.00	100.00	0.00
1.10	49.66	0.82	7.50	99.92	0.12	51.00	100.00	0.00
1.30	60.43	0.93	9.00	100.00	0.00	61.00	100.00	0.00
1.50	69.07	0.98	10.50	100.00	0.00	73.00	100.00	0.00
1.80	79.11	0.99	12.50	100.00	0.00	87.00	100.00	0.00
2.20	88.36	0.92	15.00	100.00	0.00	103.00	100.00	0.00
2.60	93.93	0.81	18.00	100.00	0.00	123.00	100.00	0.00
3.10	97.63	0.67	21.00	100.00	0.00	147.00	100.00	0.00
3.70	99.34	0.53	25.00	100.00	0.00	175.00	100.00	0.00
4.30	99.68	0.46	30.00	100.00	0.00			
5.00	99.69	0.44	36.00	100.00	0.00			

Figure A.2. Size distribution (µm) of DNase I particles.

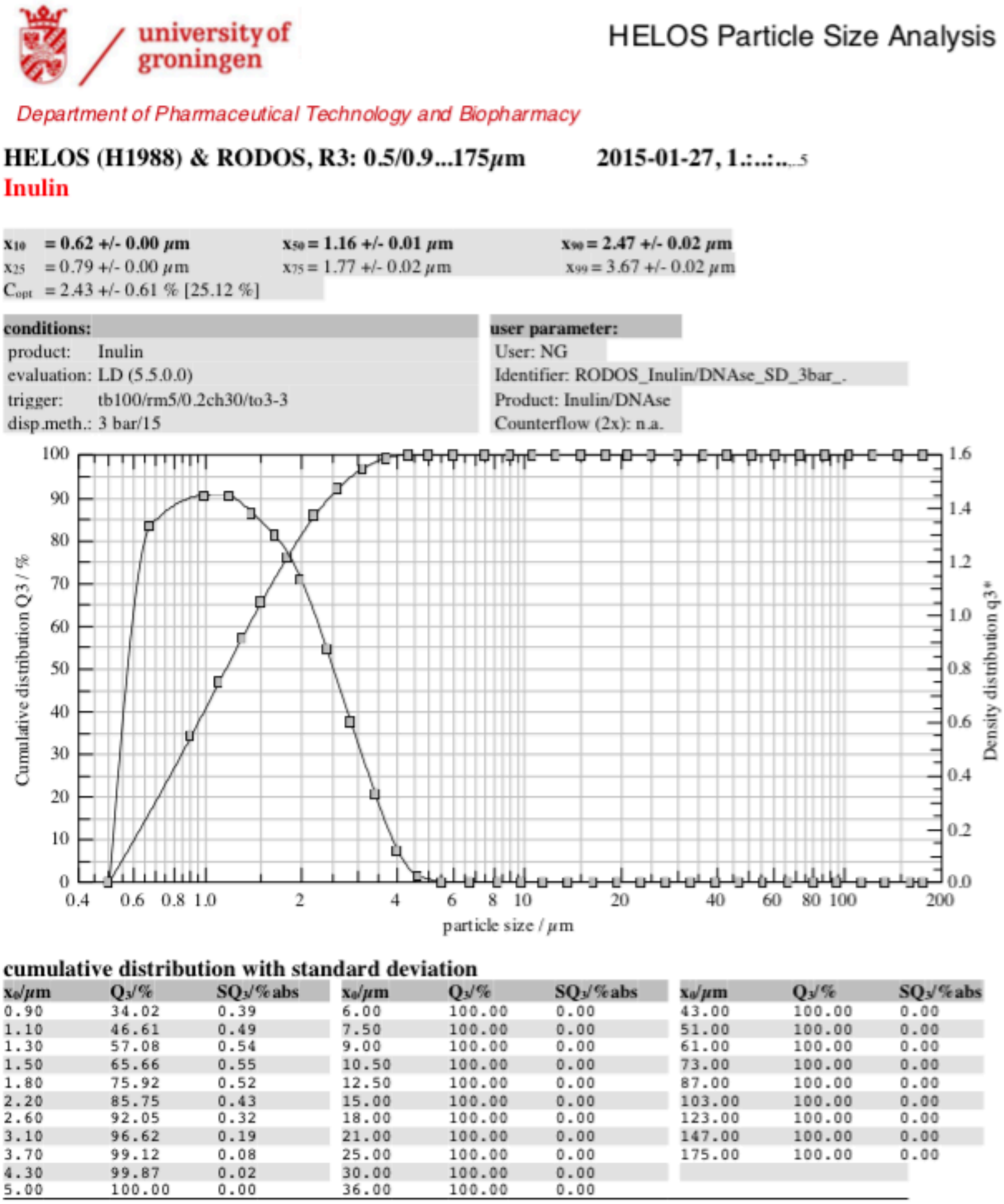

university of groningen

HELOS Particle Size Analysis

Department of Pharmaceutical Technology and Biopharmacy

HELOS (H1988) & RODOS, R3: 0.5/0.9...175µm **2015-01-27, 1.:..:...5**

Inulin

x_{10} = 0.62 +/- 0.00 µm **x_{50} = 1.16 +/- 0.01 µm** **x_{90} = 2.47 +/- 0.02 µm**
x_{25} = 0.79 +/- 0.00 µm x_{75} = 1.77 +/- 0.02 µm x_{99} = 3.67 +/- 0.02 µm
C_{opt} = 2.43 +/- 0.61 % [25.12 %]

conditions:
product: Inulin
evaluation: LD (5.5.0.0)
trigger: tb100/rm5/0.2ch30/to3-3
disp.meth.: 3 bar/15

user parameter:
User: NG
Identifier: RODOS_Inulin/DNAse_SD_3bar_.
Product: Inulin/DNAse
Counterflow (2x): n.a.

cumulative distribution with standard deviation

x_0/µm	Q_3/%	SQ_3/%abs	x_0/µm	Q_3/%	SQ_3/%abs	x_0/µm	Q_3/%	SQ_3/%abs
0.90	34.02	0.39	6.00	100.00	0.00	43.00	100.00	0.00
1.10	46.61	0.49	7.50	100.00	0.00	51.00	100.00	0.00
1.30	57.08	0.54	9.00	100.00	0.00	61.00	100.00	0.00
1.50	65.66	0.55	10.50	100.00	0.00	73.00	100.00	0.00
1.80	75.92	0.52	12.50	100.00	0.00	87.00	100.00	0.00
2.20	85.75	0.43	15.00	100.00	0.00	103.00	100.00	0.00
2.60	92.05	0.32	18.00	100.00	0.00	123.00	100.00	0.00
3.10	96.62	0.19	21.00	100.00	0.00	147.00	100.00	0.00
3.70	99.12	0.08	25.00	100.00	0.00	175.00	100.00	0.00
4.30	99.87	0.02	30.00	100.00	0.00			
5.00	100.00	0.00	36.00	100.00	0.00			

Figure A.3. Size distribution (µm) of inulin-packaged DNase I (ratio 4:1) particles.

Appendix B – DNase I and inulin calibration curves

Calibration curves were performed for further DNase I and inulin quantification. Calibration curves of DNase I (Figure B.1) and of inulin (Figure B.2) reflect the relationship between the concentration (μg/ml) of these substances and optical density (595 nm or 630 nm, correspondingly).

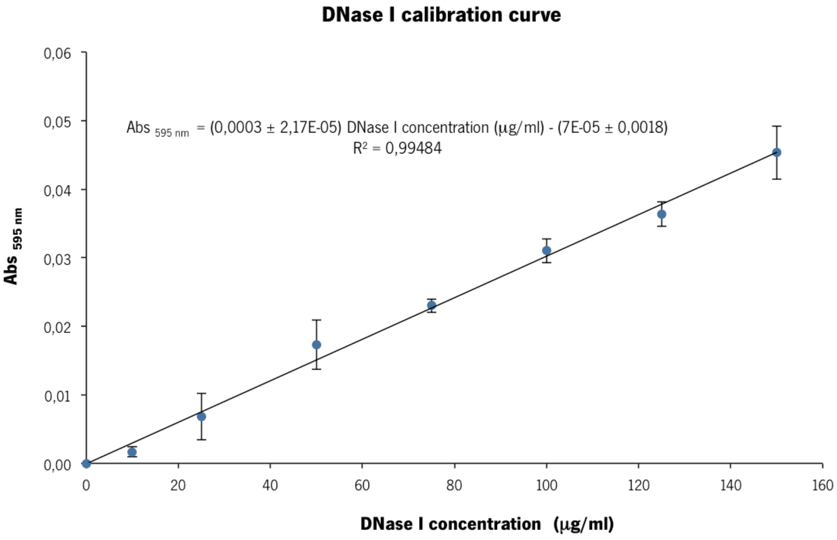

Figure B.1. Calibration curve of DNase I (595 nm) solution as a function of their concentration in solution (μg/ml) obtained spectrophotometrically. Error bars indicate SD over three experiments with separately prepared DNase I solutions.

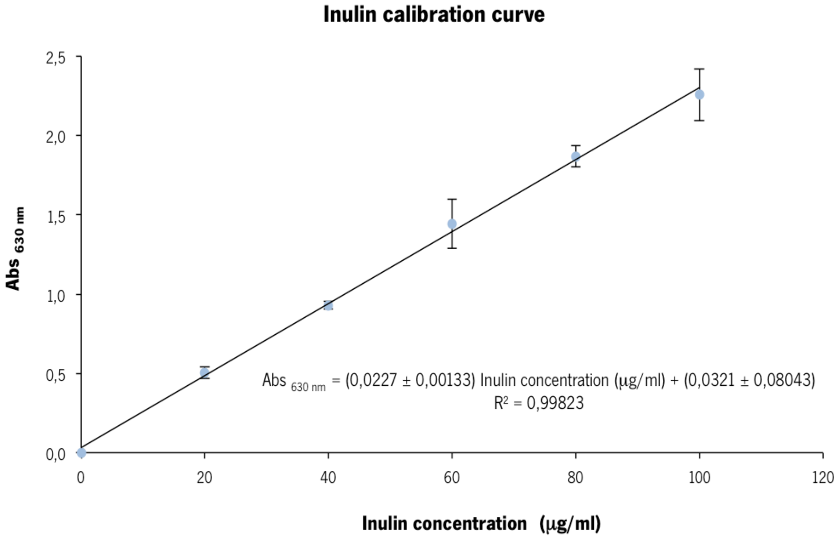

Figure B.2. Calibration curve of inulin (630 nm) solution as a function of their concentration in solution (μg/ml) obtained spectrophotometrically. Error bars indicate SD over three experiments with separately prepared inulin solutions.